Acoustic Studies on Wood

A Thesis

Submitted to the University of Canterbury

in partial fulfilment

of the requirements for the Degree

of

Masters of Forestry Science

by

Helge Hansen

The New Zealand School of Forestry

University of Canterbury

2006

Wood is just a monosyllabic word, but behind it there is a world of myths and miracles.

Theodor Heuss
President of the Federal Republic of Germany, 1949-1959

Table of contents

List of tables

List of figures

Acknowledgements

I wish to thank John Walker for being my supervisor and supporting me throughout the entire masters programme. Big thanks to Luis Apiolaza, my co-supervisor, especially for his advice and expertise in statistics.

The support from the staff of the school of forestry is also highly appreciated: thank you Jeanette, Vicki, David, Nigel, Lachlan, Marco and all the others.

The summer work for Forest New South Wales was a great opportunity to get some work experience, explore a new country and to make good friends. Special thanks to Carolyn Raymond for the support, assistance and advice with the study on the Blenheim Pruning Trial.

I also would like to say thank you to Roddy MacKenzie from Napier University, Edinburgh, for the cooperate research on laminated beams. Thank you for having me as a guest at your university and for showing me parts of beautiful Scotland.

Financial support from a masters scholarship granted by the University of Canterbury is highly appreciated.

Thank you to my Christchurch friends for keeping me from working too much on my thesis and for a good time in New Zealand.

Finally I would like to thank my German friends for showing me that they have not yet forgotten me; and my parents and brother for their incredible, limitless support, their patience and their love.

Abstract

Several acoustic techniques have been used to determine elastic and damping properties of trees, logs and beams.

Time of flight (TOF) measurements in the outerwood of 14-year-old *Pinus radiata* trees showed that pruning operations increased the outerwood stiffness by up to 25% compared with unpruned trees. However, at the most 5% to 10% of the increased stiffness can be explained by the fact that the outerwood of the pruned trees is free of knots, as TOF measurements are little affected by knots. Thus, it is not known what causes the increase of outerwood stiffness in the pruned trees. One possible explanation could be a smaller microfibril angle (MFA) in the S2 layer of the outerwood cells, which would cause a significant increase in stiffness. Thinning operations decreased the outerwood stiffness by up to 8%.

In small *Eucalyptus nitens* and *Pinus radiata* logs, which had branch nodes and nodal whorls at specific locations, MOE calculations (using the resonance technique) based on different harmonics gave different results. This indicates that defects do interact with acoustic waves.

Acoustic tests on laminated beams with artificial defects (holes filled with dowels) at specific locations also had a significant impact on the MOE. Moreover, it was evident that the damping ratio (evaluated from the Q- factor) of the beams increased with increasing diameter of the holes.

However, it was found that holes in laminated beams decreased stiffness while branch nodes and nodal whorls increased stiffness. This shows that relatively small defects, occupying a small volume of the beam, have an impact on acoustic measurements. It is not appropriate to base the MOE calculation on a single harmonic, considering that different harmonics investigate different parts of the specimen.

Chapter 1: General Introduction

1.1 Aim of the study

Wood is a natural material which has been used for millennia for many purposes. Today, wood is used as a raw material for a variety of products, such as furniture, structural timber in housing, wood-based panels and pulp and paper.

Wood shows large variation in its properties. The properties of wood mainly depend on its cellular, anatomical and chemical characteristics (Zobel and van Buijtenen, 1989). These properties determine the behaviour of wood during processing; moreover, they have a major impact on the features of the final product and as a consequence, the value of the wood mainly depends on its properties. Different sectors of the wood industry demand wood that has different specific requirements. Therefore it is crucial to sort or to grade wood according to its properties. Log grading systems around the world are still based on length, diameter, straightness and branch size which are all external assessments and provide almost no information about intrinsic wood properties. However, the result of such grading and sorting systems is often not sufficient, neither for forest owners, nor for the wood industry and their customers. Only with the most accurate information is it possible to achieve the greatest value recovery from the logs and to use the raw material efficiently and effectively (Xu and Walker, 2004). Therefore more consistent methods have to be used to assess wood, in particular the intrinsic properties of logs and timber. During the last decade a reasonable amount of effort has been made to develop methods and tools for the non-destructive assessment of wood properties in logs and timber and also in standing trees. One promising area is acoustics.

This thesis covers three acoustic studies:

- Chapter 3 examines the use of the time of flight (TOF) method to evaluate the outerwood stiffness of young *Pinus radiata* tress which have received various pruning and thinning methods.

- Chapter 4 discusses the resonance method applied to small *Eucalyptus nitens* and *Pinus radiata* logs. Acoustics is a relatively new method to assess wood properties, and there may be uncertainties in using these recently developed acoustic tools. Branches and nodal whorls may have an impact on the acoustic behaviour of wood, although the general opinion is that acoustic waves, which roughly match with the size of the sample, are not affected by disturbances that are much smaller than their wavelength.

- Chapter 5 explores measuring various acoustic parameters in an engineered wood product which has a controlled degree of inhomogeneity. The impact of artificial defects, introduced at specific locations of the test specimens, on the elastic and damping properties is examined.

In Chapter 4 and 5 it is demonstrated that the resonance method can give different results when testing the same specimen under the same test configuration.

1.2 Wood characteristics and properties

Wood is a complex and highly ordered material. The overall performance of wood can be best described by its characteristics and properties. Often the term wood quality is used instead. When discussing wood quality one has to take into consideration that wood is used for many purposes and itself is highly variable. Different end products demand different types, or qualities, of wood. Therefore it is reasonable to describe wood by its characteristics and/or properties.

According to Walker and Nakada (1999), wood characteristics relate to the "elemental" cellular and chemical components of wood (for example. density, cell length, cell diameter, cell wall thickness, microfibril angle and content of (hemi-) cellulose, lignin and extractives). In contrast, wood properties refer to features of wood that affect its processing (for example. stability, machinability). Zobel and van Buijtenen (1989) state that many wood scientists refer to wood properties as "the cellular, anatomical, and chemical characteristics of the wood within and among

trees". A good general definition of quality has been given by Gibson (1980, cited in Zobel and van Buijtenen 1989): "quality is the totality of the attributes of a product which contributes to the satisfaction of needs".

1.2.1 Basic characteristics

Wood structure

Wood is a complex, inhomogeneous and anisotropic material based on hierarchical structure with cellulose microfibrils and lignin as its most basic components. The proportions of the components show large variation between and within species, stand and also within a single tree. Typical composition of coniferous wood and hardwood is shown in Table 1-1.

Table 1-1: Typical composition of conifers and hardwoods (Walker, 2006)

Components	Conifers	Hardwoods
Cellulose	42 ± 2%	45 ± 2%
Hemicellulose	27 ± 3%	30 ± 5%
Lignin	28 ± 2%	20 ± 2%
Extractives	3 ± 2%	5 ± 3%

Considering the hierarchical structure of wood at a macroscopic level, the tree trunk is composed of millions of individual cells. The vast majority of the cells are aligned more or less parallel to the axis of the stem. The cells themselves have a length to width ratio of approximately 100:1 for conifers and 50:1 for hardwoods. They consist of a double-layered cell wall (a very thin primary layer (P) and the secondary layer (S)) which encases the cell lumen. The cells are "glued" together by the middle-lamella which mainly consists of lignin. The cell wall itself is made of millions of polymeric cellulose chains forming crystalline microfibrils which are surrounded by hemicelluloses (non crystalline) and embedded in amorphous lignin. The secondary cell wall is divided into three main layers, each of which shows a characteristic

alignment (microfibril angle) of the microfibrils. The dominant layer is the S2 layer, in which the microfibrils are aligned at an angle of approximately 15-30˚ from the longitudinal axis of the cell. Hence, the configuration of the S2 layer plays a major role in terms of wood properties and characteristics.

The wood structure of conifers is much simpler compared with the structure of hardwoods. The wood of conifers consists of up to 95% of vertical tracheids, up to 5% horizontal ray cells and some resin canals. The more complex wood of hardwoods has short and large diameter vessel elements, tracheids, longitudinal parenchyma and it has rays with differing types of cells (Macdonald and Franklin 1969). The distribution of the vessels has a major impact on the properties of hardwoods. Within the hardwoods diffuse porous wood, where the vessels are evenly spread across one growth ring, may be distinguished from ring porous wood where the vessels are laid down almost side by side in the early wood band of each growth ring.

Density

Wood density is the oldest and most widely used criterion for the evaluation of wood. According to Bamber and Burley (1983) “it has a considerable influence on strength, machinability, conversion, acoustic properties, wearability, paper yield and properties and probably many others”.

Owing to the fact that the density of cell wall material of any wood species is almost constant (1530 kg/m^3), wood density is mainly determined by the amount of cell wall material in relation to the voids. The amount of moisture in the wood has to be considered when the density is determined. Density can therefore be expressed as: green density, oven-dry density, air-dry density or basic density. The latter is a standardised method that gives a precise measure of the ratio of water saturated cell wall material to void space.

In conifers, the growth rings have high density latewood and low density earlywood zones. The density variation within growth rings can be extremely high for some

species such as Douglas fir, where the ratio between earlywood (thin-walled cells with large lumen) and latewood (thick-walled cells with small lumen) is around 1:5. In radiata pine the difference in density between earlywood and latewood is much smaller (1:1.8), which can be considered as beneficial in terms of machinability (Harris, 1981). In conifers, a reduced percentage of latewood can partly explain low density (Smith, 1980).

A study by Cown et al. (1991) on radiata pine showed that the trend for density variation within trees is that density increases radially with distance from pith and decreases vertically with increasing distance from the base of the tree.

Within the hardwoods the density contrast between earlywood and latewood is greatest in ring porous trees. In diffuse porous trees the difference is less pronounced, although the wood tissue produced early in the growing season is of lower density than the thick-walled latewood tissue.

Microfibril angle

Microfibril angle (MFA) is defined as the deviation of the microfibrils from the long axis of the cell. The MFA of conifers in the first growth rings around the pith can be as high as 45˚. It then decreases rapidly across the next 10 or so growth rings before stabilising at an angle between 5˚ and 20˚ degrees (Megraw et al., 1998). However, hardwoods usually have a smaller initial MFA (20˚ to 25˚) near the pith compared with softwoods (Fang et al., 2006). Butterfield (2003) reports that the axial stiffness of the cell is inversely related to the mean MFA of the S2 layer. A five-fold increase in axial cell wall stiffness for *Pinus radiata* can be attributed to a decrease of the MFA from 40˚ to 10˚ (Cave, 1968).

Stiffness

Stiffness is defined as the resistance of an elastic body to deflection or deformation under an applied force. The Young's modulus of elasticity (MOE) can be thought of as a measure of the stiffness of a material. The stiffness of a structure is of principal importance in many engineering applications. In recent years stiffness has been more frequently used to describe the mechanical properties of wood, especially the properties of structural timber (Burdon et al., 2004). The MOE of wood can be determined by static bending tests but it can also be estimated by using acoustic techniques.

Studies on radiata pine by Tsehaye (1995) and Xu (2000) revealed that stiffness varies in both the vertical (bottom to top) direction and the radial direction (pith to bark). The microfibril angle is thought to be the most important factor affecting stiffness

1.2.2 The concept of juvenile and mature wood

In a broad sense, juvenile wood is produced at a young cambial age. Thus it can be found around the pith of the stem (Barnett and Jeronimdis, 2003). Cown (1992) gave a "New Zealand" definition for juvenile wood which is "the wood within the 10 rings of the pith". Consequently the wood outside the 10^{th} growth ring should be called mature wood. However, it is not possible to draw an exact line of demarcation between juvenile wood and mature wood. The region where the wood starts to mature is often referred to as transition wood (Zobel and Sprague, 1998). In literature the term "corewood" is sometimes used instead of juvenile wood and mature wood is often replaced by the term "outerwood". The wood characteristics and properties of juvenile wood can be very different from those of mature wood, especially in conifers. Probably the most important feature of juvenile wood is that it shows high variation in its characteristics and properties. In general it can be assumed that juvenile wood, in comparison with mature wood has the following features: lower density owing to thin-walled cells; high percentage of reaction wood (compression wood with a higher

lignin content and shorter tracheids in gymnosperms, and tension wood with a higher cellulose content in angiosperms); a larger microfibril angle causing low stiffness and higher longitudinal shrinkage; high grain spirality; and relatively high moisture content (prior to heartwood formation) (Zobel and van Buijenten, 1989). Differences between corewood and outerwood lead to a well known radial (pith-to-bark) change of some wood properties, especially for softwoods like *Pinus radiata* or *Pinus taeda*. This is reflected by increasing stiffness, strength and stability from pith-to-bark. All of these wood properties are crucial for structural timber (Burdon et al., 2004).

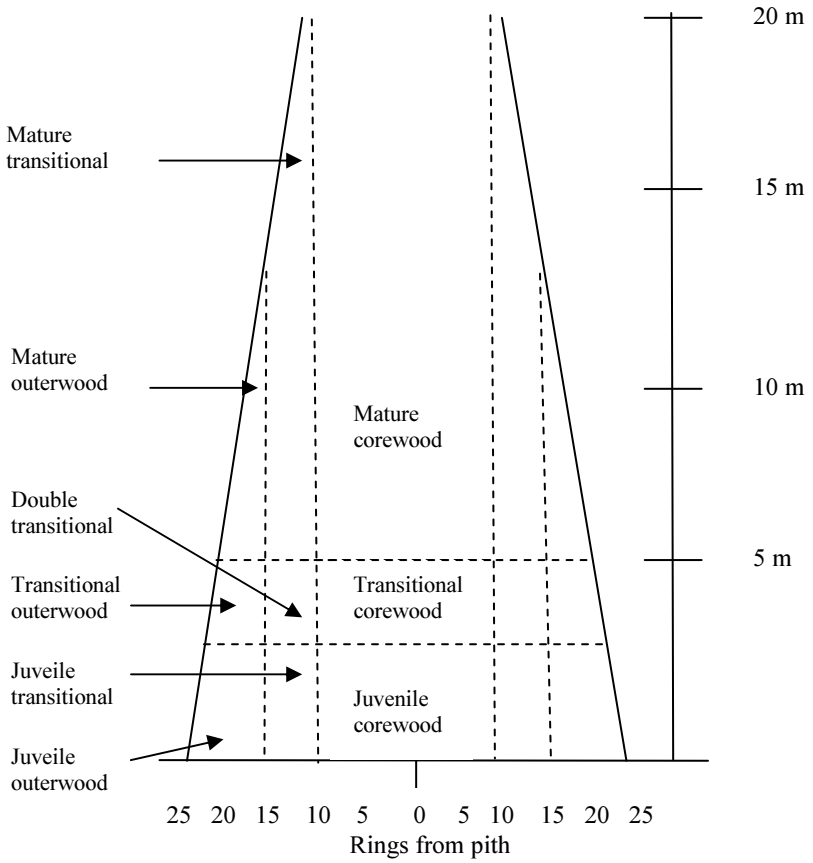

Figure 1-1: Schematic section of a typical P. radiata stem showing new categorisation of wood zones. (adapted from Burdon et al., 2004).

Burdon et al. (2004) have suggested a more accurate definition of juvenile wood, and redefined juvenile wood as "the wood near ground level of trees grown from seed, irrespective of ring number from the pith". Moreover, Burdon et al. (2004) divided the

stem in a new two-way classification of wood zones (Figure 1-1). This includes a radial progression from corewood to outerwood and a vertical progression from juvenile to mature wood. The authors argue that their new classification better matches the well-established botanical concept of maturation.

A study by Xu and Walker (2004) on 62 *Pinus radiata* trees showed that the wood with the lowest stiffness is found in the centre of the butt log (Figure 1-2). One reason for this is probably the high microfibril angle near the base of the tree. Also a significant stiffness gradient is still evident in the first, second or third log. It also clearly reveals that the poorest quality wood is laid down in the very early or juvenile years in the life of the tree which might justify or support the new classifications made by Burdon et al. (2004).

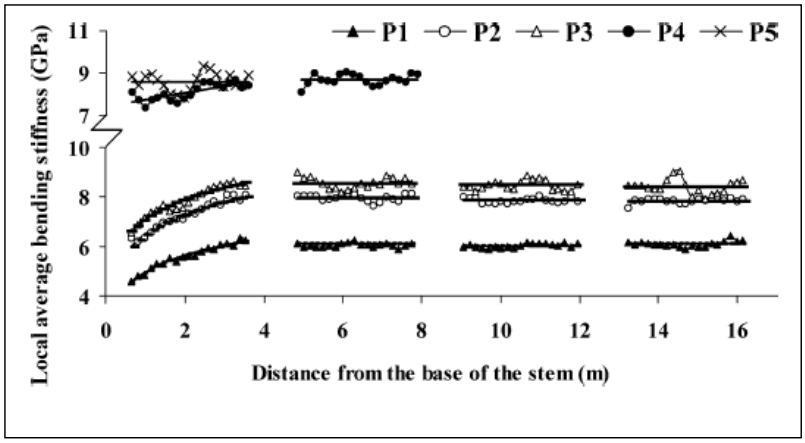

Figure 1-2: Bending stiffness according to the distance from the base of the stem and the distance from the pith. P1, P2 … refers to the numbering of boards which have been stress graded. P1 boards are centre boards while P4 boards are cut from the periphery. (adapted from Xu and Walker 2004).

For tree growers it is of great interest to know more about the transition process from juvenile wood to mature wood in conifers. They are interested in minimising the amount of juvenile wood in their stands which would yield higher prices for their logs. The situation is even more important in short rotation plantations, where the percentage of juvenile wood is much higher compared to stands with longer rotation periods.

Studies of Larson (1963) and Fabris (2000) suggest that the location of the crown is an important factor which affects the quality and quantity of wood produced along the stem. It is assumed that juvenile wood is produced within the crown and mature wood below. This assumption is based on the fact that growth regulators (hormones) produced by the foliage and the apical meristem may inhibit the formation of mature wood. Thus, while those growth regulators move downwards to the base of the tree they become less effective and consequently mature wood can be produced. However, this issue is controversial and studies of Sundberg et al. (1993), Funada et al. (2001) or Savidge (2001) did not corroborate this lowered effect of plant growth regulators below the crown.

Gartner et al. (2002) tested the assumption that the bole of softwoods produces juvenile wood within the crown and mature wood below. They compared growth ring areas and widths and wood density components of the outer three growth rings in disks sampled from various vertical positions of 34-year-old Douglas-fir which had a wide range of heights from base to live crown. Gartner et al. found no statistically significant difference at p= 0.05 for any of the factors studied supporting the hypothesis that the formation of mature wood is dependent on the position of the green crown.

1.3 *Pinus radiata* D.Don

1.3.1 Taxonomy and nomenclature

Pinus radiata D. Don. belongs to the subgenus Pinus (syn. Diploxylon) (‘hardpines’), section Pinus. Within that section it has recently been reassigned, along with the closely related *Pinus muricata* and *Pinus attenuata*, to a new subsection called Attenuatae van der Burgh (Price *et al.*, 1998 and Millar, 2000). *Pinus radiata* hybridises naturally with *Pinus attenuata*. These three species are commonly referred to as the California closed-cone pines. *Pinus radiata* has three varieties: var.

cedrosensis, var. *bianta* and var. *radiate.* Some other common names for Pinus *radiata* are Monterey pine, remarkable pine and insignis pine. California pine is also a trade name.

1.3.2 General description

Pinus radiata is an evergreen tree of 20-35 m height and a DBH of 40-100 cm when growing in its natural area of distribution. These figures are highly dependent on stocking and site fertility as both play a major part in the growth pattern. However, exotic plantings can reach heights of 55 m and diameters of up to 250 cm. The wood of *Pinus radiata* is of low to medium density and its mechanical properties are comparable to other common softwoods, although the properties of *Pinus radiata* are highly influenced by factors like genetics, environment, age and silviculture.

1.3.3 Geographic Distribution

Natural Distribution

The natural latitude range limits of *Pinus radiata* from north to south are 37˚N to 28˚N. It occurs naturally only in five distinct populations. Three of them are on the mainland along the fog belt of the central Californian coast (Año Nuveo, Montery and Cambria) at altitudes ranging from sea level to 420 m, and the other two are found off the coast of the Baja California Peninsula, Mexico on Guadalupe Island and Cedros Island at altitudes ranging from 300-1200 m. All these natural habitats represent a special and highly localized variant of the dry to mesic Mediterranean climate which is caused by a cold ocean current and characterized by mild summer temperatures, rainfall of 700 mm or less mainly during winter and sea fogs during the mainly rainless summer period. These fogs provide a crucial amount of precipitation in the form of fog drip. Another very distinct feature is that *Pinus radiata* does not grow naturally more than 8 km inland (Libby et al., 1968 and Forde, 1966).

Locations of introductions

The main countries where *Pinus radiata* has been planted on a massive scale are New Zealand and south central Chile (approx. 1.5 million ha each). There are also considerable plantations in southern Australia (> 700.000 ha) and northern Spain (approximately 220000 ha). Other significant plantations have been established in South Africa, Ecuador Argentina and Italy. This comes to a total *ex situ* plantation area of more than 4 million ha, which is more than 99.7 % of the global estate (Lavery and Mead, 1998).

1.4 *Eucalyptus nitens* Maiden

1.4.1 Taxonomy and nomenclature

Eucalyptus is a diverse genus of trees within the plant family Myrtaceae. A new formal classification of the genus Eucalyptus was recently developed by Brooker (2000). It includes 13 subgenera in the concept of the whole genus *Eucalyptus*, six of them consisting of only a single species. Within the 13 subgenera are more than 700 species, most of them native to Australia. Only a few species are found in adjacent parts of New Guinea and Indonesia and one as far north as the Philippines. *Eucalyptus nitens* belongs to the distinctive group of eucalypts that are characterised by very remarkable, large, sessile, glaucous juvenile leaves to the tall sapling stage, seen most prominently in *E. globulus* (Brooker, 2000). Some other common names for *Eucalyptus nitens* are shining gum and silvertop.

1.4.2 General description

Eucalyptus nitens is a fast growing hardwood tree that can grow to a height of 70 m. The bark of *Eucalyptus nitens* is smooth throughout or has a thin zone of rough grey bark in the basal metre of the trunk. Further up the trunk the predominantly smooth bark is pale grey to greenish-grey but with patches of white, cream or pale brown with some horizontal black scars. The usually straight grained wood of *Eucalyptus nitens* has an air-dry density of approximately 700 kg/m^3. The medium textured heartwood is of straw colour with pink or yellow tints (Bootle, 2005). The wood is used for general building construction, flooring, joinery, panelling, furniture and pulp.

1.4.3 Geographic Distribution

Eucalyptus nitens is native to the high altitude country on both sides of the Victoria-New South Wales border and the mountain areas of eastern Victoria, Australia. Most eucalypts will grow rapidly even in poor soil conditions. Together with many other eucalypt species *Eucalyptus nitens* has been introduced to many parts of the world, notably USA (California), Chile, Brazil, Morocco, Portugal, South Africa, Israel and Spain (Galicia).

Chapter 2: Introduction on Acoustics

Acoustics can be used for non-destructive testing of wood. Ross and Pellerin (1994) state, that "nondestructive materials evaluation is the science of identifying physical and mechanical properties of material without altering its end-use capabilities". Acoustic techniques can be applied to get a fast estimation of the elastic and damping properties of wood. The material's elasticity can be described by the relation between stress and strain. In the elastic range (the linear region between stress and strain) Hooke's law relates stress and strain by the means of the MOE:

$\sigma = E\varepsilon$

where;

σ= stress, E= Modulus of elasticity and ε= strain.

Damping reduces the amplitude of oscillations in an oscillatory system by dissipating vibration energy into heat. Damping is often characterised by the loss factor which is defined as the ratio of lost energy to the vibratory reversible energy during one cycle of vibration (Ouis, 2002).

The dynamic properties of solid materials are often frequency- and temperature-dependent. Unlike many other solid materials, the damping and elasticity properties of wood become frequency-dependent at a few kHz. It was found that the dynamic MOE tends to increase with frequency. Ferry (1980) reports that the curve of frequency variation of the MOE of organic polymers passes a turning point at about the same frequency as when the loss factor goes through a maximum. Thus, it can be assumed that elastic and damping properties are dependent on each other (Ouis, 2002).

Areas where acoustics can be applied are:

- Defect assessment in sorting and grading of wood and timber
- In-place assessment of wooden members
- Health monitoring of trees.

2.1 Wave propagation in wood

Wood is regarded as an orthotropic solid having three mutually perpendicular planes of elastic symmetry: longitudinal, radial and tangential (Bucur, 1996). Consequently the propagation of sound in wood is much more complex than in isotopic materials. Wave propagation in isotropic materials should be considered first. Longitudinal waves, where particle motion is along the propagation direction can be distinguished from shear waves or transverse waves where the particles vibrate perpendicularly to the propagation direction. However, in wood, longitudinal and transverse waves can also travel out of their principal symmetry direction. Surface waves, which can propagate in any direction, are found in isotropic and anisotropic materials.

The mathematics for anisotropic material like wood are more complex than those of isotropic materials. Nevertheless, it is possible to apply acoustics in anisotropic materials. There are considerable differences in propagation speed of acoustic waves along these directions; for example, the velocity in the longitudinal direction is five times greater than in the radial direction (Harris and Andrews, 1999).

To meet the requirement of homogeneity, the wavelength must have a greater magnitude than the inhomogeneity of the sample (Feeney et al. 1996).

2.2 Acoustics used to determine the elastic properties of wood

Using acoustic waves to determine the elastic properties of the tested material by measuring the velocity of the waves is a well-established science. In the 1950s Jayne (1959) conducted one of the first acoustic studies in wood by assessing the dynamic stiffness of clearwood samples of Sitka spruce, using transverse vibration techniques. His testing was motivated by interest in the fundamental proposition of NDT of wood. His assumption was that “the energy storage and dissipation properties of wood materials which can be measured by various NDT techniques are controlled by the

same mechanisms that determine the static behaviour of such material" (Ross and Pellerin, 1994).

The most common way to introduce acoustic waves into logs or lumber is a light tap with a hammer. To generate compression waves that travel along the length of the specimen, one of the cut ends of the specimen has to be excited. From the point of impact the waves start to spread out into the specimen and only two propagation speeds are evident: the dilatational speed of compression and the shear speed of distortions. There are multiple interferences and reflections of these two wave types within the boundary conditions of the sample; however, after the travelling signal has passed a certain distance it can be identified as a plane wave if the lateral dimensions of the rod are small in comparison to its length (Andrews, 2002). The way a sound wave (stress wave) propagates through a body is correlated with the body's intrinsic properties. By measuring the velocity of the travelling wave and by using the one-dimensional wave equation:

$$MOE = E = V^2 \times \delta$$

it is possible to calculate the dynamic MOE where;
MOE or E (Pa) stands for the Modulus of Elasticity, V (m/s) for velocity and δ (kg/m³) for the density of the wood.

However, this equation is idealized for elastic materials shaped as a long slender rod (Buccur, 1995). In theory the one-dimensional wave equation is valid for uniaxial stress. This is not the case when wood is excited, since there is radial inertia (kinetic energy of the material that flows radially outward under compression); nor is it the case when the waves interact with the external surfaces (free surfaces) of the specimen (Meyers, 1994). In wooden materials the application of the one dimensional wave equation might also be affected by various factors, such as knots, grain angle, moisture content, wood temperature, as well as by the materials dimensions and geometric form.

2.3 Factors affecting stress wave-transit time in timber

According to Gerhards (1982), who summarized the results of previous studies in this area, as a rough approximation, the propagation speed of stress waves decreases by 1% when the moisture content increases by 1% within the hygroscopic range. Further, a rise in temperature by 1˚ Fahrenheit (between 0 and 200˚ Fahrenheit) causes a drop in the propagation speed of approximately 0.05% for timber at moisture content of 12%. This temperature dependence of stress wave velocity in timber is also affected by the moisture content. With increasing moisture content the influence of temperature on the stress wave velocity becomes stronger.

As summarised by Gerhards (1982), various studies showed that the grain angle has a major impact on the velocity of stress waves. Sound travels along the grain about three times faster than perpendicularly to the grain. The velocity decrease is most pronounced within the first 30˚ from the longitudinal direction (probably following Hankinson's formula).

The effect of knots on the propagation speed of stress waves in timber is controversial. It is widely accepted that knots and distorted grain surrounding knots have at least some effect on the velocity of stress waves. Burmester (1965) noticed a difference of 4% in the propagation speed of stress waves between clear wood and knotty wood. However, experiments by Gerhards (1982) showed that the velocity in knot-free wood was only 1% higher than in knotty wood: these tests were conducted on a beam of 2 by 6 inches and a length of 2.5 foot containing only one knot. After testing the knotty beams, a clearwood sample of 2 by 2 inches was cut out and tested again. Gerhards (1982) investigated the shape of the wave front as it passed knots. He observed that the wave front did not remain a planar front when travelling through or around knots. Within the area that is influenced by the knot, the velocity was reduced, but once the knot was passed, the wave front reformed as a planar front.

2.4 Acoustic methods

Wood can support a variety of wave types and because of the fact that waves can only reveal things that are comparable to their wavelength, it is important to generate the right wavelength when looking at particular properties (Bucur, 1996). Many methods using different wavelengths have been studied and are used on standing trees, logs and wood products to measure elastic properties or to reveal defects. The most common are: the stress wave technique, Acoustic Emission (AE), Acoustic Ultrasonic (AU), Ultrasonic Techniques and Acoustic Microscopy (Buccur, 1996).

The common opinion is that high frequency waves have to be used to detect defects like knots or resin pockets. So-called Ultrasonic techniques use vibrations similar to sound waves but at much higher frequencies (> 20 kHz) (de Oliveira et al., 2002). A major problem of ultrasonic waves in wood is that they are strongly absorbed in green wood. However, this problem is less evident in dry wood.

In this study, the stress wave technique, operating with relatively low frequencies (audio range), is used to calculate the elastic properties (MOE) of young *Eucalyptus nitens* and *Pinus radiata* trees and the elastic and damping properties of laminated beams. There are basically two distinct acoustic methods that can be applied to assess the MOE: the time of flight (TOF) and the resonance method.

2.4.1 Time of flight method

The time of flight method, also known as the transit time method or stress wave timer, simply measures the travelling time of the wave between two sensors that are driven into the sample. A mechanical or ultrasonic impact is used to launch a longitudinal vibration into the sample, and the time delay of the signal over a known distance between the sensors allows the calculation of the velocity of the stress wave. Thus, the calculation of the velocity is based on only one observation. To overcome this problem the measurement can be repeated several times to obtain more reliable

results. The TOF method has been applied to standing trees, logs, timber and wood-based panels.

2.4.2 Resonance method

The resonance method can only be applied when the sample has two cut ends, thus it is not suitable for measuring MOE in standing trees. A stress wave is introduced at one end of the sample from where it travels forwards and backwards between the two cut faces of the log introducing standing waves. The signal is usually picked up from the other end of the sample using a microphone or an accelerometer.

The resonance method provides more information and also gives more reliable results than the TOF method, which is mainly due to the fact that the velocity of the wave is calculated on up to several hundred passes through the sample (Grabianowski, 2003). Resonance methods produce standing wave patterns called harmonics or modes, which match the size of the sample.

Standing waves are formed as the result of the perfectly timed interference of two waves passing through the same medium (Kane and Sternheim, 1988). A standing wave pattern is not actually a wave; rather it is the pattern resulting from the presence of two waves (sometimes more) of the same frequency moving in opposite directions within the same medium. This study focuses on compression waves, thus they are discussed in more detail than, for example, bending waves.

A compression wave can be described as a disturbance carrying energy from one location to another. A compression wave has characteristics just like any other type of wave, including amplitude, velocity, wavelength and frequency. The wave length of a compression wave equals the length between two maximum compressions (Figure 2-1).

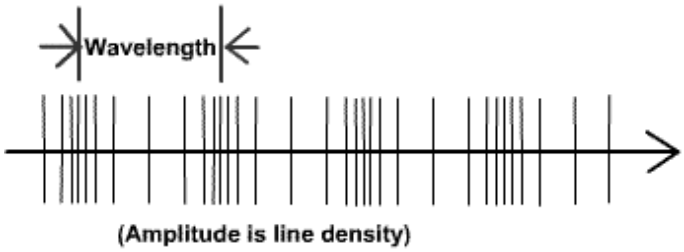

Figure 2-1: Wavelength and amplitude of a compression wave

A blow by a hammer at one end of a specimen (log or beam in this study) will force the particles close to the impact to move in the direction of the impact. As a consequence, the adjacent particles are also pushed in that direction, creating an area of high compression which proceeds to pass through the specimen. Meanwhile, the particles at the impact end will vibrate back. It is the elasticity of the medium which controls the return of the displaced particle towards its equilibrium position. Due to the inertia of the particle the particle will pass its equilibrium position and thereby pulling particles apart, creating a low pressure region. This low pressure area then follows the high pressure area. Thus, a compression wave, where particles are pushed back and forward parallel to the direction of the transmitted energy, consists of areas of high compression and areas of low compression (rarefactions). When the wave front hits the other end of the specimen it is reflected and starts to interfere with the waves coming from the opposite direction. If it now happens that the compression of one wave meets up with the compression of a second wave, the pressure at that particular location will be even greater. Such a scenario is called constructive interference. Constructive interference also occurs when two low pressure areas travelling in opposite directions meet and thereby create an area of even lower pressure. Locations where constructive interference continually occurs are known as antinodes. Antinodes are therefore locations where the specimen undergoes maximum positive and negative change in pressure.

The opposite of constructive interference is destructive interference, which is a result of the interference of compression and rarefaction. Particles at a location where this

takes place will not be pressurized, as the tendency of compression to push particles together is cancelled out by the tendency of rarefaction to pull particles apart. If destructive interference continually occurs at the same location, then this region will form a node. A standing wave pattern always consists of an alternating pattern of nodes and antinodes. However, once a medium starts to vibrate, different standing wave patterns, called harmonics, can be obtained (Halliday, Resnick and Walker, 1997). The wave pattern with the longest wavelength that fits into a medium (in this study, a log or a beam) is referred to as the fundamental mode and has a wavelength of twice the log length. The next possible pattern, called second harmonic or first overtone, which fits inside the log has a wavelength that is equal to the log length. The distribution of the nodes and antinodes along the specimen is of great interest.

The distribution of pressure and displacement within the specimen

When a log is put into longitudinal vibration (excited by a hammer blow at one end) and not clamped down at its ends, it will show areas of maximum positive and negative displacement (antinodes) at either end. However, in terms of pressure there will always be a node at both ends of the specimen. The first harmonic has an antinode for pressure at midspan. This means that two compression waves meet at midspan in a way that constructive interference occurs. Exactly at midspan, the particles will not be displaced at all. They will stand still. To simplify the situation one could divide the specimen in two parts of equal length. When two compressions meet at midspan they will travel through each other and pressurise the particles to a maximum, or in other words pushing the two parts of the specimen together. When now two rarefractions meet at midspan they will pull the particles apart causing maximum negative pressure, or pulling the two parts of the specimen apart. Thus the specimen will experience maximum force (stress) at the cross section at midspan, which is the imaginary boundary between the two parts of the specimen. Hence the largest internal forces in the specimen always appear where the specimen has nodes for displacement or antinodes for pressure. The pattern for antinodes and nodes in terms of pressure and displacement for the first three harmonics is illustrated in Figure 2-2.

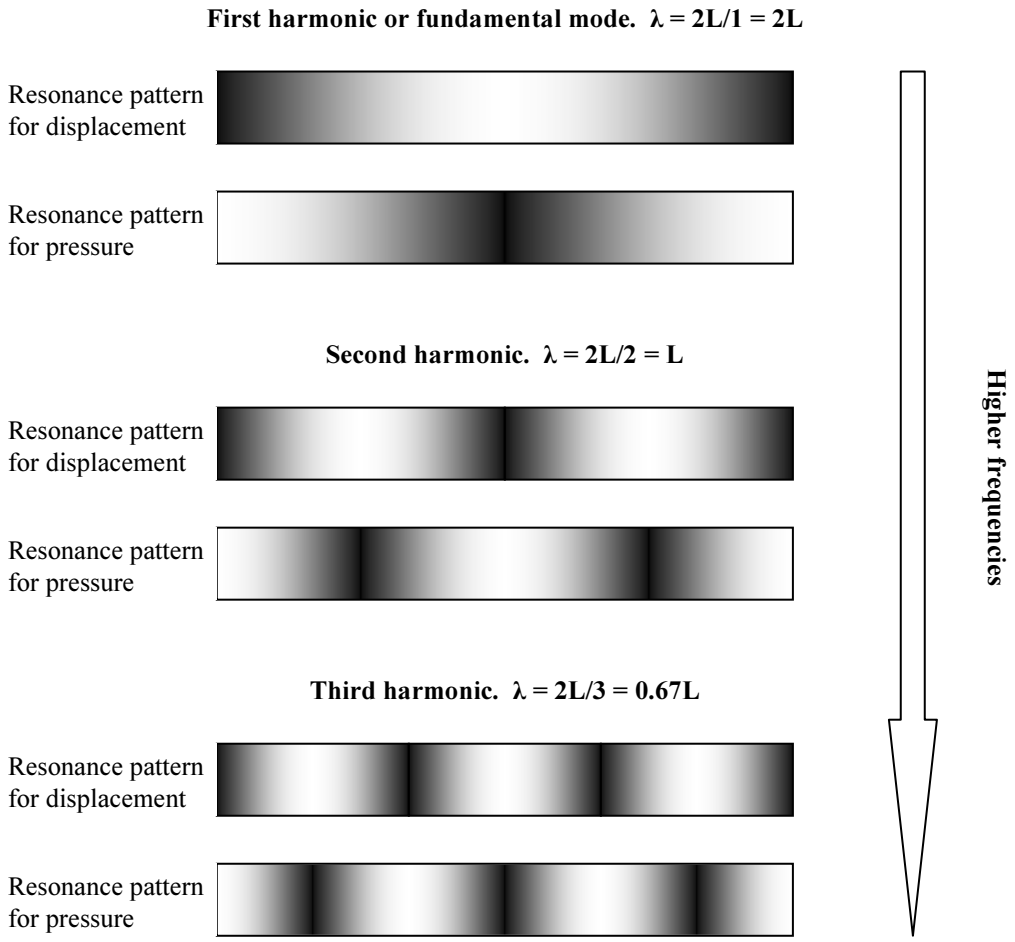

Figure 2-2: Resonance pattern for the first three harmonics. The dark areas represent anti-nodes and the lighter areas nodes.

The wavelength of the *n*th harmonic can be calculated by the equation:

$$\lambda_n = 2\ L/n$$

and the corresponding frequencies are found from:

$$f_n = (n/2L) \times V$$

where;
V = velocity, *f* = frequency, λ = wavelength and L= (log) length

A vibrating log in which compression waves are travelling forth and back can be described by a set of masses and springs. The positions where the log has antinodes for displacement refer to a mass. The masses are connected with springs (Figure 2-3).

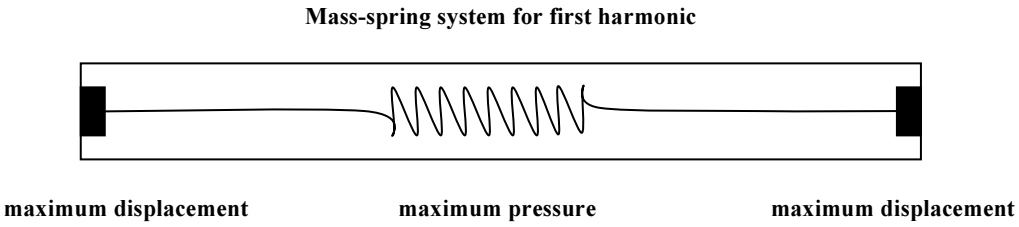

Figure 2-3: Mass-spring system of a log for the 1st harmonic as sensed by acoustics.

Applying Hooke's law and using the definition of Young's modulus with the definitions of stress σ = *Force/Area* and strain ε= *Δl/l*, this becomes:

$$\frac{F}{A} = E\frac{\Delta l}{l}$$

Therefore, in tension or compression the force on an object is proportional to its elongation:

$$F = k\Delta l$$

where k is the spring constant which is defined by:

$$k = \frac{EA}{l}$$

From the definition of k it follows that the spring constant can be changed by altering the cross-sectional area. An increase of the cross-sectional area will increase the spring constant.

2.4.3 TOF method versus resonance method

Andrews (2002) compared acoustic speeds measured by the TOF and the resonance method. Observations in the past have shown that there is some discrepancy between both methods, especially in short samples. Once a wave is introduced into an elastic material only two propagation speeds can be found: the dilatational speed of compression and the shear speed of distortions. Andrews' (2002) examinations

showed that there is a provable difference in velocity between the TOF and the resonance method when measuring the same logs. The TOF speed was significantly higher (approximately 1.25 times) than the resonance speed. The time that is needed to travel through the log (during a single pass) was calculated based on the multi pass resonance method. Looking only at the first pass between both ends, Andrews observed that there was a small amount of energy which was arriving earlier and thereby stopping the time measurement. However, the explanation for this is that some energy travels faster than the main wave front. This weak signal, called incremental speed, travels in a straight line from one end to the other end of the sample without being reflected from the edges of the sample (Andrews, 2002). However, this faster travelling energy dies away inversely with distance squared and the measurable wave becomes a plane front. This is the reason why this phenomenon can be ignored when acoustic velocity is measured by resonance methods.

To obtain the right data from TOF tools, it is crucial to distinguish between the fast incremental and the slower propagation speed of the developing plane wave. Thus, the sensitivity and the setting of the detecting probes have a major impact on the performance of the tool. The influence of the incremental speed is highest in short samples. The reason is twofold: as already mentioned, the incremental speed dies away inversely with distance squared; and secondly the time difference between the incremental speed and the “main” wave is relatively higher over short distances. According to Andrews, the consequences of this are that acoustic velocities based on TOF measurements are often overestimated by a factor up to 1.3, especially in relatively short samples with a high diameter to length ratio. The following equation can be used to avoid an overestimation of the MOE when measuring very short samples:

$$MOE = \left(\frac{V}{1.3} \right)^2 \delta$$

When the length is about ten times the diameter, it can be assumed that the correction factor can be neglected. However, Andrews (2002), advocates further research to verify this length to diameter ratio.

2.5 Damping properties of wood

Damping is evident in all real systems. Even in systems with small damping the system will still oscillate and the amplitude of the vibration will decay exponentially with time. In an over-damped system, no vibration will be found and after excitation the mass will return slowly to its original position. If a system is critically damped it just fails to oscillate and returns to its original time in the fastest possible time: for example, suspension systems of vehicles should be critically damped. The damping ratio compares the damping constant of the system with the critically damped case, and thereby expresses the viscous damping of the system (Smith, Peters and Owen, 1996). The damping ratio (often expressed as a percentage) for lightly damped systems is approximately half the loss factor.

There are three main factors that affect the damping properties of wood: the geometry of the sample and the material characteristics of scattering and absorption. Scattering and absorption are highly dependent on frequency, anisotropic direction and wood species (Buccur, 2005).

2.5.1 Methods to calculate damping

There are many different methods that can be applied to calculate damping. They can be divided into three groups:

- Vibration decay measurements (time domain)
- Bandwidth determination of measured modal resonances (frequency domain)
- Steady-state measurements of input and stored energy

This study does not deal with the steady-state technique which is based on the energy balance of vibrationally excited structures.

The complete dynamic behaviour of a structure can be described by its individual modes (harmonics) of vibration. The so-called modal parameters characterize the modes in a given frequency range (Brüel & Kjær, 1994). The modal parameters are:

- The resonance or modal frequency
- The damping of the resonance – the modal damping
- The mode shape

Damping can be described by many factors which are all interrelated; for example, loss factor, damping ratio, quality factor, reverberation time and logarithmic decrement.

Quality Factor method

The quality factor or Q factor is an indicator of the "quality" of a resonant system. Resonant systems respond to frequencies which are close to their natural frequency much more strongly than they respond to other frequencies. The Q factor measures the sharpness of the resonance peak, as displayed in a frequency response function (FRF) spectrum or by fast fourier transform (FFT), and therefore this method belongs to the frequency domain category. Systems with a high Q factor resonate with greater amplitude at the resonant frequency compared with systems with a low Q factor. Damping within the system decreases the Q factor.

The Q factor is defined as the resonant frequency (frequency of the peak) f_0 or f_c divided by the bandwidth between the half power point values. When the Y axis is converted to a decibel scale, the half power points are located on either side of the peak where the energy is lower by 3 dB (Figure 2-4). Decibel is the standard unit in acoustics for measuring the level or level difference. The decibel scale is based on the

ratio $10^{1/10}$ which takes account of the fact that the perception of loudness of the human ear is roughly logarithmic.

The Q factor can be calculated by the following equation:

$$Q = \frac{f_c}{f_2 - f_1} = \frac{f_c}{\Delta f}$$

where;
Q = Q factor, f_2 = the upper, f_1 = lower half-power frequency, $\Delta f = f_2 - f_1$ and f_c = frequency of the peak

The Q factor is related to the damping ratio by the following equation:

$$\xi = \frac{1}{2Q}$$

where;
Q = Q factor and ξ= damping ratio

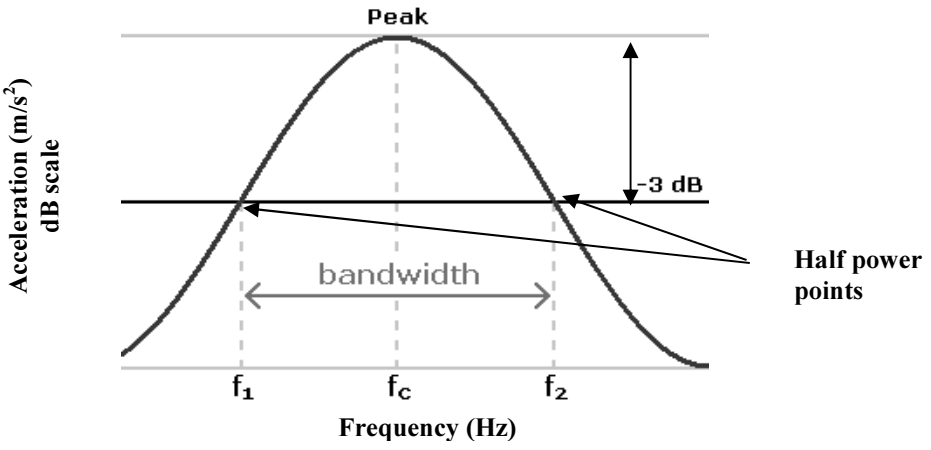

Figure 2-4: Bandwidth of a resonant peak.

The accuracy of the frequency measurements is determined by the frequency resolution of the measurement. The accuracy can be increased by reducing the

frequency range of the baseband, or making a zoom measurement around the frequency range of interest.

Whenever the Q factor was used in this study, it was given by the auto damping function of the "PULSE" unit which is based on the fundamental frequency. This automated function is very useful especially in terms of time efficiency. However, it is also possible to calculate the Q factor on subsequent harmonics. In this study calculating the damping based on the fundamental frequency was chosen. The reason for this is twofold. Firstly the fundamental frequency is usually the strongest mode in the FRF spectrum and secondly, higher frequencies receive higher damping which might affect the accuracy of the frequency measurement of subsequent harmonics.

Logarithmic Decrement

The logarithmic decrement provides a variable which tells how quickly the motion decays. It therefore belongs to the time domain measurements. It is important to point out that the logarithmic decay curve displays the whole frequency spectrum; therefore logarithmic decrement measurements give accurate results when only one resonance is present (Brüel & Kjær, 1994). Figure 2-5 shows a typical decay curve (of a homogeneous cylinder of plastic) where the time is plotted against acceleration. Logarithmic decrement can be calculated by the following equation:

$$\delta = \frac{1}{n} \log_e \frac{X_1}{X_n}$$

where;
δ = logarithmic decrement and X_1 and X_n are two amplitudes n cycles apart.

Logarithmic decrement is related to the damping ratio (ξ) by the following relationship:

$$\xi = \frac{\delta}{2\pi}$$

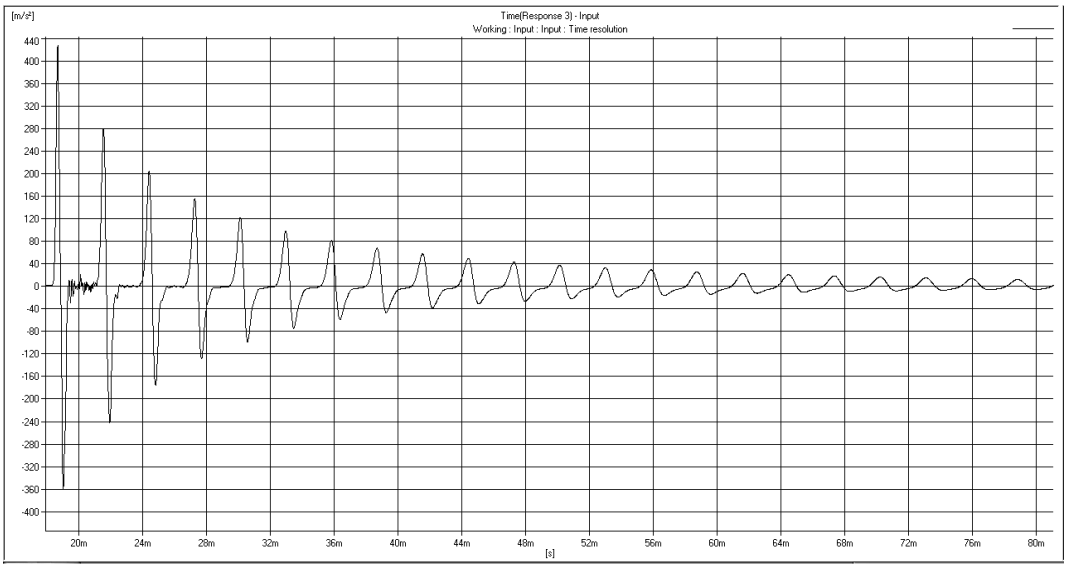

Figure 2-5: The logarithmic decay in amplitude (of accelereation) of the stress wave with time of a plastic cylinder as measured by "PULSE".

Impulse Response method

The impulse response method in its simplest form is used by woodmen to judge the quality of a tree trunk by ear. When the trunk is hit with a hammer (impulse) the vibrational response is detectable by the human ear owing to the low resonance frequencies of a log (< 20 kHz).

For accurate calculations, the specimen is excited by a short pulse (for example a hammer blow) and the impulse response is detected by means of a vibration sensor, most often by an accelerometer as in this study. Essentially, this method calculates the logarithmic decrement by isolating the signal to the fundamental frequency (or subsequent harmonics) and converting the signal to a logarithmic dB scale where the decay can be observed as a straight line (Figure 2-6). The damping can then be extracted from the measured slope of the decay curve.

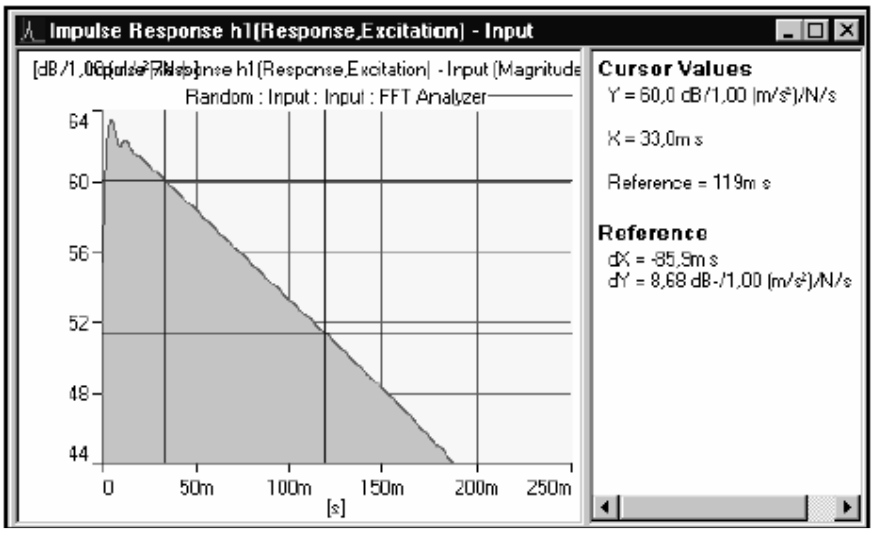

Figure 2-6 Impulse response of an isolated mode displayed on a logarithmic scale.

The decay rate σ for the isolated mode is related to the time constant τ by (Brüel&Kjær, 1999):

$$\tau = \frac{1}{\sigma}$$

The decay corresponding to time constant τ is given by the factor e^{-1}, or in dB:

$-20\log_e = -8.7$ dB.

The damping ratio ξ is related to the decay rate by:

$$\xi = \frac{\sigma}{2\pi f} = \frac{1}{\tau 2\pi f}$$

Reverberation Time method

Reverberation time measurements are usually used to assess the amount of sound absorption in a room. By using Schroeder's elegant "Method of Integrated Impulse Response" the impulse response is first squared and then integrated backwards to obtain the energy decay curve from which the reverberation time can then be calculated. However, Ouis (2000 and 2002) applied this method successfully to detect

decay and knots in logs and timber. The reverberation time T60 is the time that is required for the energy of the system to drop to one millionth of its initial value, or alternatively, the time within 60dB decay in energy or amplitude can be observed. The following equation can be used to calculate the loss factor based on reverberation time (Cremer and Heckl, 1988):

$$\eta = \frac{\ln 10^6}{2\pi f T_{60}} \approx \frac{2.2}{f T_{60}}$$

2.6 Acoustic tools used in this study

2.6.1 The TreeTap time of flight tool

The TreeTap TOF was designed by the Department of Electrical and Computer Engineering at the University of Canterbury, New Zealand. It is similar in appearance to the Fakopp 2D and uses the Fakopp piezo-elements transducers as active probes. An inert start probe (metal spike) is used to launch the acoustic impulse into the sample by a light tap with a 200g hammer. The timing of the impulse wave begins as it is detected passing the first stop transducer, and the clock is stopped when the impulse wave is detected by the second stop probe. The clock is only triggered if the received signal reaches a certain threshold (the lower and upper threshold are pre-set at 40 mV and 50 mV respectively, but they can be adjusted if necessary). Thus, actually two arrival times are measured, one at 40 mV the other one at 50 mV. This then allows back-calculation of the arrival time of the wave at the zero-voltage threshold. The acoustic velocity can be found by dividing the distance between the two stop probes by the transit time.

2.6.2 The WoodSpec resonance Tool

Woodspec was designed and build by Industrial Research Ltd. The WoodSpec tool consists of a flexible pc-based data acquisition and spectral analysis package which provides a graphic presentation of the time trace and its spectral analysis. The acoustic signal reverberates within the sample and from the frequency of the reverberation the acoustic velocity is determined using the following relationship:

$$V = 2 \times l \times f$$

where;
V stands for velocity, f for frequency and l for (log) length.

It is possible to run WoodSpec in three different modes: trigger, sweep and monitor. The trigger mode can be either used with a microphone or an accelerometer to pick up the acoustic vibrations from one end of the sample. The acoustic vibrations are launched into the sample by hitting the other end with a ball bearing on a string. The display of the trigger mode shows the amplitude of the signal with time (decay curve), and in a second window the peaks of the acoustic spectrum, which refer to subsequent harmonics, are displayed. In a third window the velocity of the acoustic signal is shown. Moreover, the frequencies of the first harmonic (fundamental mode) and detectable subsequent harmonics (overtones) are displayed. A detune factor, based on the first harmonic (fundamental mode), is calculated for subsequent harmonics. In an isotropic material the frequency of the n^{th} harmonic is exactly n times the fundamental mode. However, in anisotropic and inhomogeneous materials the overtones are usually detuned, indicating the inhomogeneity of the tested material. Swept frequency testing uses a speaker either to generate a single tone sweep or a multitone signal which penetrates the sample. An accelerometer is used as a transducer to detect and analyse the signal. The output of the sweep mode is similar to the trigger mode. The monitor mode basically was designed to check the system by determining whether or not the received signal levels match expectations.

2.6.3 The “Pulse” multi channel analyser

The “PULSE” multi-channel analyser platform, developed and distributed by Bruel and Kjær (B&K, UK), is a windows PC-based tool that uses up to nine signal channels to perform simultaneous sound-level or acceleration measurements. By using an endevco 8202 model hammer and 3608-B TEDS cubic uniaxial accelerometers (also by B&K), the transducers used and the calibration history are recorded automatically by the PULSE. These accelerometers have a reccomended upper limit of 8 kHz. These signals are then subject to a variety of real-time analytical applications, including time response, impulse response, Fast Fourier Transform (0% overlap, 4600 lines), automated damping ratio and reverberation time calculations, and up to 1/24 octave Constant Percentage Bandwidth analysis. This allows for imediate validation of the test. It facilitates a singal generator, including fixed and swept sine or dual sine waves and random pink or white noise generation. The “PULSE” has a maximum frequency limit of 26.6 kHz. Features include the ability to cross-reference signals from the impact energy and the response from the accelerometers, multipe trigger settings and a recording facility.

2.6.4 The Pundit tester

The PUNDIT 6 concrete tester, by CNS Farnell (UK), is primarily desinged for concrete testing but can also been used for testing wood. The company specifies 150-220 kHz transducers for the testing of timber specimens but these would be unlikely to be able to transmit the required distance that was measured in this study so instead a 54 kHz transducer was used. An electric pulse from the transmitting head produces a longitudinal wave which is detected at the receiving probe, which must be aligned directly opposite from the transmitter due to the high directivity of the wave. Both transducers were manually held in place with a thin layer of grease or similar conductive liquid to allow transmission and reduce fluctuation in the signal. The device is calibrated regularily (after and before each test) on a known velocity metal bar. Since it produces a very high frequency wave, relative to a low frequency

hammer impact, there is no issue with modelling the result as for infinite lateral dimensions.

Chapter 3: The Impact of pruning and thinning on young *Pinus radiata* trees

3.1 Introduction

The acoustic properties of 14-year-old *Pinus radiata* trees, growing in 12 plots (two replicates) which had been treated differently in terms of pruning and thinning, were measured to investigate whether there is any correlation between acoustic velocity in the outerwood and the pruning schedule and different thinning treatments. The impact of pruning and thinning on the basic density, DBH, tree height and taper was also examined.

3.2 Literature review

Wang et al. (2000) investigated the effects of thinning and pruning in a 20-year-old Taiwania (Taiwania cryptoerioide) trial on wood quality using an ultrasonic wave method (SYLVATEST^{TM}). In their study thinning, pruning and their interaction had a significant impact on DBH and (Table 3-1). They found that a heavy thinning treatment with no pruning increased DBH growth and non-thinning with heavy pruning inhibited DBH growth. Also the longitudinal velocity was significantly influenced by thinning and pruning and the longitudinal velocity in unthinned treatments was significantly greater compared to heavy thinning treatments.

The largest longitudinal velocity was found in the unthinned and unpruned treatment (3566 m/s), while the lowest value was found in the heavy thinned and medium pruned plots. The longitudinal velocity in the wood of unpruned and heavily pruned stands was greater than that of medium pruning. However, there was no significant impact of thinning on the transversal ultrasonic wave speed.

Table 3-1: ANOVA table of DBH, transverse velocity, and longitudinal velocity by Duncan's multiple range test. (The different letters at the right-upper corner represent 5% significant level) Wang et al. (2000).

	heavy	medium	none	F	Pr>F
DBH					
Thinning	26.29±4.71 A	23.05±5.34 B	16.69±5.53 C	115.84	0.0001
Pruning	22.28±6.2 B	21.16±5.26 B	24.08±5.89 A	12.43	0.0001
Thinning× Pruning				19.00	0.0001
Transverse velocity					
Thinning	1809.6±98.7 A	1841.8±135 A	1793.9±89.7 A	1.84	0.1646
Pruning	1779.5±1298 B	1818.9±71 AB	1853±115.4 A	3.57	0.0321
Thinning× Pruning				1.50	0.2095
Longitudinal velocity					
Thinning	3300.5±228.2 B	3346.2±292 AB	3459.3±260 A	3.51	0.0339
Pruning	3411.6±280.6 A	3245.6±246 B	3473.5±227 A	6.91	0.0016
Thinning× Pruning				0.39	0.8127

In a more recent study on the same plantation Wang et al. (2005) repeated the acoustic measurements after trees were harvested (tree age approximately 22 years) and also did mechanical bending tests to verify the results from acoustic testing. This time measurements were on air-dried beams (2.2 m long and a cross-section of 8.9×3.8 cm) and air-dried small clear specimens (24×1.5×1.5cm) cut from approximately breast height position.

Wang et al. (2005) found that higher values for dynamic MOE, static MOE and MOR were obtained in the following order: unthinned > medium thinning > heavy thinning. The trend for the pruning treatments was: medium pruning > no pruning > heavy pruning. However, not all results were statistically significantly different. For example, both the dynamic MOE and the static MOE revealed a significant ($P < 0.05$) difference between the heavy-thinned and the unthinned treatments. It is also interesting to note that the dynamic MOE was approximately 20% higher than the static MOE (the same observations were made in Chapter 4 of this study). Both studies by Wang et al. (2000 and 2005) concluded that better average qualities of lumber can be obtained from unthinned stands that have received a medium pruning treatment (3.6 m from the root base upward).

Cown (1973) examined 10-year-old radiata pine trees which had undergone severe silvicultural treatments. Of interest were growth rates and intrinsic wood properties.

Cown reported that stem diameter growth was reduced by pruning treatments, but only for a short period after treatment. Moreover, pruning increased the mean wood density by up to 7%, but this effect also tapered off after 2-3 years. The only significant change in intrinsic wood properties was a reduction in tracheid length caused by thinning.

Pape (1999) reported that thinning reduced the juvenile wood content in stands of Norway spruce (Picea abies). Zobel and van Buijtenen (1989) also pointed out that thinning generally decreases the juvenile wood content.

Lasserre et al. (2004) investigated the influence of initial stand density and genetic population on corewood dynamic stiffness of 11-year-old *Pinus radiata*. They found a significant impact of planting density ($P < 0.001$) and genetic population ($P < 0.01$) on stiffness. Plots with high initial stocking showed an MOE that was on average 1.7 GPa or 34% higher than plots with low initial stocking. The DBH was negatively related to MOE ($P < 0.01$). However the interaction of planting density and genetic population had no significant impact on stiffness. When DBH was introduced to the model as a covariance, the variation in stiffness and genetic population was reduced but still significant. According to Lasserre et al. (2004), initial stocking is a very important factor in terms of stiffness. It is of interest, that initial stocking and genetic population independently affect stiffness.

3.3 Location and site-characteristics of the Blenheim Pruning Trial

The study material came from Blenheim State Forest No 993, also known as the Blenheim Pruning Trial in the Macquarie region of New South Wales, Australia. The trees were planted in 1992 and the plots were established in November 1996. In December 1996, the plots were non-commercially thinned to 1000 stems/ha.

The elevation of the site is approximately 1160 m above sea level. The average annual rainfall is 750 mm. February and March are the driest months (average 40 mm) and

the months with maximum rainfall are June–August (average 75 mm) (Kovac et al. 1990). The average temperature in this region is 12˚C, with the warmest months in January and February (average 17˚C) and the coldest months in June–August (average 4˚C).

The Blenheim Pruning Trail lies in the Oberon landscape, which covers an extensive area of undulating to rolling low hills with elevations ranging from 980- 1336 m and slopes from 6-20%. Red earths are the dominant soil type especially on the mid to upper slopes. The geological unit is the Rockley Volcanics and Triangle Group. The parent rock code consists of andesite, tuff, grey slate, quartz and feldspathic greywacke. The topsoil of a typical red earth can be described as a dark-reddish brown, fine-sandy loam with weak structure and a pH of 6.0 at a depth of 20 cm. The subsoil gradually changes to dark-reddish brown, sandy clay loam with weak to moderate structure and a pH of 6.0.

3.3.1 Layout of the Pruning Trial

The trail is divided into 12 plots, all of which have been treated differently in terms of pruning and thinning (Table 3-2). The trial consists of two replicates (Figure 3-1).

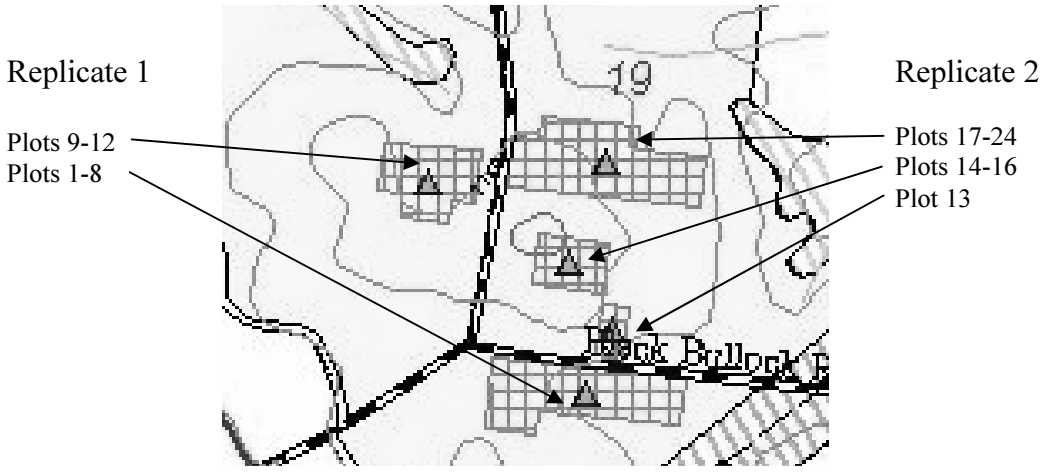

Figure 3-1: Layout of the Blenheim Pruning Trail

The trees of the rectangular-shaped plots were planted in rows running east to west. The initial stocking of the plots in replicate 1 was approximately 1000 stems/ha. The initial stocking of the plots in replicate 2 was approximately 1400 stems/ha. The difference between the replicates is due to the fact that cuttings were used in replicate 1 while seedlings were used for replicate 2. When the trees were planted it was not intended to use them for a trial study. The trial was established in 1996. At this time the plots of replicate 2 were thinned to 1000 stems/ha. The plots are aligned in a north to south direction. The plot size for the 1000 and 500 trees/ha thinning treatment plots is 0.126 ha. They are spread over 21 rows with six trees in a row. The actual measurement plot consists of 30 trees, which are surrounded by at least two rows of buffer trees (belonging to the same plot) to avoid undesirable interaction with the treatment of adjacent plots. The plot size of the 250 trees/ha thinning treatment plots is 0.186 ha, with 31 rows of six trees. These plots consist of 13 measurement trees only. The combination of treatments of the 24 plots are summarized in
Table 3-2.

Table 3-2: Combination of pruning and thinning treatments

Thinning Treatments	**Pruning Treatments**			
	Unpruned	3m green crown remaining	5m green crown remaining	7m green crown remaining
1000 Stems/ha	1000 Stems/ha (Treatment A/Up)	1000 Stems/ha (Treatment A/3)	1000 Stems/ha (Treatment A/5)	1000 Stems/ha (Treatment A/7)
500 Stems/ha	500 Stems/ha (Treatment B/Up)	500 Stems/ha (Treatment B/3)	500 Stems/ha (Treatment B/5)	500 Stems/ha (Treatment B/7)
250 Stems/ha	250 Stems/ha (Treatment C/Up)	250 Stems/ha (Treatment C/3)	250 Stems/ha (Treatment C/5)	250 Stems/ha (Treatment C/7)

Plot 7 in replicate 1 and plot 24 in replicate 2 were treated as control plots since they did not receive any treatment after they had been thinned to 1000 trees/ha in 1996. It has to be emphasised that this trial is not a spacing trial. When the plots were thinned, trees of abnormal growth form, such as double leaders, broken tops or butt sweep, were preferably cut out, and those trees showing good form retained.

In this trial, the distance between the base of the tree and the green crown was not the criterion for the pruning schedule. The green crown starts where a whorl has at least three live branches. The crucial criterion was the length of the green crown that remained after pruning. Thus, the plots had to have a certain average tree height before pruning was possible. The pruning treatment was started in 1997 when the trees were five years old. The plots with the 7 m green crown were pruned in the following year because the tree height was only around 7 m in 1997. The plots were thinned at the same time as when they received their first lift, which was between 1996 and 1998. The unpruned plots (excluding the control plots) were thinned in 1997. The plots received a second and a third lift to readjust the length of the green crown to either three, five or seven metres. The maximum delay between the 1st and the 3rd lift was three years. Thus the last plots received the final lift in 2001.

3.4 Methodology

3.4.1 Sampling strategy

Toulmin and Raymond (2007) developed a sampling strategy for measuring acoustic velocity in standing radiata pine using the TreeTap time of flight tool. They over sampled the variables of interest to determine the sample size required to estimate the mean of one side, tree, plot and stand to a level of precision with a 95% confidence interval. The variance component (σ^2) was used to determine the sample size required (n) to estimate the mean of the side, tree, plot, and stand to a required level of precision (± L) with a 95% confidence interval (which is a common level in applied science), using the equation (Snedecor and Cochran, 1967):

$$n = 4\sigma^2 / L^2$$

Toulmin and Raymond (2007) found that the variation within an individual side of a tree was extremely low: only one measurement per side would be sufficient to fulfil a

95% confidence interval (Figure 3-2). The variation increases with the age of the trees.

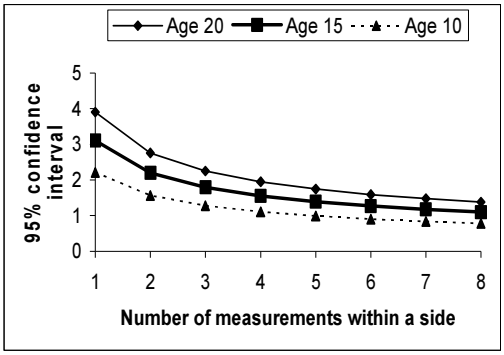

Figure 3-2: Number of measurements to be taken in order to estimate the individual side mean to various levels of precision. Confidence interval is expressed as percentage of the mean (Toulmin and Raymond 2007).

Due to the fact that it takes less than one second per tap, but between one or two minutes to attach the probes to the tree, a couple of extra taps would not cost too much extra time, but would double the accuracy of the results. Another advantage of capturing up to eight readings a side is that the display of TreeTap does not have to be watched that carefully for false readings, as they can be easily rejected when analyzing the data. False readings mainly occur when the probes are not driven in far enough to get in touch with the xylem (which can be a problem for trees with thick bark) or when the angle between the spike and the stem is above 45˚ (towards the right angle). Moreover, errors can be caused when the face of the hammer does not hit the surface of the spike properly, for example not centred or at an angle. Toulmin and Raymond (2007) concluded that tapping one side between four to eight times is an appropriate sampling strategy.

Toulmin and Raymond (2007) conducted acoustic measurements on four sides (90˚ apart) which have shown that there is considerable variation in outerwood velocity around the circumference of the stem. Thus, when only one side was measured the mean would be estimated to ± 12%. When a second side was measured, the estimate of overall outerwood stiffness could be improved significantly, and is ±7-8%,

therefore within the desired precision. When data from four sides were captured, the precision increased only slightly. Thus, mainly in terms of time efficiency it was concluded that it is not worth measuring more than two sides of one tree. These should be on opposite sides, for example north and south. When choosing the sides to measure the main wind direction (stem lean) and the slope of the stand, if any, should be considered.

The study by Toulmin and Raymond (2007) revealed that there is very high variation of outer wood velocity between trees of the same stand (Figure 3-3). The variation between trees decreased with age.

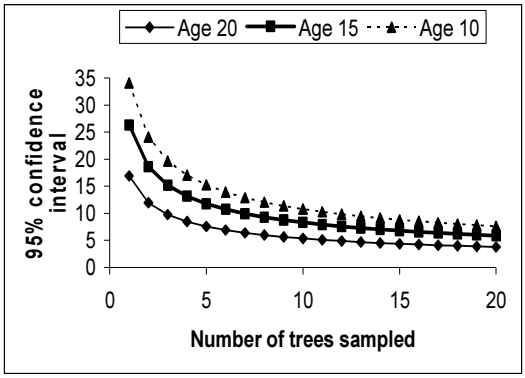

Figure 3-3: Number of trees to be sampled within a plot in order to estimate the plot mean to various levels of precision. Confidence interval is expressed as a percentage of the mean. (Toulmin and Raymond 2007).

Once the number of sampled trees exceeds 10 to 12, the accuracy for mean stand values is at around ± 10% and to measure additional trees would not improve this value significantly. Hence, they suggested sampling only 12 trees per plot.

3.4.2 Data collection

The trees in the measurement plots are permanently numbered and the 12 first trees with normal form (no double leaders or broken tops) of every plot were chosen for this study. However, some of the 250 trees/ha plots only had 10 or 11 reasonable trees

as some of the numbered trees had blown over or died during recent years. The tree height and the DBH are measured annually (in June or July) by Forest New South Wales research staff.
The taper (cm/m) of the tree was estimated by using the following formula:

$$\text{Taper} = \frac{\text{D base} - \text{D top}}{\text{Distance}}$$

where;
D base = diameter at breast height in cm, D top = diameter at the top and therefore equals 0 and distance = tree height (m) – 1.3 m.

The acoustic TOF tool TreeTap was used to measure the velocity of sound of the outerwood. The upper probe was driven in at approximately 1.9 m above ground and the lower probe 1.3 m below that. The spike, through which the shock waves were launched into the tree by a light tap with a hammer, was driven in approx 15 cm (hand span) below the lower probe. Sixteen measurements were taken on each tree, eight on the western side and eight on the eastern side. To measure the green density, which is required to calculate the MOE of the trees, one increment core of the five outer growth rings was taken at breast height (1.3 m) from the northern side of the tree. The northern side was chosen because it should be less affected by compression wood as the main wind direction is from the west. To avoid any unnecessary loss of moisture the cores were put into plastic straws immediately after they have been taken and stored in a cool box. At the end of the day the straws were put in a freezer where they remained until the basic density was measured in the laboratory. The green density was derived from the basic density by using the following equation:

$$\delta_{green} = 1 - \left(\frac{\delta_{basic}}{1500} + \frac{\delta_{basic}}{1000} \right) \times 1000$$

However, a common practice in other projects is to assume 1050 kg as an average green outerwood density for *Pinus radiata* to avoid sampling increment cores. This is

acceptable as the moisture content above fibre saturation point does not have a significant impact on the velocity of sound. Nevertheless, the value of the green density will affect the calculation of the acoustic MOE, since acoustic MOE is the product of the squared velocity multiplied with the density (Schniewind, 1989).

In this study the average green density of the five outer growth rings was 1132 kg/m^3 with a standard deviation of only eight kg/m^3.

3.5 Results

All statistical analyses were undertaken using SAS (SAS-Institute-Inc., 2002). It is thought that the acoustic waves find their fastest path within a distance of approximately 0.5 to 2.5 cm from the cambium and the wood tissue in this area was produced approximately two years ago. Growth data from 2004 was considered suitable to characterise the trees.

The following basic linear regression model was used to analyse (proc mix) the gathered data:

$$y_i = \mu + b_0 x_{i1} + b_1 x_{i2} + b_2 x_{i3} + \left(b_1 x_{i2} \times b_2 x_{i3}\right) + \varepsilon_i$$

where;
yi = is the response variable, e.g. MOE, taper, DBH,
μ = mean of y, b_0 = replicate, b_1 = thinning, b_2 = pruning and εi = error factor

The dataset that was created included basic and green density; outerwood velocity; MOE; and height to green crown after last lift. It also included DBH, tree height, taper, length of green crown and percentage of green crown measurements from 1996 to 2006. This was done to monitor the impact of pruning and thinning on these parameters. Table 3-3 shows some of these parameters

Table 3-3: Means of MOE, DBH, height, taper and basic density for various thinning and pruning treatments. (with DBH and height measurements from 2004, trees 12 years old), based on 286 trees, planted in 1992.

Treatment		MOE (GPa)	DBH (cm)	Height (m)	Taper (cm/m)	Basic density (kg)
thinning						
1000		10.16	23	16.82*	1.49	401.7
500		10.05	28.2	17.43	1.76	387.6
250		9.31	31.8	16.5	2.1	395
pruning*						
3		10.92	25.4	15.94	1.74	403.1
5		10.25	27.4	17.12	1.74	390.5
7		10.37	27.4	17.6	1.7	392.6
Up		7.81	30.5	17.02	1.96	392.9
thinning	pruning**					
1000	3	11.45	20.8	14.64	1.56	416.2
1000	5	10.31	22.8	17.07	1.45	405.6
1000	7	10.48	22.7	17.75	1.38	399.3
1000	Up	8.39	25.8	17.81	1.57	385.7
500	3	11.03	26.8	17.74	1.63	388.7
500	5	10.52	27.9	17.18	1.78	382.3
500	7	10.58	28.6	18.39	1.68	382.5
500	Up	8.01	29.5	16.37	1.96	397.3
250	3	10.28	28.5	15.43	2.02	404.3
250	5	9.93	31.3	17.13	2.00	383.6
250	7	10.02	31.2	16.63	2.05	396.1
250	Up	7.04	36	16.84	2.38	395.8
Replicate 1		10.46	27.9	17.71	1.68	396.1
Replicate 2		9.22	27.5	16.13	1.89	393.5
Trial		9.84	27.7	16.92	1.78	394.8

*** surpressed trees probably decrease the mean tree height**
**** length of green crown**

The impact of thinning and pruning and their interaction on the MOE

The ANOVA for the basic regression model when using MOE as the response variable indicated that thinning and pruning had a significant impact on the MOE of the outerwood (Figure 3-4).

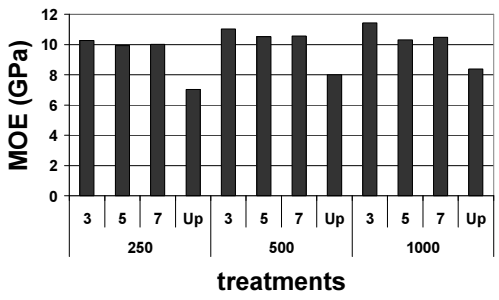

effect	MOE (GPa)		Tukey grouping
	Mean	Std.error	
thinning			
1000	10.16	0.18	A
500	10.05	0.18	A
250	9.31	0.18	B
pruning			
Up	7.81	0.21	A
7	10.36	0.21	B
5	10.25	0.21	B
3	10.92	0.21	B

Figure 3-4: Mean MOE of the 12 different treatments and Tukey grouping. Treatments with different letters are significantly (P < 0.05) different from each other.

The P-values for the F-test for thinning were < 0.05 and for pruning < 0.001 respectively (P < 0.05 is usually regarded as significant to reject the null hypothesis), thus there is strong evidence against the null hypothesis that there is no relationship between thinning or pruning and the MOE. However, the null hypothesis that there is no relationship between the interaction of thinning and pruning and the MOE can not be rejected owing to a P-value for the F-Test of 0.81.

Thinning had the following effect on MOE: 1000 stems/ha (10.16 GPa) > 500 stems/ha (10.05 GPa) > 250 stems/ha (9.31 GPa), indicating that an increased thinning is negatively related to MOE. The trend for pruning was: 3>7>5>Up which indicates that intensive pruning increases the MOE of the outerwood. The MOE of the unpruned trees was 7.81 GPa and therefore 3.11 GPa (28%) lower compared with the trees that received the 3 m remaining green crown treatment (10.92 GPa). The difference between the 5 m and 7 m pruning treatment was only 0.12 GPa.

The ANOVA only indicates that both thinning and pruning have a significant impact on the MOE, but it does not tell which means within the different thinning and pruning methods are significantly different. To determine significant differences between means within different treatments, a post hoc test was applied. The Tukey Test is a post hoc test designed to perform a pair wise comparison of the means to see which are significantly different. The Tukey Test revealed that the 250 stems/ha

treatment is significantly different ($P < 0.05$) from the 1000 and 500 stems/ha treatment, but that there was no significant difference between the 1000 and 500 stems/ha treatment. Moreover, there was a significant difference ($P < 0.001$) between the unpruned and the 3, 5 and 7 m green crown treatments.

The highest mean MOE (11.45 GPa) was observed for the intensively pruned plots with a stand density of 1000 trees/ha, while the lowest MOE (7.04 GPa) was observed for the heavily thinned and unpruned treatment, which shows up a difference of 4.41 GPa or 39%.

When DBH was introduced as a covariance to the model, the impact of thinning just failed to be significant. However, the impact of pruning on the MOE was still significant ($P < 0.001$).

The impact of thinning and pruning and their interaction on basic density

Pruning and thinning as well as their interaction had no significant impact on basic density (Figure 3-5). However, the trend was that thinning slightly decreased basic density while pruning slightly increased basic density.

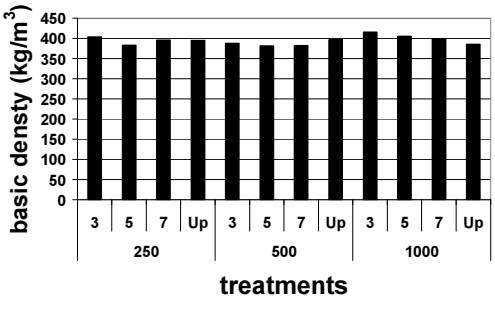

effect	Basic density (kg/m^3)		Tukey grouping
	Mean	Std.error	
thinning			
1000	401.66	4.57	A
500	387.61	4.57	A
250	394.88	4.57	A
pruning			
Up	392.75	5.27	A
7	392.57	5.27	A
5	390.45	5.27	A
3	403.09	5.27	A

Figure 3-5: Mean basic density for the 12 treatments and Tukey groupings.

The highest basic density (416.2kg/m^3) was found in the 1000 trees/ha treatment with intense pruning, and the lowest MOE (382kg/m^3) was found in the 500 trees/ha

treatment that received medium pruning. Figure 3-6 shows that there is only a weak correlation (r^2= 0.11) between MOE and basic density. Thus, at least in this trial, basic density could not be used as a reliable indicator for stiffness.

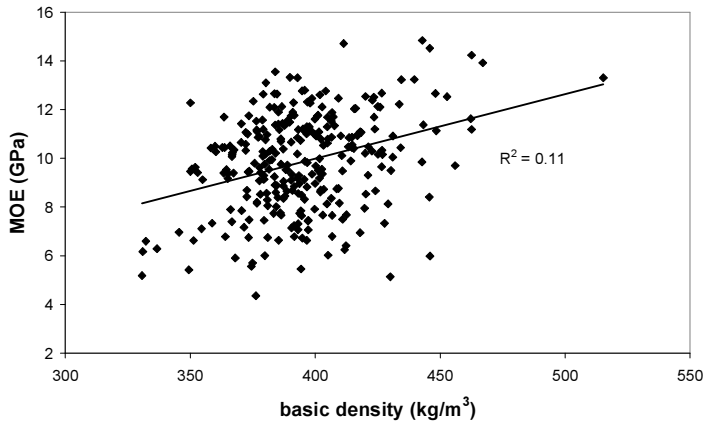

Figure 3-6: Correlation (r^2) between MOE and basic density.

The impact of thinning and pruning and their interaction on DBH

Both thinning ($P < 0.001$) and pruning ($P < 0.05$) had a significant impact on DBH. Their interaction could not explain the variation in DBH on a significant level.

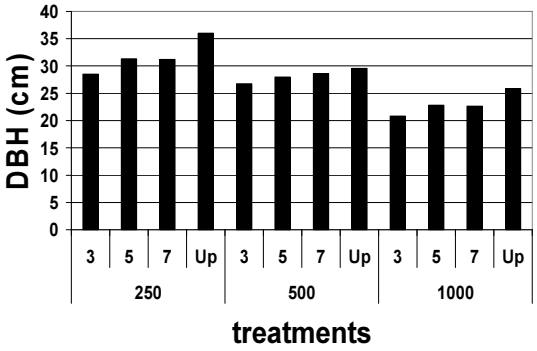

effect	DBH (cm)		Tukey grouping
	Mean	Std.error	
thinning			
1000	23	0.74	A
500	28.2	0.74	B
250	31.8	0.74	C
pruning			
Up	30.4	0.86	A
7	27.5	0.86	A B
5	27.4	0.86	A B
3	25.4	0.86	B

Measurements 2004

Figure 3-7: Mean DBH for the 12 treatments as measured in 2004 and Tukey grouping of the 2005 measurements.

The effect of thinning on DBH was the following: 250 trees/ha (31.8 cm) > 500 trees/ha (28.2 cm) > 1000 trees/ha (23 cm), indicating that thinning (reducing stand density) is positively related to DBH. The trend for pruning was: Up>7=5>3, showing that intensive pruning decreased DBH. The DBH of the unpruned trees was with 30.4cm, larger by 5 cm (17%) than the smallest DBH (25.4 cm) observed for the intensely pruned trees.

The Tukey test showed that the means of the three different thinning treatments were significantly different from each other. In terms of pruning only the unpruned treatment and the 3m green crown remaining treatments were significantly different from each other.

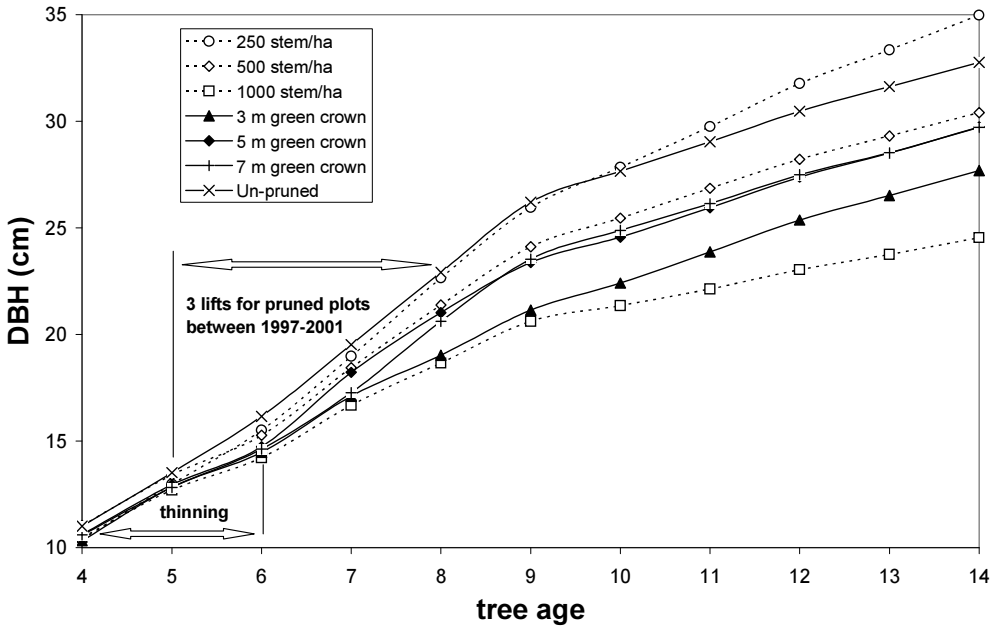

Figure 3-8: DBH over tree age.

Figure **3-8** shows that thinning had stronger effect on DBH than pruning. The main response by DBH to thinning and pruning occurred immediate following these operations. After the age of 9 the trees showed a more uniform increase in DBH. Only the 1000 stem/ha treatment still showed a smaller increase compared to the other treatments while the 250 stem/ha still gained diameter at higher rate.

The impact of thinning and pruning and their interaction on the tree height

The basic model could not explain the variation in tree height at a sufficient level of significance. However, the trend was that higher trees were found in medium thinning and medium pruning treatments.

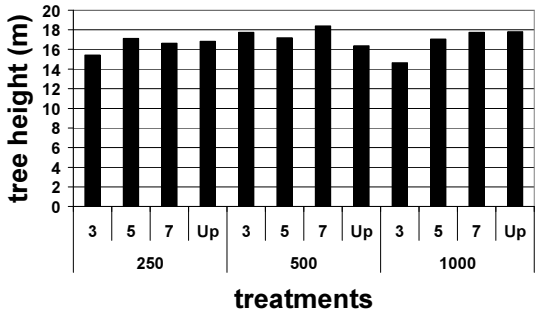

effect	Tree height (m)		Tukey grouping
	Mean	Std.error	
thinning			
1000	16.8	0.41	A
500	17.4	0.41	A
250	16.5	0.41	A
pruning			
Up	17	0.48	A
7	17.6	0.48	A
5	17.1	0.48	A
3	15.9	0.48	A

Measurements 2004

Figure 3-9: Mean tree height for the 12 treatments as measured in 2004 and Tukey grouping of the 2004 measurments.

Intense or non-pruning as well as heavy thinning and low thinning produced trees of smaller height. The interaction of a 7 m green crown remaining and a stem density of 500 stems/ha (medium thinning) produced the highest mean tree height (18.39 m). The smallest mean height (14.64 m) could be observed in the plots that have a stem density of 1000 stems/ha and received intense pruning (Figure 3-9). The mean height in the 1000 stems/ha treatment was probably reduced by the presence of some suppressed trees. If these suppressed trees had been neglected, the highest mean tree height should have been observable in the 1000 stems/ha treatment.

When DBH was introduced to the model as a covariance, thinning and pruning had a significant ($P < 0.001$) impact on tree height. Their interaction was also significant at $P < 0.05$. The Tukey test revealed that the three different thinning treatments were all significantly ($P < 0.001$) different from each other. In terms of pruning it was only the unpruned plots that were significantly different from the other pruning treatments.

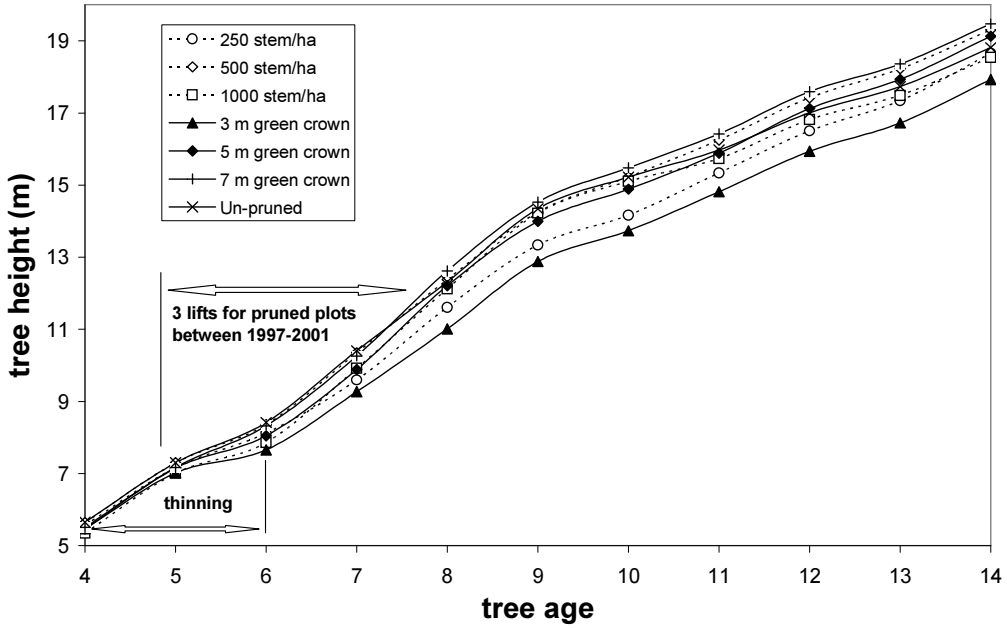

Figure 3-10: Tree height over tree age.

The plots that received heavy pruning and heavy thinning did gain less height during the pruning period (Figure 3-10). After the last lift the effect of pruning on height growth tapered off quickly.

The impact of thinning and pruning and their interaction on taper

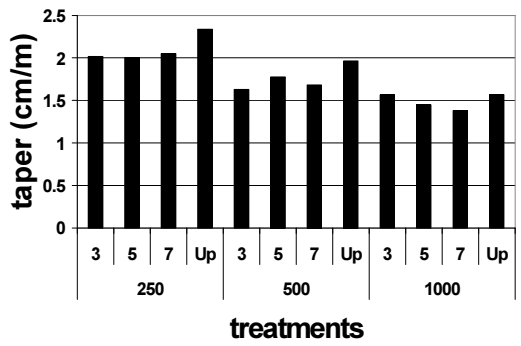

effect	Taper (cm/m)		Tukey grouping
	Mean	Std.error	
thinning			
1000	1.5	0.03	A
500	1.8	0.03	B
250	2.1	0.03	C
pruning			
Up	2	0.03	A
7	1.7	0.03	B
5	1.7	0.03	B
3	1.7	0.03	B

Measurements 2005

Figure 3-11: Mean taper for the 12 treatments as measured in 2004 and Tukey grouping of the 2004 measurements.

The basic model showed that taper is influenced by thinning and pruning ($P < 0.001$) (Figure 3-11). However, their interaction could not be used to explain the variation of taper. Thinning increased taper (1000 stems/ha < 500 stems/ha < 250 stems/ha), and the three different thinning treatments were significantly ($P < 0.001$) different from each other, whereas only the unpruned trees were significantly different from all the pruning treatments. The trees with the smallest taper value (1.38 cm/m) were found in the 1000 stem/ha treatment that was pruned in such a way that 7 m of green crown remained. The maximum amount of taper (2.38 cm/m) was evident in the heavily thinned and unpruned plots.

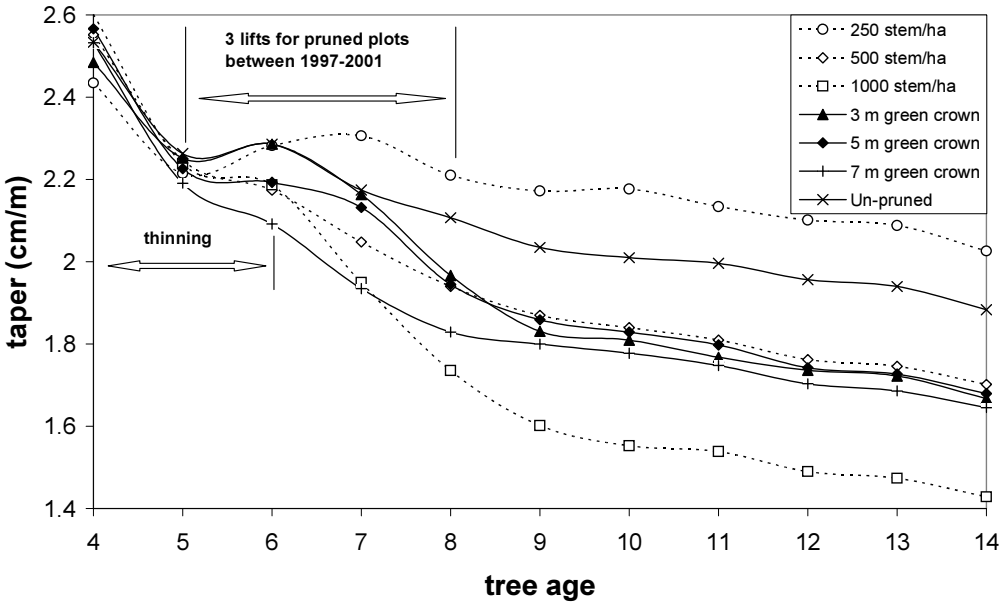

Figure 3-12: Taper over tree age.

3.6 Discussion

The statistical analyses of the data gathered from the Blenheim Pruning trial underlines that both pruning and thinning play a key role in crucial parameters such as MOE, DBH, height and taper. Basic density was not significantly influenced by either thinning or pruning. This outcome is in accordance with a study by Gartner et al.

(2002) on Douglas fir in which they could not find a significant correlation between the location of the green crown or stand density (trees/ha) and basic density.

In this study, there was only a weak correlation between MOE and basic density. Owing to the fact that pruning and thinning both significantly influenced the MOE, the question of whether basic density is a good indicator for predicting mechanical wood properties has to be asked.

This study shows that pruning had a strong positive effect on the MOE of the outerwood. Pruned trees were approximately 25% stiffer than unpruned trees. However, the differences in MOE among the three different pruning methods were relatively small. MOE also increased (by up to 8%) when the initial stand density of the trial was not further reduced by thinning.

What causes the higher MOE in the pruned plots?

One approach to explain the higher velocities of the pruned trees is to look at the grain angle of the outerwood. Knots will cause a deflection of the fibres around the knot, thereby creating an area of disturbance through which the acoustic waves have to travel. It can be assumed that the branch scars caused by pruning would have been well overgrown because the branches at the height where the acoustics measurements were taken had been pruned at least five years before. Thus the fibres of the two or three outer rings should not have been be deflected by any disturbing impacts of knots. This could partly explain the lower acoustic velocities in the unpruned plots (Table 3-3), since the compression waves in the unpruned trees are likely to be deflected by knots that are present within the span between the two probes of the TreeTap tool. However, as reported by Gerhards (1982) and Burmester (1965), the impact of knots on stress wave velocity is relatively small, Gerhards reported a 1% difference, and Burmester, 4%. Even a 4% increase of velocity would raise the MOE by less than 10%. Thus there have to be other “effects” of pruning that cause the formation of stiffer outerwood.

Another factor worth examining is the distance from the base of tree to the green crown. If there is an impact of growth hormones, which are produced in the live crown and thought to inhibit the formation of mature wood within the live crown, a pruning trial should be a good example to test this assumption. The trees in the plots that received pruning should then start to produce mature wood at those positions of the trunk from which the branches have been removed, and they should do this sooner than the unpruned trees. Keeping in mind that one of the differences between juvenile and mature wood is a decreased microfibril angle of the S2 layer, this then could be used to explain the significantly higher stiffness of the outerwood in the pruned plots since a decrease of the microfibril angle increases stiffness.

A first glance at the results of this trial would support the theory that the live crown inhibits the formation of mature wood at that part of the trunk which belongs to the green crown. If 5-10% of the increase in stiffness is attributed to the abundance of knots in the pruned plots, the missing 10-15% could be attributed to a decrease of the microfibril angle. However there is one problem that arises when looking at the control plots (1000 stems/ha and Up). The distance to the green crown in the control plots was the same as in the pruned plots (Figure 3-13). Moreover, Figure 3-13 shows that there is no difference in the distance to the green crown between the three pruning treatments.

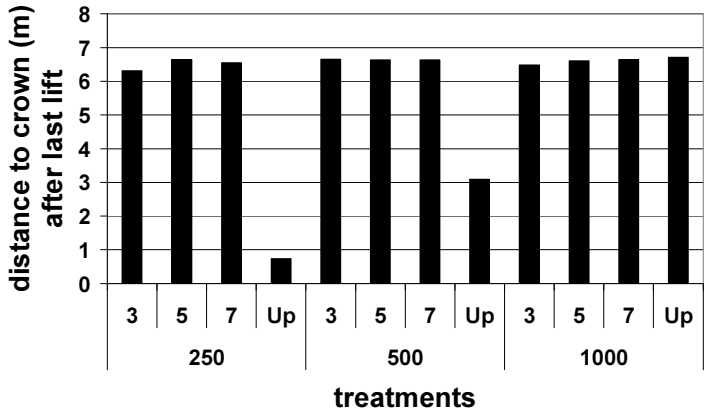

Figure 3-13: Mean distance from the base of the tree to the green crown of the 12 treatments as measured in 2006.

When the distance to the green crown in the control plots is the same as in the pruned plots, it should be asked, why is the MOE of the trees in the control plots lower by approximately 20%? The trees in the control plots still had the dead branches attached to the trunk, will causes a slight decrease of the MOE. Unfortunately, the height to green crown was measured only once in the space of 14 years, in 2006. Thus, it could be argued that some of the branches might have only died recently, and that the distance to the live crown was significantly shorter two or three years ago. It is thought that the fastest path of the shock waves is between 0.5 and 2 cm inwards from the cambium. Hence, this wood tissue could still have been under the control of the green crown when it was laid down. However, the outerwood of the pruned trees at the base of the tree was freed from the direct impact of the green crown at least seven years ago (in 1999 when the last pruned plot received its first lift). Thus, it is not known precisely when a certain part of the tree growing in the control plots was freed from the impact of the live crown.

Why is there only a small difference in the MOE between the three pruning treatments?

The difference between the 3 m green crown treatment and the 7 m and 5 m green crown treatment was relatively small, only 0.62 GPa or 6%. When the height to green crown after the last lift is plotted, it can be seen that there is almost no difference in distance from groundlevel to the green crown between the pruning treatments Figure 3-13. This is due to the fact that the plots were not pruned at the same time. The parameter that controlled the time frame for pruning was the mean tree height of the plots. Thus, plots were pruned when the trees reached a mean height that allowed (re)-adjustment of the green crown to the scheduled length. Consequently, pruning of plots with the 3 m green crown remaining could have started in 1997, while some of the 7 m green crown plots were not pruned before 1999. Likewise this means that the 7 m green crown plots received their last lift in 2001, while the pruning for the 3m green crown could have been finished in 1999.

Figure 3-14 shows that the measured length of the green crown after the last lift matches well with the target length. However, in 2004 the differences in the length of the green crown between the three pruning treatments were relatively small. In other words, that means that the trees that received heavier pruning operations showed an increased height growth.

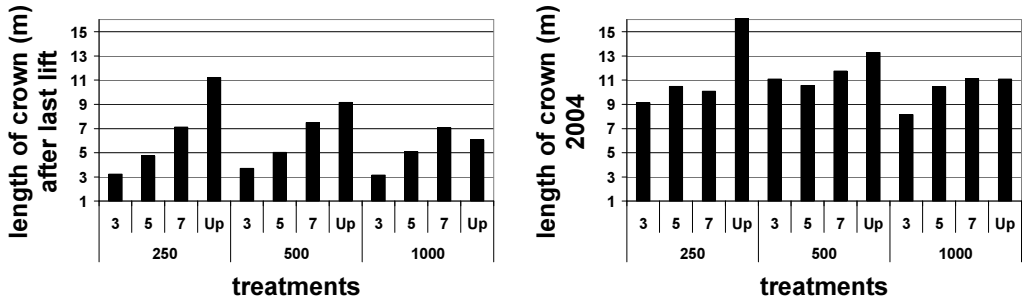

Figure 3-14: Mean length of green crown after the last lift (1999-2001) and in 2004.

Considering that there is no significant difference in distance from the tree base to the bottom of the green crown between the three pruning treatments, the effect of this on the MOE cannot be very strong. The fact that there was a time difference between the pruning operations of the three treatments may be the only factor that has an impact on the formation of the wood tissue that was produced after the plots were pruned. Thus, the number of growth rings that are free of knots at the position from which the acoustic measurements were taken is greater compared with those plots that were pruned in later years. This also means that this area was less affected by hormones (growth regulators) which are produced in the live crown and are thought to inhibit the formation of mature wood. Thus it might be argued that those plots that received the 3 m pruning treatment have a smaller microfibril angle in the S2 layer since they started to produce mature wood one or two years earlier. The fact that the time window of two years is relatively short might explain why there is only a small difference in the MOE of the outerwood between the three pruning methods.

The issues discussed above lead to the assumption that the Blenheim Pruning Trial seems not to have been effective in investigating whether the distance to the green

crown has an impact on the wood formation process. To do so, a pruning trial in which the trees are pruned to different heights at the same time would be more suitable. In subsequent years the acoustic measurements should be repeated to see how fast the cambium responds to pruning operations.

Two factors that have not been considered so far are basic density and the dimensions of the trees.

The basic density of the unpruned plots was the lowest among the unthinned treatments. Basic density increased systematically with pruning intensity within the 1000 stem/ha treatment. This might just have been chance, as there is no such trend within the other thinning treatments. For example, in the 500 stem/ha treatment the highest basic density was found in the unpruned plots.

The trees in the control plots have similar dimensions compared to the other unthinned plots. Only the height and the DBH of the trees of the 3m green crown treatment are significantly smaller. The fact that the trees with the 3m green crown pruning treatment were on average 1m shorter than the average tree of the trial means that they were less exposed to wind. A study by Bascuñán et al. (2004) showed that trees that are more exposed to wind (edge trees) had reduced outerwood stiffness (around 10% less). They state that wind increases the microfibril angle which could explain the decrease in stiffness. However, it is questionable whether wind is a major factor in this trial, since the difference in average tree height between the plots is not very big. Nevertheless, the stiffest trees were found in the plot that had the smallest mean tree height. But in this study, wind probably is just one (minor) factor among many that together determine the stiffness of the tree.

What causes the difference in MOE between the three different thinning methods?

When comparing the three different thinning treatments, the heavily thinned plots showed the lowest MOE (9.31 GPa) followed by the medium thinned plots (10.05 GPa). The highest MOE (10.16 GPa) was measured in the unthinned plots. Higher stocking usually increases the competition for light, which tends to increase height growth while DBH growth is reduced. Moreover, the diameter of the branches of trees growing in high stocked stands is smaller compared with the diameter of branches of trees growing in low stocked stands. Smaller branches will cause less disturbance within the woodstructure and might give faster TOF velocities compared with trees that have bigger branches. Another trend is that the canopy in high stocked stands closes earlier compared to low stocked stands. Due to a shortage of light the branches start to die from the base upwards when the canopy starts to close.

3.7 Conclusion

Substantial improvements of the MOE of the outerwood in *Pinus radiata* were gained by pruning operations. The MOE in the unpruned plots was significantly lower (25%) than the MOE in the plots that received pruning. The variation in MOE between the three different pruning methods was relatively small. The trees with the stiffest outerwood grow in the plots that were heavily pruned and had a stand density of 1000 trees/ha (highest in the trial). It is not absolutely clear what causes the increased MOE in the pruned plots. The higher MOE can be partly explained by the fact that the knot free outerwood of the pruned trees will lead to stress wave velocities that might be up to 4% higher than in knotty wood.

The theory that the distance to the green crown has an impact on the type of wood (juvenile or mature) that is produced at a certain position of the trunk, could not be tested in this study. The pruning operations of the Blenheim Pruning trial did not allow this, because the trees were all pruned to the same height. It would not have

been practical to do acoustic measurements further up the trunk when measuring standing trees. To confirm that pruning frees the pruned part of the trunk from growth hormones that might inhibit the formation of mature wood, the microfibril angle of the outer growth rings should be analysed. If the microfibril angle decreases more rapidly in the pruned trees than in the unpruned trees, this might indicate that pruning can shorten the time in which juvenile wood is produced.

Thinning activites also had an impact on the MOE, although not as strong as pruning. By decreasing the stand density the MOE was reduced while DBH and taper were increased.

No significant influence of pruning and thinning was found on basic density. However, pruning tended to slightly increase basic density while thinning caused the opposite.

Thinning and pruning also had a significant impact on DBH and taper. When DBH was introduced to the model, the tree height was also significantly influenced by pruning and thinning activities.

Chapter 4: MOE measurements on small eucalypt and pine logs

4.1 Introduction

In this chapter acoustic tools based on the resonance method are shown to give different answers (for example MOE) using an identical physical configuration. In particular the influence of branch nodes and nodal whorls on the resonance frequencies of small roundwood specimens is examined. For this, stems of young eucalypt and pine trees were cut in a way that knots were located at specific positions along their span.

4.2 Material

The study required green stem wood with long internodes. Moreover, branch nodes had to be of sufficient size to represent a zone of disturbance inside the model material. Young eucalypts meet such requirements, and testing material was taken from a 10-13-year-old *Eucalyptus nitens* stand growing on the Port Hills, Christchurch. The study also included acoustic measurements of a *Pinus radiata* clone (number 870), which was bred for long internodes, growing on a 15-year-old plantation at Burnham, west of Christchurch.

4.2.1 Eucalypt samples

Several trees were felled and delimbed. Seventeen stems with a length of approximately 2 m (1.516 - 2.185 m) and a diameter at midspan of approximately 12 cm (7.1 – 15.8 cm) were cut. Thus the samples could be handled by a single person in the laboratory. Three different groups with branch nodes at specific locations were

selected: Group 1 (only three samples)[1] had branch nodes at either end; Group 2 (five samples) had branches only at midspan; Group 3 (five samples) had branch nodes at ¼ and ¾ of the span. Ideally there would be clearwood in between these branch nodes. However, as far as the eucalypt samples are concerned, it was not always possible to avoid having some small branches between the main branch nodes. Moreover, the location of the branch nodes was not exactly at the specified locations, for example a group of two or three branches might be spread over a distance of about 20 cm along the axis of the bolt. If so, the sample was cut in a way that the centre of this group roughly coincided with one of the specified locations. Branches rarely grow perpendicular to the pith so the shape of knots inside the stem could be described as an inverted cone around which the fibres and sap flow. Thus, the centre of the nodal whorl or a single knot is not directly under the knot on the cambial face of the log. The acuter the angle between the axis of the knot and the pith, the more the true knot centre (inside the bolt) and the wood tissue that is influenced by the knot shift towards the base of the stem.

The bolts were taken from at least 2 metres above the ground. The reasons for this are; the wood at the base of the stem significantly differs from the wood in other parts of the stem (high percentage of tension wood) and; second, due to the fact that mainly suppressed trees had been chosen from which to collect the samples, the lower part of the stem had self-pruned itself and therefore only some branch scars could be found on the bark; and third, the proportion of knot wood, especially in suppressed trees, is reduced compared to other parts of the stem.

4.2.2 *Pinus radiata* samples

Fifteen samples (5 samples each group) with dimensions that are similar to the eucalypt samples were taken from a 15 year old plantation in Burnham. All samples were cut from the same clone. This clone typically has long internodes, which is ideal

[1] Two samples that were original cut to be put in group 1 showed branch nodes at undesired positions after they had been debarked. Thus, these samples could not be used and group 1 consisted only of three samples.

for this project. Moreover, the nodal whorls were mostly well defined, which made it easier to cut samples according to the three specified groups. Again the butt log was not used.

4.3 Methods

4.3.1 Data collection

Once cut, the samples were numbered and the bottom and the top ends of the bolts marked. While transporting to the laboratory (approximately 1 hour), the ends of the bolts were wrapped in poly bags to minimize evaporation. Immediately after arriving at the laboratory a disc (approx. 2.5 cm) from either end of all samples was cut and numbered (indicating top or bottom and number of bolt). Then the green density of the debarked discs was measured by using the displacement method. The process of measuring the green density took about 1 hour, and during that time the discs, except the disc that was just processed, were stored in a polythene bag to minimise evaporation.

After cutting the discs, the bolts were stored in a fridge and chilled to 6 °C. If acoustic measurements needed to be repeated or if more samples for further testing were required, it was possible to repeat the measurements under the same conditions. This is crucial as the temperature of wood has a small impact on its mechanical and acoustical properties.

Green density, length and the frequencies of the acoustic waves are the only parameters that are required to calculate the MOE of the bolts. Since eucalypts are the main emphasis of this study, several other parameters of the bolts have been measured for the eucalypt groups only. These parameters were: diameter at the top, middle and bottom of the bolts (with bark and debarked), moisture content, green density of the bark, weight of the bolt, weight of the bark, position and size of knots (smallest and largest diameter of the node and percentage of cross section) and the centre of gravity.

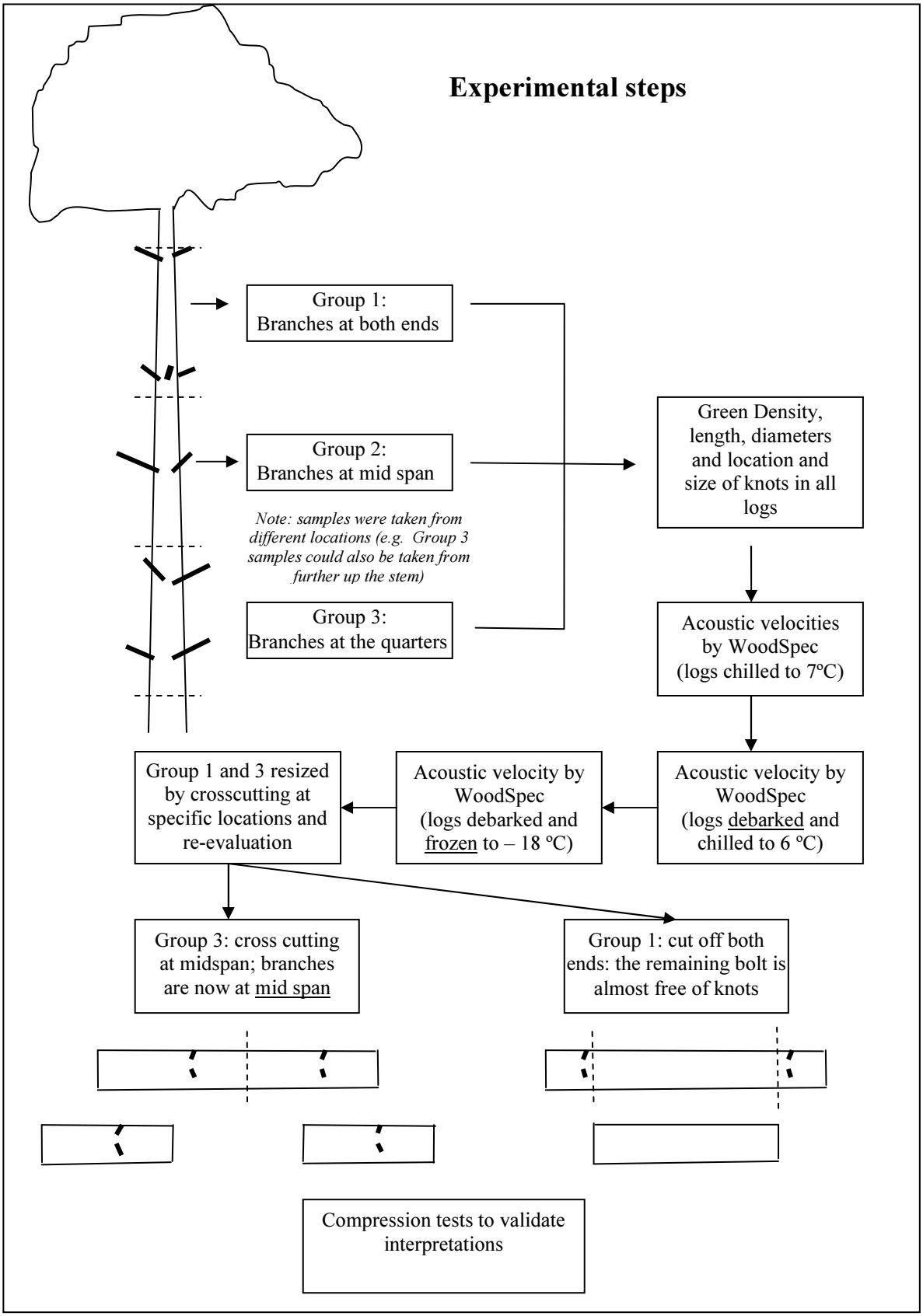

Figure 4-1: Experimental steps in this study.

4.3.2 Impact of branches on the wood structure

When investigating the influence of knots at specified positions along the length of the bolt with respect to the velocities of the fundamental mode and its overtones, it is crucial to describe every knot exactly. Small knots that have been overgrown were neglected. As the branches usually grow at an angle of 40°–80° to the pith, the cross section of the knots after delimbing is more or less oval-shaped. The 'real' diameter of the knot is the smallest diameter which is usually found along the tangential direction of the bolt. To calculate the percentage of the cross section of the bolt, which is occupied by a particular knot the knot itself was considered as an isosceles triangle (Figure 4-2). Consequently the area of the knot can be calculated by using the following equation:

$$\text{Area} = (g \times h)/ 2$$

where;
g= the smallest diameter of the knot as measured at the cambial face of the bolt and h=the radius of the cross section.

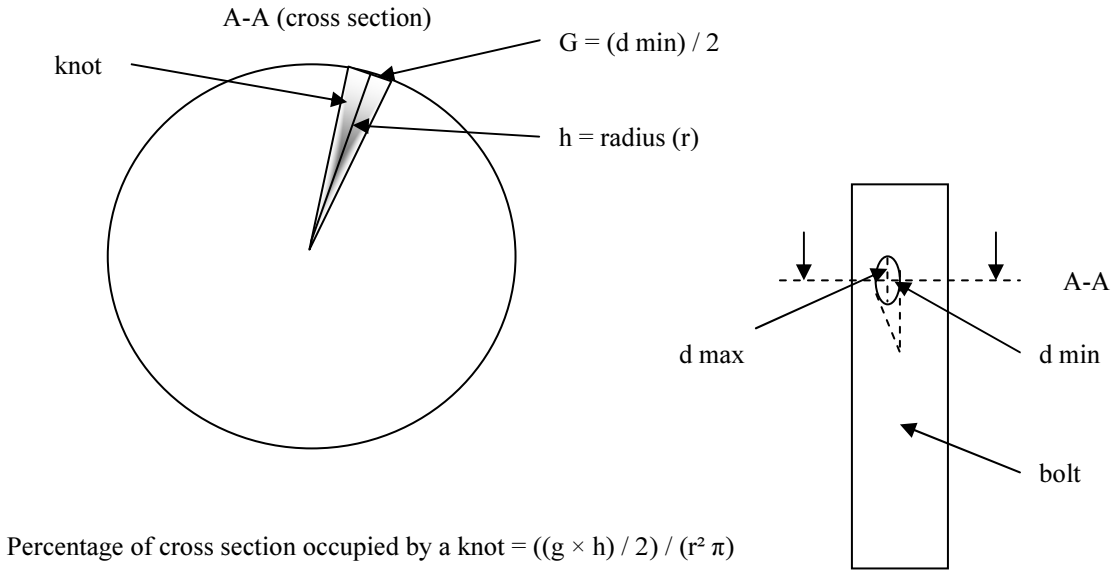

Figure 4-2: Method for calculating the percentage of cross section occupied by a knot.

To obtain the percentage of the cross section that is directly influenced by the knot, the area (triangle) of the knot is divided by the area of the cross section of the bolt at that particular location. However, as mentioned, the influence of the knot on the deviating wood tissue is about 1-3 times larger than the knot itself.

On average each bolt had seven branches; four–five of them were located at the specified locations while two-three significantly smaller knots were placed elsewhere. The area of the cross section that was occupied by a small knot (e.g. 17 × 20 mm) is around 5%, while a large knot (60 × 90 mm) could occupy around 20% of the total cross section. As far as the pines are concerned the knots were located at well defined knot whorls. Thus, the areas of all individual knots from a whorl could be added together. On average a whorl had 5 branches which occupied approximately 25% of the stem's cross section. Considering that the area of disturbance around a knot can be up to three times of the size of the knot, 50% of the cross section at the nodal whorls is affected by knots. However, it is more complicated to characterise the impact of branch nodes on the wood structure of the eucalypts due to the fact that the knots are spread around the specific location.

It can be assumed that a knot which overlaps exactly with an antinode for pressure has a considerably higher impact on the acoustic properties than a knot that is placed mid-way between a node and an antinode. The impact of this knot probably is not 50% of the maximum impact but more likely around 25%. Further work would be required to confirm this assumption. Figure 4-3 illustrates the average eucalypt bolt of each group.

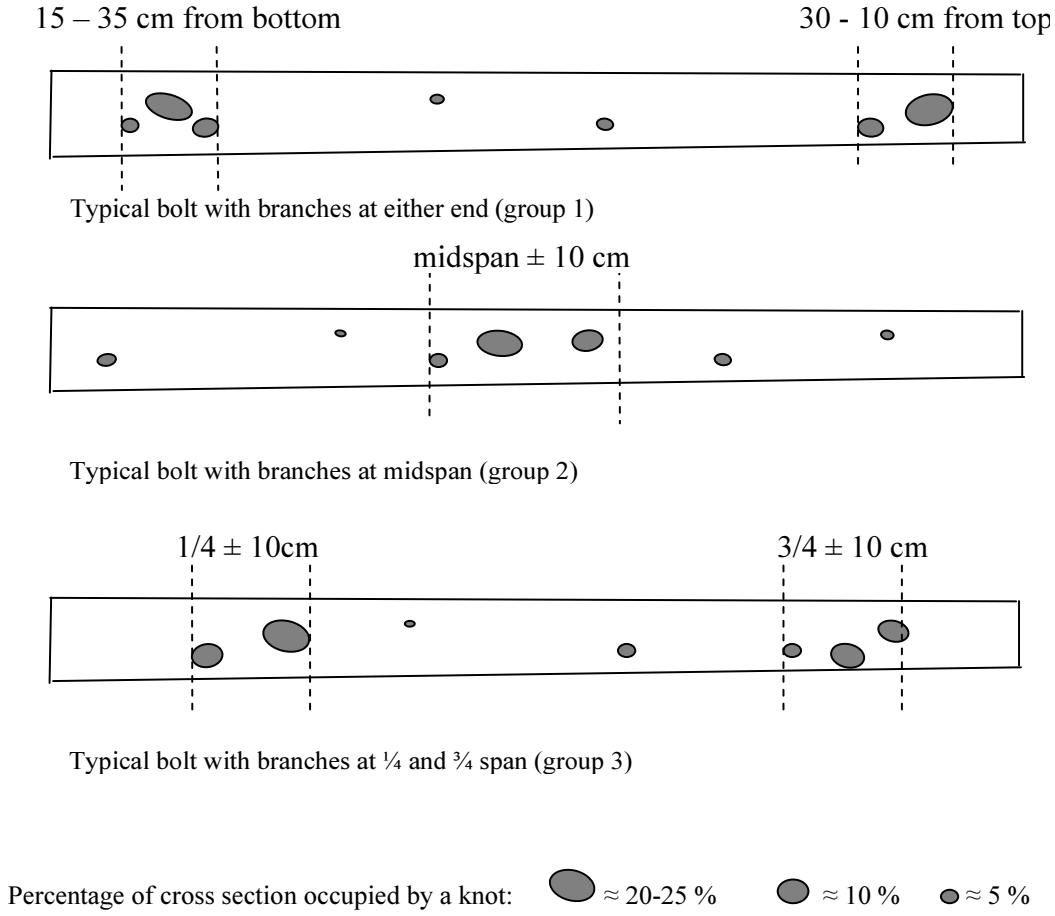

Figure 4-3: Typical eucalypt bolts of the three different Groups.

4.3.3 Acoustic velocity measurements with WoodSpec

For this study the trigger mode of Woodspec with a microphone as a transducer was used to determine the frequencies of the fundamental mode and its overtones. The reasons for preferring the microphone to the accelerometer were twofold: preliminary studies indicate that the microphone tended to detect more overtones than the accelerometer. Moreover, the accelerometer has to be physically connected to one end of the sample by putting a dab of silicone grease on one end of the bolt and pushing the accelerometer into the grease, which is time consuming. Another, more important reason is that the acoustic measurements were also conducted on frozen (-18°C) logs.

Where the temperature of the grease drops below 0°C it might have an impact on the accuracy of the measurements, as the grease might lose its stickiness.

Figure 4-4 illustrates the experimental setup of WoodSpec as used in this study. The bolt was supported at two points: ¼ and ¾ span. A pad of bubble wrap was placed between the log and the supports to minimise interactions between the vibrating log and the supports. The distance between the log and the microphone was approximately 5 cm.

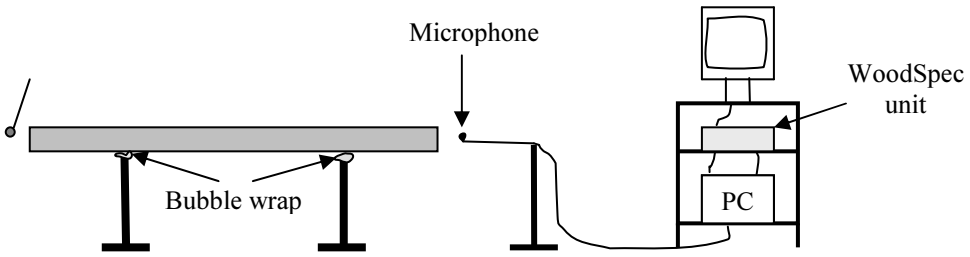

Figure 4-4: Experimental setup of the WoodSpec unit.

4.3.4 Acoustic measurements under various conditions

After the samples had been stored in the fridge for two days, to allow the whole log to equilibirate to 6°C, the acoustic velocities of the eucalypt and the pine logs with bark were determined. One log at a time was taken from the fridge, and before starting the measurements by WoodSpec, the length of the log was measured. Immediately after the acoustic measurements, which took 5-10 minutes for each pine bolt, the pine bolts were put into the freezer.

Further parameters were gathered for the eucalypts. Diameters at the top, middle and bottom were measured with bark on; moreover, the bolts were weighed using a balance with an accuracy of 50 grams. Then the bolts were debarked and all the measurements were repeated. Two pieces of the bark from each bolt (approximately

100 × 40 mm) were taken to measure the green density of the bark, again using the displacement method. The required time for this part of the measurements was between 20 and 30 minutes for each log.

The bolts were stored in the freezer (-18°C) for at least 48 hours to guarantee that the entire log was at the same temperature. The acoustic measurements were repeated on the frozen logs.

The bolts were then resized in such a way that the branch nodes were at different positions. Thus, it was possible to test the same material under different configurations. For instance the bolts of group 3 (branches at ¼ and ¾ span) were crosscut at midspan and the two resized samples now had branches at midspan. Group 1 (branches at either ends) was resized in such a way that both ends of the sample were cut off and the remaining bolt just had a few small branch nodes at unspecified positions. In this case, the middle part was used to compare the values for clearwood with the values of knotty samples and the ends of the original bolts were used to test whether it is possible to conduct acoustic measurements based on the resonance method if the diameter to length ratio falls below 1:3.

4.3.5 Areas of the bolts examined by the first, second, third, fourth and fifth harmonic

When standing waves are introduced into bolts, each harmonic has nodes and antinodes at specified locations along the length of the bolt. The idea of cutting samples with branch nodes at specified locations was to examine whether or not the acoustic waves are influenced by knots, which represent a region of disturbance inside the logs. The fibres in knots are aligned more or less perpendicular to the grain of the stem. Knot wood itself has a high content of reaction wood and can be highly resinified, consequently knot wood can be 2-3 times as dense as stem wood (Walker, 2006). The area of disturbance is not just the volume of the branch inside the log. The fibres surrounding the knot are deflected and cause a region of wild grain around

knots. Thus, the disturbance is around 2.5 times greater than the size of the knot. Moreover, the density and the chemical components of the knot-surrounding wood are highly affected by the presence of reaction wood. Figures 4-5 to 4-7 illustrate the overlapping of the branch nodes of the three different groups with nodes and antinodes in the first five harmonics.

The branch nodes of Group 1 (branches at either end) are mainly placed between 12-25% and 78- 90% of the length of the bolt (Figure 4-5). The branch nodes for the 1st harmonic are situated between the nodes and the antinode for pressure. The 2nd and the 3rd harmonics have antinodes for pressure close to the place where the branch nodes are located, and for the 5th harmonic the branch nodes overlap with nodes for pressure.

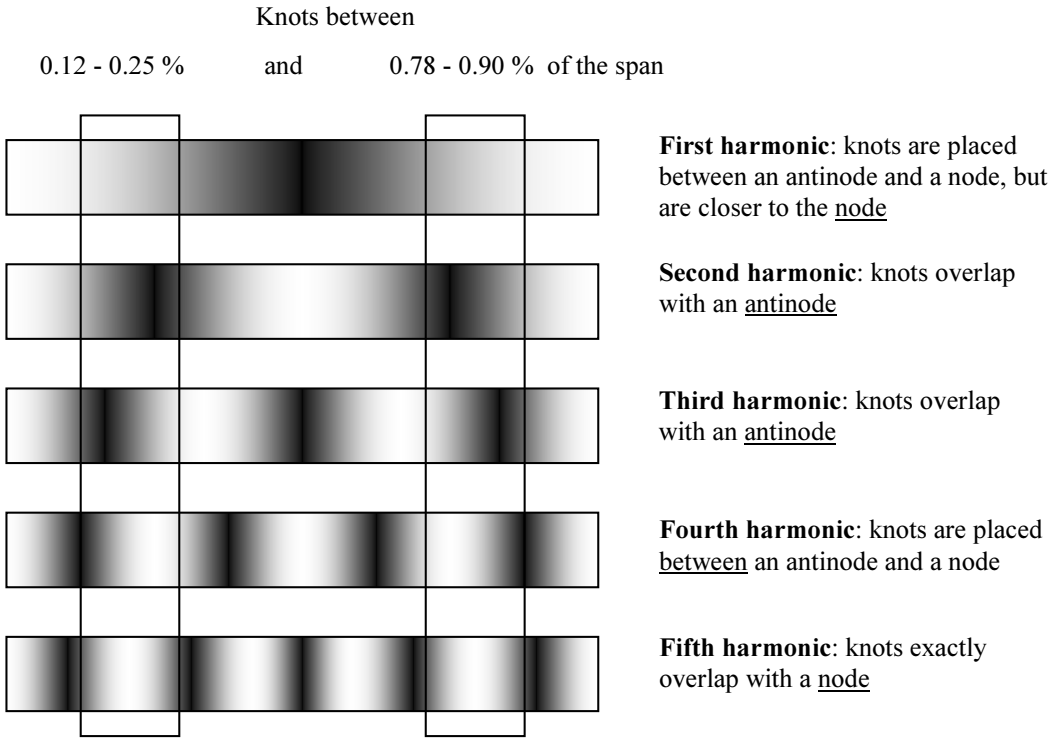

Figure 4-5: Overlapping of branches at either end (Group 1) with the nodes and antinodes of the first 5 harmonics. The dark areas refer to antinodes for pressure (nodes for displacement). The light areas are nodes for pressure (antinodes for displacement).

Group 2 has branches at midspan (Figure 4-6). The 1st, 3rd and 5th harmonics have antinodes for pressure at midspan and the 2nd and 4th harmonics have nodes respectively. With increasing harmonics the distances between nodes and antinodes get shorter and shorter. Consequently, knots that are not exactly placed at midspan might not be sensed by the antinode for pressure at midspan of the 5th harmonic.

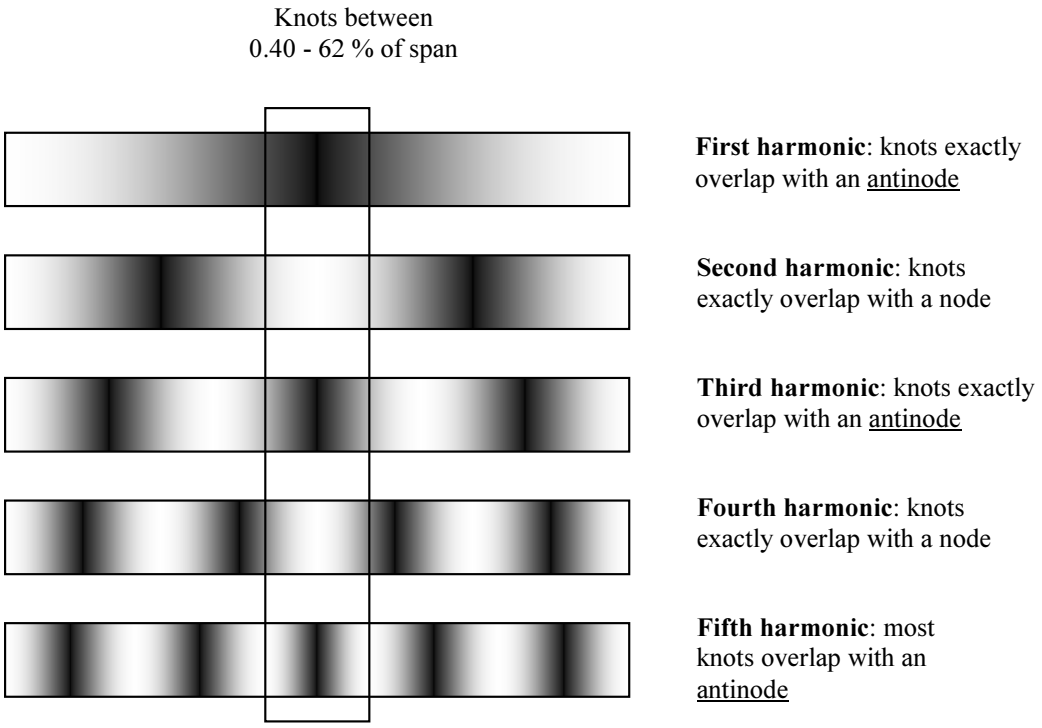

Figure 4-6: Overlapping of branches at midspan (Group 2) with the nodes and antinodes of the first 5 harmonics. The dark areas refer to antinodes for pressure (nodes for displacement). The light areas are nodes for pressure (antinodes for displacement).

The branch nodes of Group 3 (branches at approx. ¼ and ¾ span) are overlapping with antinodes for pressure of the 2nd harmonic, and with nodes for pressure of the 4th harmonic (Figure 4-7). Hence, if knots have an impact on acoustic velocities, the MOE calculated from the 2nd harmonic should be significantly different from the MOE based on the 4th harmonic.

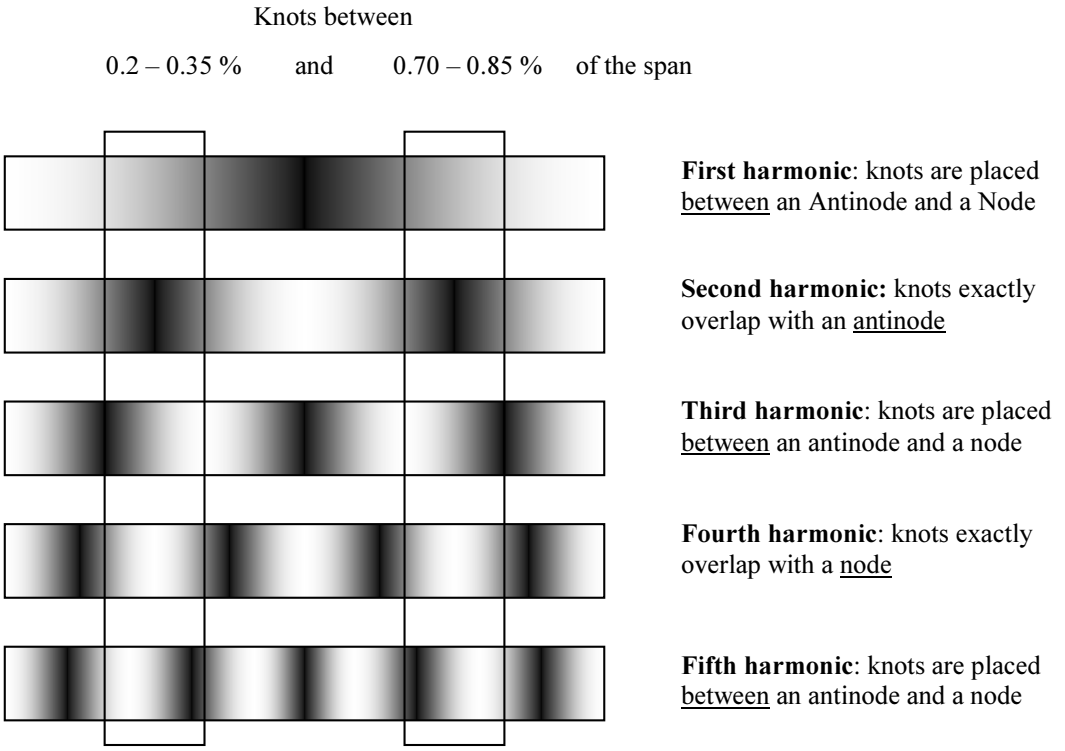

Figure 4-7: Overlapping of branches at ¼ and ¾ span (Group 3) with the nodes and antinodes of the first 5 harmonics. The dark areas refer to antinodes for pressure (nodes for displacement). The light areas are nodes for pressure (antinodes for displacement).

4.3.6 Static MOE determination by compression tests

A procedure to validate acoustic measurements by compression tests was developed by Lindström et al. (2002). Instead of using WoodSpec, they conducted sonic testing with Sylvatest which is based on the time of flight method. Lindström et al. (2002) cut internodal bolts of four-year-old radiata pines that were 400 - 700 mm long. After sonic testing the samples were recut to a diameter to length ratio of 1:3. The stress-strain behaviour of the bolt was measured using an Instron machine and two linearly

variable differential transformers (LVDT's) that were attached directly to opposite sides of the bolt. A LVDT element basically consists of a cradle which is pressed into the bolt by a needle and a moving core element that rests against an independent support plate. The LVDT's measure the displacement between the needle of the cradle and the needle of the support plate under the load applied by a 50 kN load cell. The following equation can be used to calculate static MOE of the bolts:

$$Bolt\ MOE\ (Static) = \frac{\Delta Load}{\pi r^2} \div \frac{\Delta l}{l}$$

where;
Δ Load (N) is the load difference within the elastic region, r = the average radius in the test zone, *l*(m) = the distance between the 2 needles attaching the cradle and support plate and Δ *l*(m) = the displacement between the 2 needles when the applied load increases by Δ Load (N).

The results of the study by Lindström et al. (2002) showed good correlation between acoustic and static measurements of MOE.

4.4 Results

4.4.1 Green density, basic density, bark density and moisture content of the samples

The mean green density (measured from debarked discs) of all eucalypt samples was 1097.98 kg/m³ with a standard deviation of 19.92 kg/m³. The average basic density was 0.486 (standard deviation of 0.035) and the mean bark density was 730.7 kg/m³. The standard deviation for the bark density, which was 93.9 kg, was considerably higher compared to the standard deviations for the green and basic density. The reason for this is that the bark of *Eucalyptus nitens* trees usually consists of two layers: the inner and the outer bark. The density of the inner bark is much higher

compared to the density of the outer bark. However, there is high variation of the ratio inner to outer bark. Thus, the variation of the bark density shows high variation too. The trend is that with increasing diameter the amount of outer bark tends to increase while the thickness of the inner bark remains approximately constant. The average moisture content of the eucalypt bolts was 127% (standard deviation of 14.4%) and. The mean length of all eucalypt samples was 1.925 m with a standard deviation of 0.241 m.

The mean green density (measured from debarked discs) of all pine samples was 734 kg/m³ with a standard deviation of 106 kg/m³. The high standard deviation can be explained by the fact that radiata pine has a significant, but also quite variable proportion, of "dry" heartwood. The average basic density was 0.36 having a standard deviation of 0.05 and the average moisture content was 180% with a standard deviation of 17%.

4.4.2 MOE calculations for the bolts by the first 5 harmonics

The MOE for the eucalypt bolts was measured both with bark on and debarked; with both measurements at 6°C wood temperature. The debarked bolts were also measured at a temperature of -18°C. The mean MOE (average of the 1st and 2nd harmonic) of all eucalypt samples with bark on was 7.72 GPa, with bark off 8.82 GPa (which is 114% of the values for samples with bark on) and 13.30 GPa for the frozen bolts (which is 172% of the chilled samples with bark on or 151% of debarked and chilled bolts). The mean MOE of all pine bolts with bark and chilled to 6°C is 6.78 GPa and the value for frozen pine bolts is 10.45 GPa (which is 154% of the chilled samples). The following graphs show the MOE of the bolts as calculated by the velocities for the first, second, third, fourth and fifth harmonic. However, it was not always possible to detect the 3rd, 4th and 5th harmonic. The trend was that more harmonics were detectable on frozen wood. To make the MOE values comparable within the groups and also between the groups, the MOE of the harmonic that gave the highest MOE for each bolt under a particular condition was referred to as 100%, and the other detectable harmonics of

that bolt were expressed in relation to that. Then, the average values (in percentages) of the 1st, 2nd,3rd, 4th and 5th harmonics for all samples (Figure 4-8) as well as for each of the three groups separately were calculated.

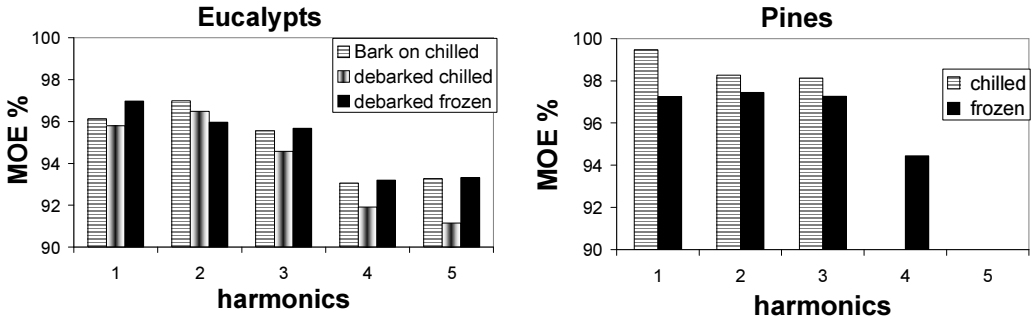

Figure 4-8: MOE (%) calculated from the detectable harmonics of all eucalypt and pine samples in chilled and froze condition.

Figure 4-8 show that for both species, the eucalypts and the pines, the differences between the first five harmonics of all samples were relatively small. In particular, the first three harmonics of all samples were very similar with less than 3% deviation. Moreover, it was evident that the relations between the harmonics are not significantly influenced when debarking or freezing the logs. It is clear that the velocities increased after debarking and in particular when measuring frozen logs, but the relation between the frequencies does not change significantly. One important distinction between the eucalypt and the pine is that it was mostly not possible to detect more than the 1st and the 2nd harmonics when testing chilled pines while it was possible in the most cases to detect the first 4 harmonics for the chilled eucalypt bolts. When measuring frozen logs it was more often than not possible to obtain a clear 4th harmonic for the pines, and for approximately 40% of the eucalypts it was possible to detect the 5th harmonic. Thus, frozen logs support more overtones.

Differences between the MOE based on the first 5 harmonics of Group 1 (branches at either end)

The MOE based on the 2nd harmonic was always the highest (Figure 4-9). For the eucalypts, the value was 100%, indicating that the MOE for the 2nd harmonic for each of the five bolts of Group 1 was at all times the highest value measured. The MOE of the 3rd harmonic was on average 3% lower than the MOE of the second harmonic. The MOE calculated from the 1st, 4th and 5th harmonics was considerably lower (around 9%) compared to the values of the second and third harmonics.

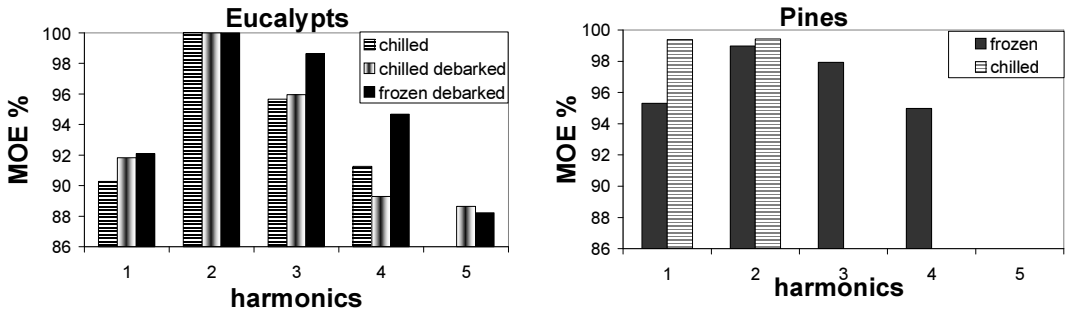

Figure 4-9: MOEs of the first five harmonics of group on (knots at either end).

When looking at the wave patterns inside the bolts it is obvious that the 2nd and 3rd harmonics have areas of little vibration (nodes for displacements or antinodes for pressure) at the locations where the knots are placed (see Figure 4-5). The 5th harmonic led to the lowest MOE value and two of its nodes for pressure exactly overlap with the branches at either end of the bolts.

For the pines, it was not possible to detect a 5th harmonic for the frozen samples and no 3rd, 4th and 5th harmonics for the chilled samples. However the difference of the frozen samples between the MOE based on different harmonics is less pronounced but still shows the same pattern as for the eucalypts.

Differences between the MOE based on the first 5 harmonics of Group 2 (branches at midspan)

As shown in Figure 4-10 the MOE of the 1st harmonic was significantly higher than the MOE based on the second and fourth harmonics.

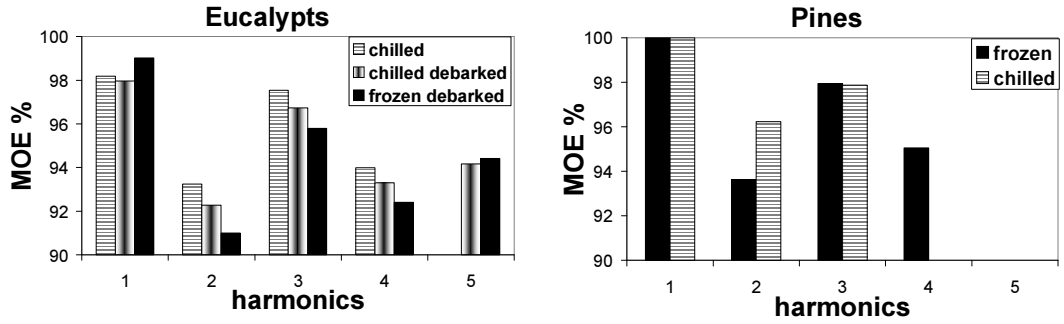

Figure 4-10: MOEs of the first five harmonics of group two (knots at midspan).

The 1st, 3rd and 5th harmonics have antinodes for pressure at midspan. Thus, there is minimum vibration, but maximum force around the knots at midspan. The MOE based on the 3rd harmonic was about 2% smaller and the MOE calculated from the 5th harmonic was about 4% smaller than the MOE based on the 1st harmonic. The 2nd and 4th harmonics have areas of maximum vibration but minimum force at midspan. The MOE calculated according to the 2nd harmonic was about 7.5% smaller than the maximum value based on the 1st harmonic, and the MOE based on the 4th harmonic was reduced by approximately 5%. The graphs for the samples under various conditions (chilled bark on, chilled bark off and frozen bark off) look very similar. However, the differences between the MOE calculated from the first 5 harmonics was highest when measuring the bolts in a frozen condition and smallest when probing chilled samples with bark on.

The graph for the pines looks similar, but only the first three harmonics were detectable when the bolts were measured chilled and the first four harmonics were detected in the frozen condition.

Differences between the MOE based on the first 5 harmonics of Group 3 (knots at ¼ and ¾ span)

The results of this group are comparable with the results of Group 1 (branches at either end).

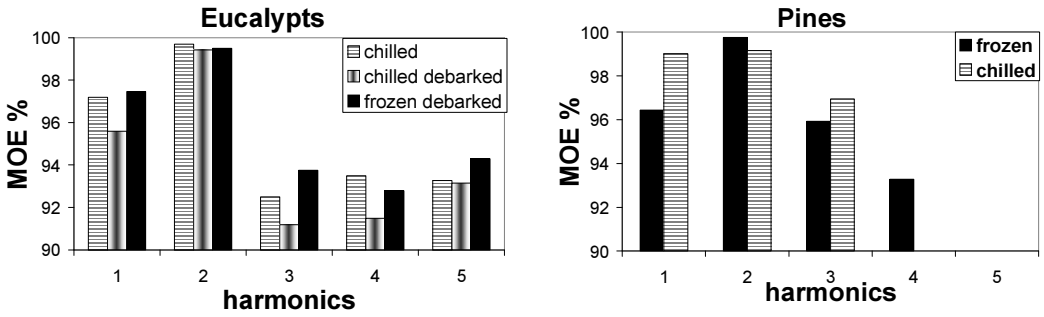

Figure 4-11: MOEs of the first five harmonics of group 3 (knots at 1/4 and 3/4).

The 2nd harmonic has its antinodes for pressure at exactly ¼ and ¾ of the span and again the MOE based on the 2nd harmonic, which causes no vibration but maximum force at the knotty areas, led to the highest MOE value. The MOEs calculated from the 3rd, 4th and 5th harmonics were significantly lower and again the wave patterns of these harmonics show areas of considerable movement at the locations of the knots.

Results of the re-evaluation of the resized samples

Group 1 of the eucalypts was resized by cutting off the knotty ends. Thus, the remaining middle parts of the logs, which had a length of approximately 1.2 m (diameter to length ratio of approx 1:10) consisted mainly of clearwood. Acoustic measurements on the chilled and resized bolts only revealed the first two harmonics. The reason for this is probably the higher diameter to length ratio. The average deviation between the 1st and 2nd harmonic was less than 0.5% (Figure 4-12). When measuring the frozen bolts it was possible to detect the first three harmonics with an average deviation of less than 1.2%.

Group 3 (knots at ¼ and ¾ of the span) was resized by crosscutting at midspan, so knots are now at the new midspan. Consequently two samples with approximately half the length of the originally bolt and a diameter to length ratio of approx. 1:8 were formed. Again it was only possible to detect the first two harmonics of the chilled bolts and the first three harmonics of the frozen bolts. The results are very similar to Group 2. The MOE calculated from the 1st harmonic was by approximately 9% higher than the MOE based on the 2nd harmonic. The MOE based on the 3rd harmonic was approximately 3% higher than the MOE than the MOE based on the 2nd harmonic.

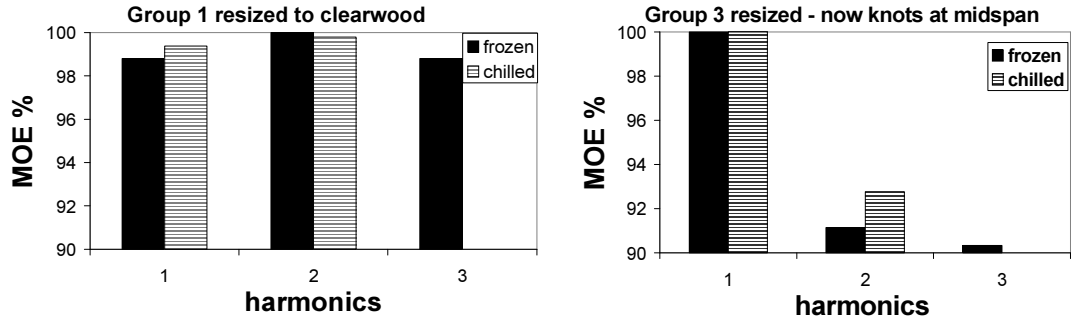

Figure 4-12: MOEs of the first five harmonics of resized samples.

4.4.3 Results of the compression tests

Twelve short (21 - 30 cm long) clearwood samples, six eucalypts and six pine bolts, with a diameter to length ratio of 1:3 were axially loaded in an Instron machine. The mini bolts were cut from the same stems that have been used in the tests described above. Two mini bolts from both species were cut from stems that showed a high acoustic MOE, two from a medium MOE stem and two from a low MOE stem. The deflection was measured by two LVDT's on opposite sides of the bolt. The measurements were conducted in both chilled and frozen condition. The deflection was measured over a distance of 6 cm. Each measurement was repeated three times. The average values for deflection on opposite sides of the bolt could differ by a factor of three in the chilled condition, whereas the deviation of frozen samples was

considerably smaller, but the deviation, in both chilled and frozen condition, of the three readings from each side was less than 4%. After the compression tests, five to six sticks (2×2 cm × length of the bolt) were cut from the mini bolts. Four outer wood sticks were taken from the positions on which the LVDT's had been attached and one stick was cut from the corewood including the pith. From three pine bolts a sample from in between the pith and the outer wood was cut. This sample was called transition wood sample Figure 4-13. No transition wood samples were cut from the other mini bolts owing to the smaller diameter of these samples.

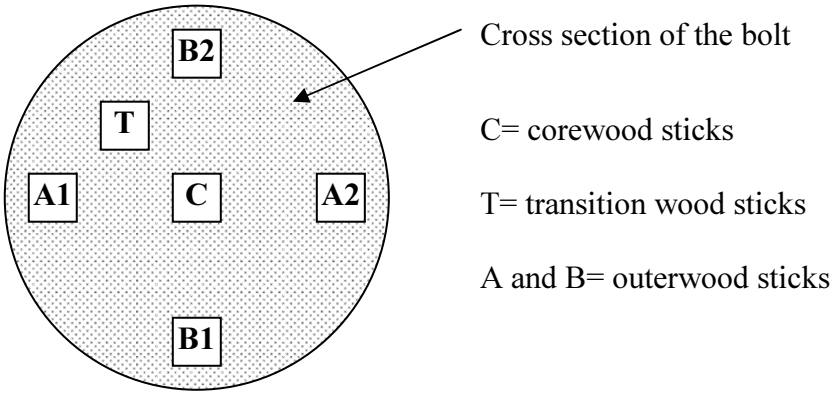

Figure 4-13: Cross section of the bolt showing the positions from where the sticks were taken.

The acoustic MOE of the sticks was measured in chilled and frozen condition.

Table 4-1shows the results of the chilled mini bolt tests and Table 4-2 shows the results of the frozen mini bolts. The values that are given in the MOE stem column refer to the acoustic MOE of the stem before they were resized. The readings displayed in the last three columns were taken from the sticks that have been cut from the mini bolts.

Table 4-1: MOE of the mini bolts as measured by static compression tests and by Woodspec in chilled condition. Values in GPa.

Sample	MOE full stem	MOE static	MOE acoustic	MOE acou. outerwood	MOE acou. corewood	MOE acou. trans. wood
Euc 1	8.07	8.80	8.93	11.13	7.33	
Euc 2	8.07	8.47	8.62	9.81	6.73	
Euc 3	9.1	8.95	9.33	9.43	8.35	
Euc 4	9.1	7.84	9.69	9.16	8.56	
Euc 5	9.61	10.77	10.56	13.41	10.62	
Euc 6	9.61	11.93	10.62	13.43	10.27	
Pine 1	4.32	4.83	4.85	4.87	2.33	
Pine 2	4.32	6.16	5.12	4.99	3.72	
Pine 3	6.30	6.64	5.09	5.17	3.51	
Pine 4	6.30	8.04	6.40	6.67	3.35	6.66
Pine 5	7.21	7.29	7.50	7.80	3.45	6.87
Pine 6	7.21	8.97	6.83	6.80	3.96	6.87

Table 4-2: MOE of the mini bolts as measured by static compression tests and by Woodspec in frozen condition. Values in GPa.

Sample	MOE full stem	MOE static	MOE acoustic	MOE acou. outerwood	MOE acou. corewood	MOE acou. trans. wood
Euc 1	11.28	9.06	13.43	13.89	11.87	
Euc 2	11.28	9.23	12.75	13.82	10.75	
Euc 3	14.1	11.49	15.72	16.84	14.99	
Euc 4	14.1	11.67	15.72	17.68	15.11	
Euc 5	12.95	8.19	13.67	14.21	12.98	
Euc 6	12.95	8.21	13.60	14.10	11.52	
Pine 1	6.97	5.30	7.17	8.02	5.40	
Pine 2	6.97	6.75	7.59	7.86	3.74	
Pine 3	9.66	8.43	9.91	9.94	6.60	
Pine 4	9.66	8.32	9.52	10.80	5.09	9.89
Pine 5	11.12	9.37	11.35	11.31	6.64	9.83
Pine 6	11.12	9.12	11.52	11.83	8.52	10.15

When comparing the MOEs measured from the chilled samples with the MOEs from frozen samples it was evident that the acoustic MOE of the chilled samples was approximately 35% lower than the acoustic MOE of the frozen samples. However, the static MOE was only lower by approximately 5% respectively. Therefore the difference between the acoustic and the static MOE of the chilled mini bolts was only 5-15% and not between 25-35% as for the frozen samples. In some cases the static MOE of the chilled bolts was even higher than the acoustic MOE.

The MOE of the outerwood of the bolts measured from four sticks per sample was by approximately 10% higher than the acoustic MOE of the bolt. The difference was more pronounced in the eucalypt bolts. The eucalypt corewood sticks showed a MOE that was approximately 10% lower than the acoustic MOE of the bolt. The corewood of the pine had a corewood MOE which was lower by about 30% compared to acoustic the MOE of the bolt.

The variation in MOE between the four outerwood sticks taken from one mini bolt was approximately 20%. In most cases the sticks which had a lower MOE were cut from position of the bolt that showed a greater deflection during the compression test. But in approximately 25% of the tests this relation was not true.

4.5 Discussion

The acoustic testing, using the resonance method, showed that the MOE of a stem calculated from different harmonics can vary by 10%. Acoustic measurements seem to be affected by the presence of knots within the sample. The average MOE of the 4^{th} and 5^{th} harmonic was considerably lower compared to the MOE as calculated by the first three harmonics (Figure 4-8). This might be partly explained by the fact that groups 1 and 3 had significantly lower values for the 4^{th} and 5^{th} harmonics, probably due to knots that overlapped with their nodes for pressure.

The difference between the MOEs as calculated by different harmonics was more pronounced for the eucalypt stems. When comparing the branch nodes of the eucalypt stems with the nodal whorls of the pine stems, it is obvious that the branch nodes in the eucalypt stems were spread over a distance of approximately 20-30 cm, while a nodal whorl in the pine stems forms a narrow zone of disturbance. Considering that the amount of disturbance caused by a knot is highly depending on the angle which is formed between the axis of the stem and the knot; this might give another reason why knots in the eucalypt stems had a greater impact on the MOE measurements. The branches of eucalypts usually grow in a steeper angle compared to branches of pines.

Moreover, the eucalypt stems tend to have knots of larger diameter compared to the knots of the pine stems.

The compression tests showed in some occasions displacements on one side of the bolt that were up to 20 times higher compared to the displacement measured on the opposite side of the sample. A questionable reason for this might be that the thin layer of plaster of Paris which was used during the compression tests to achieve optimal contact between the specimen and the load cell, might have influenced the measurements due to asymmetric loading. Moreover, it has to be taken into consideration that the static measurements based on the deflection measured by the LVDT's were conducted on a bolt which might slightly buckle under the applied load, this time because of natural inhomogeneity around the bolt. In such a case the LVDT unit at the compression side will give a considerably larger displacement than the LVDT attached to the opposite side. For most bolts (75%), the mean of the displacement of two readings taken from opposite sides of the mini bolt was close to the mean of all four readings of the bolt. This was also true for the acoustic MOE as measured from the four outer wood sticks from each bolt.

4.6 Conclusion

The results of this study led to the conclusion that knots have a modest impact on the acoustic behaviour of bolts. One important outcome of this study is that the MOE of a bolt can differ by almost 10%, depending on the positions of the knots and the harmonic that was used to calculate the MOE. The MOE calculated from harmonics where antinodes for pressure overlap with branch nodes was significantly higher compared to the MOE from harmonics where the antinodes overlap with areas of clearwood, whereas in clearwood samples there was less than 1.5% variation between the MOE as calculated by different harmonics.

The results for the eucalypts and the pines are very similar. However, the trend was that the eucalypt samples could support more overtones than the pine samples. Both

species could support more overtones in frozen condition. The MOE measured acoustically from frozen samples was 40-50% higher than the MOE measured from chilled samples. Moreover, it was observed that if the diameter to length ratio exceeds 1:10 it was often not possible to detect more than the first two harmonics, and if it gets larger than 1:4 only the first harmonic was obtainable. The compression tests using LVDT's to measure the deflection under axial loading led to MOE values that can be used to broadly validate the acoustic measurements.

Acoustic tests on small eucalypt clearwood sticks showed that the stiffness of the corewood is lower by approximately 15% compared to the stiffness of the outerwood. However, in the pine sticks the MOE of the corewood was lower by about 40%.

Chapter 5: Determination of the elastic an damping properties of laminated beams using various acoustic techniques

5.1 Introduction

The subject of this chapter is the modulus of elasticity (MOE) and the damping ratio in an engineered wood product having a controllable degree of inhomogeneiety. By altering the alignment of the 12 individual layers in the test specimens it is possible to create specific test configurations that are, for wooden products, highly repeatable. Artificial defects (holes filled with dowels) are introduced at specific positions along the span of the beams to investigate the impact of defects on elastic and damping properties. Various parameters, some of which are relatively new or at least seldom considered in acoustics of wood, are used to calculate the damping ratio of laminated beams. The study examines the potential use of the damping ratio to estimate mechanical properties of wood. It is also of interest to compare the response of the elastic properties and the response to the damping properties of the laminates caused by the introduced defects. Moreover, the impact of artificial defects introduced at specific locations along the beams on the fundamental frequency and its subsequent harmonics is investigated.

5.2 Literature review

In recent years several studies have been made which investigate the impact of artificial defects on the elastic and damping properties of timber.

Sandoz et al. (2000) used an ultrasound device, Sylvatest®, to investigate correlations (r^2) between the ultrasound parameters, for example stress wave velocity, maximum peak, integrated transmitted energy on a 500 ms time base, attenuation and the mechanical properties MOE and MOR. Thirty-two beams (9 x 16 x 320 cm) were studied using both four-point bending to evaluate their static MOE and MOR and the

data gathered by the ultrasound device Sylvatest®. The maximum peak value (V) of the transient signal and the transmitted energy were displayed in the time domain. The transmitted energy equals the area under the decay curve over the defined time base of 500ms. The attenuation measurement started at the maximum peak (greatest amplitude) and was calculated with an exponential approximation. The results showed a good correlation between velocity and MOE. The correlation between MOR and velocity was much weaker, which might be due to the fact that MOE is less sensitive to local defects than is the MOR where defects such as knots initiate the rupture mechanism (Table 5-1). However, they showed that MOR was best correlated with attenuation.

Table 5-1 : Correlations (r^2) between the ultrasound parameters and the mechanical properties MOE and MOR. Adapted from Sandoz et al. (2000).

	Velocity (m/s)	Peak max	Energy	Attenuation
MOE	**0.583**	**0.321**	**0.23**	**0.461**
MOR	**0.025**	**0.416**	**0.293**	**0.561**

In another experiment on a solid wood plank (2 x 17.5 x 200 cm) of high mechanical quality (presumably clearwood), Sandoz et al. (2000) made progressively deeper saw cuts (across the width) at mid-span. They showed that the propagation velocity was far less influenced by a progressive saw cut than was peak maximum and integrated transmitted energy (Table 5-2).

Table 5-2: Impact of a saw cut of increased depth at midspan on the velocity, maximum peak and energy of acousto-ultrasound in a wood plank (adapted from Sandoz et al 2000).

Saw cut depth %	Propagation velocity (m/s)		Maximum peak (V)		Energy (V.s)	
	value	loss %	value (10^{-3})	loss %	value (10^{-3})	loss %
0	5698	0	2.8	0	1.43	0
12.5	5698	0	2.48	11.4	1.31	8.4
25	5698	0	2.33	16.8	1.28	10.5
37.5	5633	1.15	2.18	22.1	1.28	10.5
50	5510	3.30	2.07	26.1	1.26	11.9
62.5	5405	5.14	1.84	34.3	1.22	14.7
75	5376	5.65	1.81	35.4	1.16	18.9
87.5	5291	7.14	1.66	40.7	0.86	39.9

The peak max dropped almost linearly as the depth of the saw cut increased. However, the transmitted energy had an equivalent loss of 40% after 87.5% of the board's depth had been cut, but responded strongly to the initial cutting to 12.5% of the board's depth and then showed little subsequent response until the two final saw cuts to 75% and 87.5% were made.

Divós et al. (2001) investigated the change in velocity and amplitude of a constant impact when introducing sawn notches halfway between the transmitter and the receiver which were placed 60 cm apart. The tests were conducted on Norway spruce (*Picea abies*) and beech (*Fagus sylvatica*) boards of a length between 80 – 200 cm and a cross-section of 2x4 cm through to 10x12 cm respectively (11-13% moisture content). Preliminary tests showed that within the first 60 cm the acoustic wave was not travelling as a plane wave front as significant differences within the cross-section of the boards were evident (near-field conditions). Beyond the initial so called near-field area a planar wave front takes over creating far-field conditions. According to Divós et al. (2001) the amplitude of the first received signal (TOF) decreases exponentially with distance once the signal is travelling in far-field conditions. Where 2mm wide saw cuts were introduced in 5-6 consecutive steps perpendicular to the longitudinal axis of the boards, the amplitude of the received signal was significantly more sensitive to the artificially created defect than was the velocity. Thus, Divós et al. (2001) concluded that measuring the signal amplitude is highly effective in terms of defect detection in wood, but this would require further research to be related to mechanical properties of wood.

From the literature that has been reviewd, it can be concluded that knots and artificial defects have an impact on the elastic and damping properties of timber. However, there there have been no studies that investigated the impact of knots on the various harmonics when using the resonance technique.

5.3 Material and Methods

The "PULSE" multi-channel analyser is a sophisticated acoustic tool that can measure a variety of acoustic parameters. Therefore, it was crucial to find the optimum test configuration for the tests conducted using "PULSE". Determination of the modal frequencies is relatively easy. The peaks that are displayed in the FRF refer to the frequencies at which the test specimen resonates. The peak with the lowest frequency is the fundamental frequency and subsequent peaks are its subsequent harmonics.

The determination of the modal damping is a more complex task. As mentioned, damping can be calculated by various methods. If the time domain is used (logarithmic decrement and impulse response method), it is crucial to obtain a very clear decay curve of the pulse, so that the required information can be extracted from that curve. One way of obtaining a clear decay curve of a pulse is to generate a pure tone, which can be the fundamental or one of the subsequent harmonics of the test specimen, and excite the specimen by means of a speaker.

During the pre-tests, various methods of supporting the specimen, different ways of excitation and different coupling agents to attach the accelerometer to the specimen were investigated.

5.3.1 Test materials

The damping ratio and the propagation speed of stress waves in wooden beams (*Pinus radiata*) cut from four laminated panels were investigated using various acoustic parameters. Each panel had a different orientation of the 12 individual layers. The advantage of testing laminated beams is that defects like knots or areas of variable properties (early and latewood, heart and sapwood or compression wood) are redistributed by peeling logs and gluing individual sheets together. The result is a reconstituted panel of improved quality compared to the raw wood material. For example, enhanced strength for LVL; or in terms of plywood reduced shrinkage and

more homogeneous strength properties along the length and across the width of the panel.

By altering the orientation of the individual layers it is possible to control the degree of inhomogeneity in the panel. This provides ideal conditions for investigating the impact of inhomogeneity on acoustic properties of wood. The beams were cut from four laminated panels (2.40 m in length, 1.20 m in width and 40 mm thick), each of which had a different combination of orientations amongst the 12 individual layers. The panels were cold pressed for 20 hours using a commercial adhesive, Sylvic S3 as hardener and resin 4260 with 69.9% formaldehyde. The configurations of the panels were as follows:

- Panel 1: All plies were laid up with the grain direction parallel (as in laminated veneer lumber, LVL-L)

- Panel 2: Four plies were laid up with their grain direction lying perpendicular to the length of the panel and sandwiched between four-face plies laid up with their grain direction parallel to the length of the panel (four longitudinal-four transverse- four longitudinal, 4L4T4L).

- Panel 3: Six plies were laid up with their grain direction lying perpendicular to the length of the panel and sandwiched between three face plies laid up with their grain direction parallel to the length of the panel (three longitudinal-six transverse-three longitudinal, 3L6T3L).

- Panel 4: Conventional plywood with alternate layers of veneers lying parallel or perpendicular to the length of the panel, (alternately longitudinal and transverse). To maintain symmetry with respect to the neutral axis of plywood, both of the core plies were laid up with their grain direction lying parallel to the length of the panel.

(adapted from Chauhan et al., 2005)

Beams can be either cut along the longest side of the panel or perpendicular to it, generating pairs of opposites. Therefore it is possible to cut eight different configurations from the four panels, each of them having a different degree of inhomogeneity. Moreover, the beams can be measured when they are supported in a

way that individual layers are aligned horizontally or vertically. For this study, first, several beams were cut from along the length of every panel. Then, a few beams were cut across the grain (width direction) from the LVL aligned panel, so the grain direction of all plies in these two beams was perpendicular to its longitudinal axis (LVL-Transverse). The cross section of the beams was chosen to be 40 × 40 mm to have the same depth and width whether the beams were aligned with the individual layers lying horizontally or vertically. The beams were cut to a length of 1.963 m, which was the length of the shortest panel. The same panels had been used for acoustic testing previous to this study (Chauhan et al., 2005).

In addition, three clearwood beams of *Pinus radiata* of the same dimensions were cut. The annual rings of the beams were aligned horizontally (or vertically depending on the reference level).

5.3.2 Consequences of supporting specimens at various positions

Tests were undertaken with the specimen supported at two points at various positions along the span. The effect of location of the supports, using triangular wedges of foam as supports, on the energy content of fundamental and subsequent harmonics of the specimen was negligible (Figure 5-1). The maximum peak of the fundamental was taken as 100% and the peaks for subsequent harmonics were expressed in relation to that. The strongest contribution of subsequent harmonics was evident when supporting the beam at both ends. However, regardless of where the specimen was supported, the peak of the fundamental was always by far the greatest. The test was repeated and showed similar results when the specimen was supported freely using two wire slings.

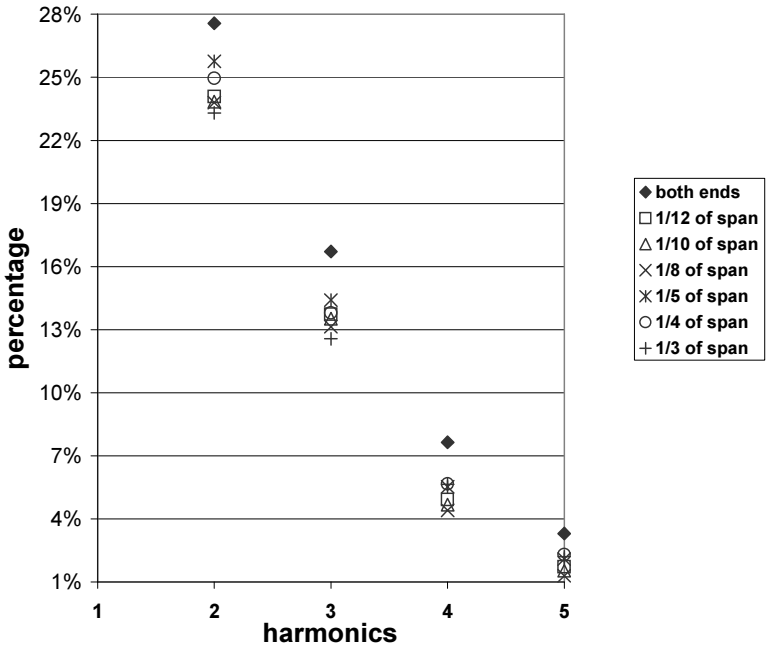

Figure 5-1: Consequences of the support position using a hammer as excitation source and triangles of foam as support on the max peak of the fundamental (100%) and subsequent harmonics.

5.3.3 Mounting the accelerometers on the specimen

To achieve optimal mounting between the accelerometer and the vibrating surface of the specimen, it is crucial to use a method of fixing that is as rigid as possible. Any flexibility between the accelerometer and the specimen would produce an unwanted 'mounting resonance' which would then reduce the upper frequency limit of the device. The best method of coupling is a steel stud that screws into both the vibrating surface and the base of the accelerometer (Smith et al., 1996). However, the accelerometers used in this experiment were not equipped with such a mechanism. Three coupling agents were considered: beeswax, vaseline and thermoplastic glue spread with a hot glue gun. All three methods gave highly repeatable results when testing the same beam. The main disadvantage of beeswax, and particularly vaseline, is that the bonding between the accelerometer and the specimen is relatively fragile. This would cause problems when drilling holes into the beams which would

inevitably result in some jiggling of the beam that might loosen or break the bond. Therefore, the thermosetting glue (Loctite glue sticks) was chosen.

5.3.4 Different ways of exciting the test specimen

During the pre-tests four different excitation methods to launch compression waves into the sample were used. A piezoelectric accelerometer was fixed with thermoplastic adhesive in the centre of the other end to acquire the structural axial response of the beam.

The first excitation method was a hammer impact with the modal hammer that can be connected to the "PULSE" unit to record the impact force and the rise time of the signal. For the other three methods a speaker was used to excite the specimen. The speaker can be used to generate pure tones, which correspond to the fundamental frequency and the various theoretical harmonics of the test specimen; a sweep tone over a set frequency range; or pink noise which is a type of random noise consisting of equal energy per logarithmic units of bandwidth (such as an octave or 1/3-octave).

For the first test series the fundamental frequency was generated by a speaker, and the test was repeated over the following distances between the speaker and the end of the specimen: 2 mm, 1 cm, 2 cm, 3 cm, 4 cm, 5 cm, 10 cm, and 15 cm. The energy (5 mVrms) of the signal was kept constant. The response for the fundamental and its subsequent harmonics was displayed using a FFT-analyser. The energy content of the fundamental was taken as 100% and the energy content of subsequent harmonics was characterised in relation to that. In other words, the harmonic distortion was measured. At a distance of 2 mm, the response showed a strong fundamental, a 3rd harmonic with approximately 20% energy of the fundamental and a weak 5th harmonic with approximately 1.5% energy respectively. When the distance between the speaker and the specimen was increased from 2 mm to 10 cm, a change in the transmitted energy content was evident. However, there was no uniform pattern which could be related to the change of distance between the speaker and the specimen.

It appears that higher frequencies become relatively stronger with increasing distance because the maximum relative response (% of 1st harmonic) for the 5th harmonic was observed at 10 cm distance. This might be due to the fact that sound at the higher frequencies is emitted in a narrower beam (like a torch) and does not spread so widely with distance. The fact that there is no uniform pattern in change of energy when changing the distance between the speaker and the specimen might be due to resonance or near-field interaction occurring within the air gap between speaker and specimen. Moreover, the various harmonics have an optimum distance at which they penetrate the specimen at a maximum level. The distance between speaker and specimen was kept constant at 5 cm and the energy of the generated pure tone (fundamental) was decreased in stages: 5 mVrms, 4.5 mVrms, 4 mVrms, 3.5 mVrms, 3 mVrms and 2.5 mVrms. When this was done, the energy content of the fundamental and subsequent harmonics decreased proportionately. At an energy level of 2.5 mVrms the subsequent harmonics were hardly detectable.

Tests using a hammer as excitation source showed that it is difficult to obtain a clear decay curve from which to calculate logarithmic decrement. The first few peaks of the decay curve usually do not show a logarithmic decay pattern (Figure 5-2).

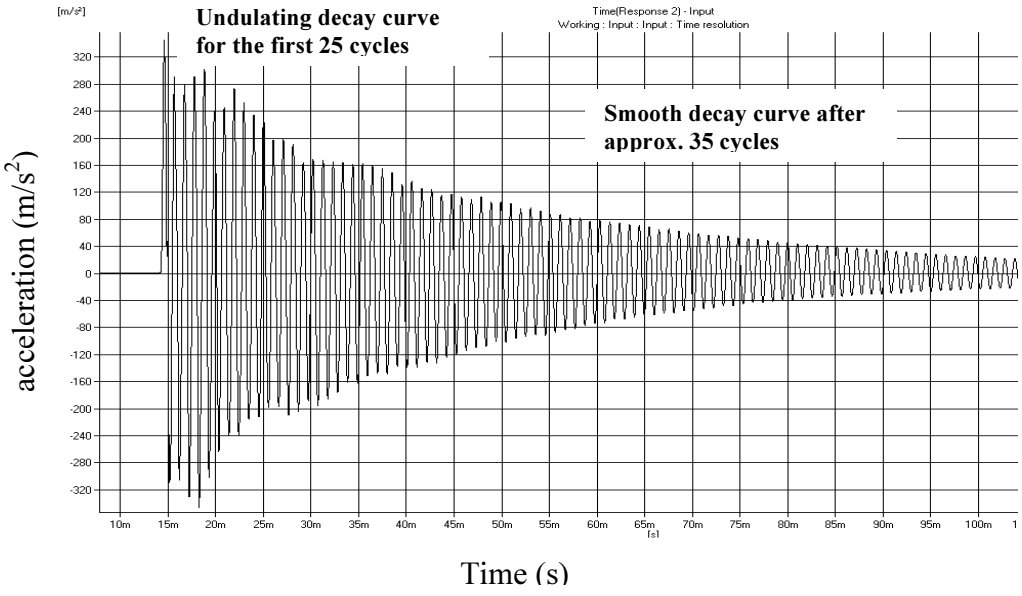

Figure 5-2: Logarithmic decay curve of a 4L-4T-4L beam when exited by a hammer tap.

This is probably due to the wide frequency spectrum that is introduced by a hammer impact, and the way they interact with each other. However, frequencies other than the fundamental and its subsequent harmonics die away quickly (probably during the first 10 cycles) and the higher harmonics decay relatively fast owing to the fact that higher frequencies are damped at a much higher level than lower frequencies such as the fundamental frequency. Therefore, after approximately 20 to 40 cycles the fundamental should be by far the strongest frequency within the remaining signal, and reliable measurements should be obtainable when calculating from the 30^{th} cycle onwards (Figure 5-2). To increase the accuracy of the damping ratio calculated from the logarithmic decay curve, the number of cycles (n) between the peaks from which the readings of maximum amplitude are taken, should be reasonably large. Test where n was chosen to be 15 rather than 5 decreased the spread of the damping ratio by approximately 15% when the test was repeated five times.

However, a broadband impact was chosen as it combines many advantages that cannot be realised when the specimen is excited by a pure tone. This means that various modes can be identified in the frequency domain by a single hammer tap and that the modal hammer that was used to excite the specimen could be connected to the "PULSE" unit which then allowed calculating the energy and the rise time of the impact. The latter is crucial to enable a cross-correlation between the impulse and its response. Moreover, a hammer hit seems to be the more sophisticated excitation method in terms of field work, especially when standing trees are tested.

5.3.5 Experimental layout

It was decided to use holes of increasing diameter instead of progressive saw cuts to mimic defects in timber. Pre-test experiments with progressive saw cuts indicated that this method is not suitable when using the resonance technique. A progressively larger peak at approximately half the frequency of the fundamental was evident with increasing depth of cut: this was probably due to some of the compression wave being reflected at the saw cut and travelling back in the opposite direction. Thus, by

introducing a saw cut at midspan the beam is behaving in part as if it were two beams of half the original length.

There are advantages of drilling holes to introduce artificial defects. Not only is the hole closer to the shape of a knot, it also can be placed at the centre of the cross-section (centreline knots) or at the edge of the cross section (edge knots) instead of always starting from one face as a saw cut must. Moreover, the waves hitting the hole are reflected in various directions, and will be attenuated quickly. Filling the holes with dowels of corresponding size keep the mass of the beam reasonably constant. Glue was used to hold the dowel in place: this was necessary because when the hole needed to be enlarged the ring-saw tool tip has to be accurately located at the centre of the dowel plugging the hole. Dowels were fitted either perpendicular or parallel to the individual layers of the beam.

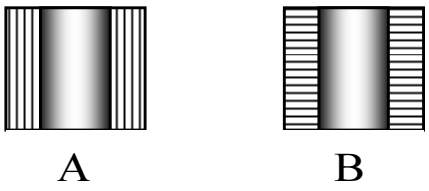

Figure 5-3: A centreline dowel drilled parallel (A) and perpendicular (B) to the individual layers of the beam.

However, pre-tests revealed that there was no noticeable difference in either the MOE or the damping ratio when the holes were not filled with dowels.

Every step of the tests was repeated three times before the knot size was increased. The graphs that are displayed below are based on the average of those three readings. The repeatability of the tests was extremely high, particularly for the “PULSE” auto-damping function, the impulse response method and the frequency measurements of the various harmonics. The “PULSE” system was set up in so that all these parameters were captured at the same time. Thus they are totally comparable as, although there might have been a slight impact depending on the way the modal hammer hit the specimen (angle, power and position), those irregularities were kept to a minimum.

The tests were conducted at room temperature (approximately 20˚C), and the moisture content of the beams was approximately 12%.

5.4 Results and discussion

5.4.1 Different methods of calculating the damping ratio

Four different methods of calculating the damping ratio of a laminated beam are compared with each other (Figure 5-4).

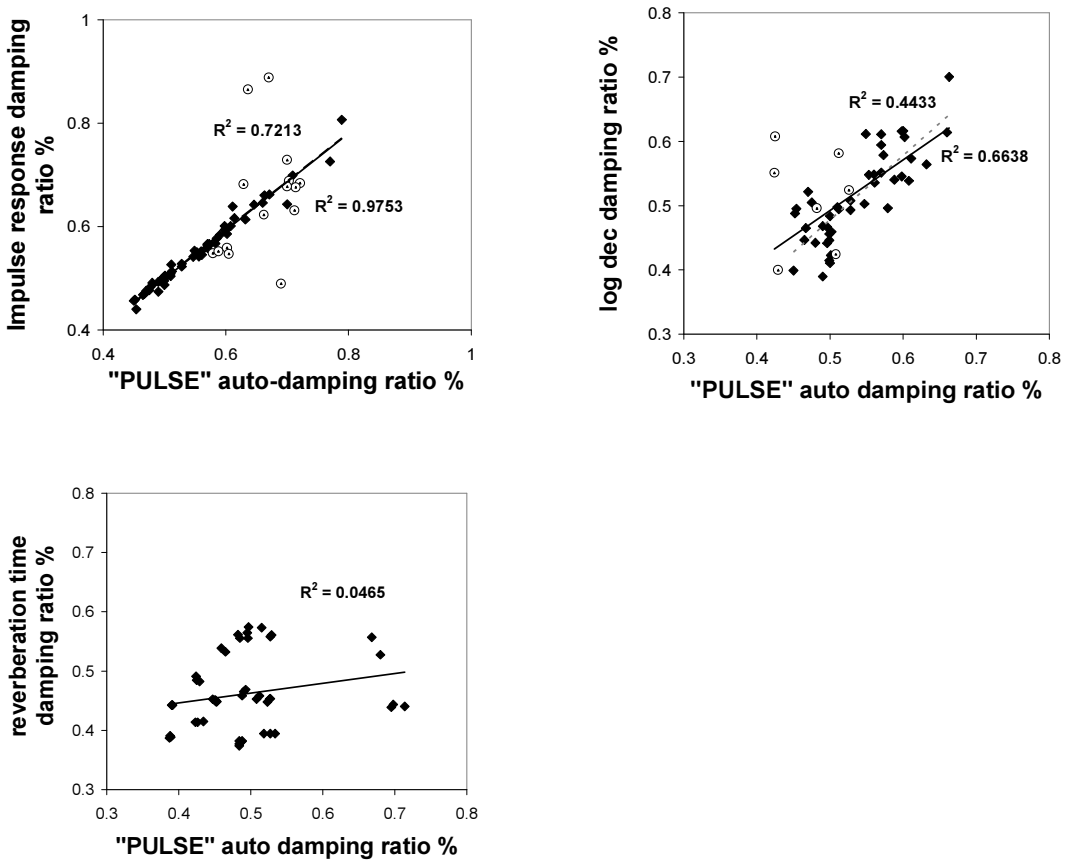

Figure 5-4: Correlation between pulse auto damping and the damping ratio based on the impulse respond method, logarithmic decrement and reverberation time

Figure 5-4 shows that the correlation between the "PULSE" auto-damping ratio and the impulse response (r^2= 0.98) were very strong. A moderate correlation was found between the "PULSE" auto-damping ratio and the logarithmic damping ratio (r^2= 0.66) and a very weak correlation for the reverberation time (r^2= 0.05), respectiveley. It was observed that the correlations calculated on the measurements of the plywood beams were significantly lower (displayed in hollow circles in Figure 5-4). The higher values for r^2 exclude the plywood beams. The lower correlations on the plywood beams might have been caused by the degree of inhomogeneity which is the greatest in the plywood beams. The "PULSE" auto-damping ratio seems to be less influenced by the degree of inhomogeneity. At least the measurements of the "PULSE" auto-damping function on the plywood beams were more consistent when compared with the other methods. Therefore, the "PULSE" auto-damping function was chosen to calculate the damping ratio. Whenever a damping ratio is given in the results part of this study it was calculated by the "PULSE" auto-damping function.

The logarithmic decrement method seems to be unsuitable when testing materials with a high degree of inhomogeneiety. Moreover, the logarithmic decrement method is usually applied when only one resonance frequency is present in the system (Brüel & Kjær, 1994). The other methods that are based on the time domain circumvent this problem by filtering the signal to the mode of interest.

The further down the decay curve the measurements are taken from, the more repeatable (accurate) the results become. If the measurements are taken right from the start of the decay curve, the logarithmic decrement is significantly higher compared with those values taken from further down the decay curve. This is probably caused by the higher harmonics which are damped at higher levels and therefore are not present further down the decay curve. For the first 20 or so cycles, the overall pattern of the decay curve usually did not show a smooth logarithmic shape (Figure 5-2). The number of cycles which showed undulation depended greatly on the configuration of the beam and the size of the knots that were introduced. The trend was that the smoothness of the decay curve decreased with the degree of inhomogeneity of the beams and with knot size.

It is also noticeable that the peaks further down the curve were sharper and showed less undulation (Figure 5-2). Nevertheless the repeatability is not sufficient. All these observations underline that it is not appropriate to use log decrement measurements on systems that are excited in a way that creates multiple resonances, especially when they have a high degree of inhomogeneity.

To demonstrate that logarithmic decrement measurements and the Q factor can be equally used to calculate the damping ratio of homogeneous materials, a plastic cylinder (201 cm × 10 cm) was tested. Both methods showed highly repeatable results. The damping ratio using the Q factor method was 1.42%. Using logarithmic decrement this compares to a damping ratio of 3.8% when measured between the 1st and the 10^{th} cycles, 1.84% when measured between the 10^{th} and the 20^{th}, 1.54% when measured between the 20^{th} and 30^{th} cycles and 1.42% when measured between the 30^{th} and the 40^{th} cycles. This indicates that after the first 30 or so cycles, both measurements can be applied equally to estimate the damping of a homogeneous material.

Cai et al. (1997) pointed out that the classical logarithmic decrement method only makes use of the peak amplitudes of the decay curve to calculate the damping properties while the other sampling points are not taken into consideration. However, it is not possible to obtain the amplitudes to a sufficient degree of accuracy. The higher the sampling rate, the more accurate are the peak amplitudes. In this study a sampling rate of 15.26 micro-seconds was used and most of the peaks look ”blunt”, indicating that the real peak value is higher. According to Cai et al. (1997) the following parameters can also lead to inaccurate logarithmic decrement measurements: coupling of transducers and material, irregularity of material and electrical noise.

5.4.2 Velocity of sound and damping ratio of the beams

Table 5-3 summarises the results of the first test series in which three beams of each configuration were tested before artificial knots were introduced. As expected, the velocity of sound in the LVL-L beams was the highest at 4799 m/s (100%) and was the lowest in the beam with all transverse laminates at 989 m/s (20.6%). The values for the plywood and the 3L-6T-3L beams, which both have six longitudinal and six transverse oriented layers were 3487 m/s (72.7%) and 3251 m/s (67.8%). The velocity of sound in the 4L-4T-4L beams, where the proportion of longitudinal to transverse layers is 2:1, was 3863 m/s (80.5%).

In the clearwood beams, the velocity was 4868 m/s and slightly higher than the velocity of the LVL-L beams: the clear, solid wood beams had narrow, flat rings and came from stiff outerwood of trees, whereas the LVL-L was a mixture of veneer from unknown parts of peeled logs.

Table 5-3 Velocity, based on the 1st, 2nd and 3rd harmonic, and damping ratio (%) of the tested beams before artificial knots were introduced (average of 3 beams per configuration).

	Velocity 1st	Velocity 2nd	Velocity 3rd	Velocity average	Damping ratio %
LVL-L	4749	4816	4831	4799	0.389
Ply	3460	3515	3488	3487	0.511
4L-4T-4L	3865	3890	3852	3863	0.447
3L-6T-3L	3286	3282	3185	3251	0.505
LVL-T	983	992	993	989	1.55
Clearwood	4848	4885	4871	4868	0.374

The Damping ratio (%) was lowest for the LVL-L beams, at 0.389 (25.1%) and was highest at 1.55 (100%) for the LVL-T beam. The values for the plywood and the 3L-6T-3L beams were 0.511 (33%) and 0.505 (32.5%) and the damping ratio for the 4L-4T-4L beams was 0.447 (28.9%). The damping ratio of the clearwood beams was 0.374 which was very similar to the LVL-L beams.

When holes were drilled at specified locations along the beam, the frequency of the fundamental and its subsequent harmonics did not always drop uniformly. Table 5-4 lists the proportion of the cross-section occupied by dowels of various diameters as well as the percentage of the beam volume that is occupied by the dowels.

Table 5-4: Percentage of cross section and percentage of beam volume influenced by dowels of various diameter.

Diameter of dowel (mm)	Percentage of cross section (%)	(volume dowel / volume beam)× 100
6	15	0.036%
10	25	0.1%
14	35	0.256%
20	50	0.4%
25	62.5	0.625%
32	80	1.024%

The relationship between the frequencies of the harmonics changed where the knots were drilled at different positions, for example, at midspan or at ¼ and ¾ of the span. To illustrate this phenomenon, the velocity as based on the first three harmonics was plotted against the total percentage knot volume of the beam (Figure 5-5).

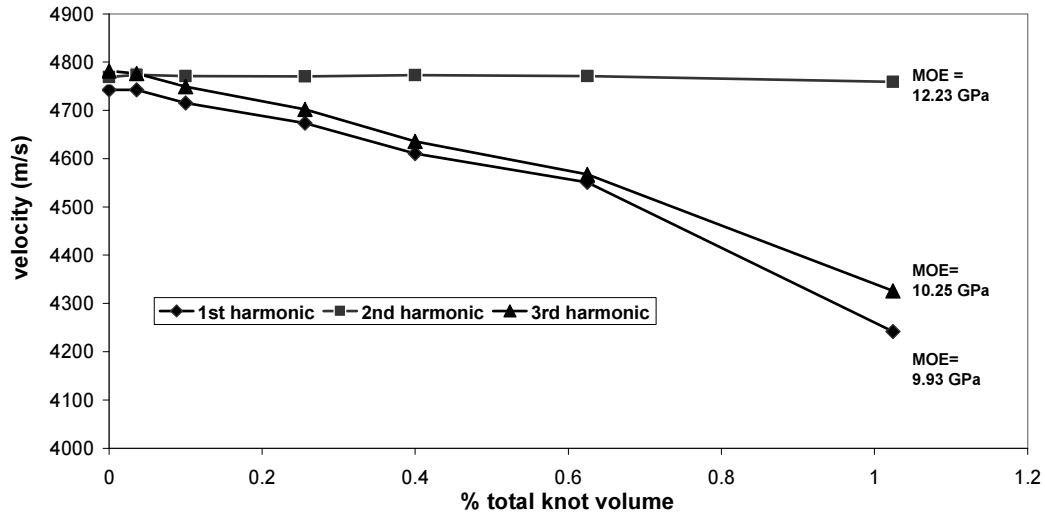

Figure 5-5: Velocity based on the first 3 harmonics versus percentage knot volume in a LVL-L beam with knots at midspan (size of the knot increases from left to right).

Figure 5-5 shows that the velocities calculated from the 1st and 3rd harmonics dropped almost linearly and with a very similar slope when the % knot volume increased (r^2 of 0.99 and 0.97). However, the velocity based on the 2nd harmonic did not change at all.

When the holes are drilled at ¼ and ¾ of the span (Figure 5-6) the velocity based on the 2nd harmonic was decreased sharply with increasing knot size. The 3rd harmonic was least affected and the 1st harmonic data lay somewhere in between those two.

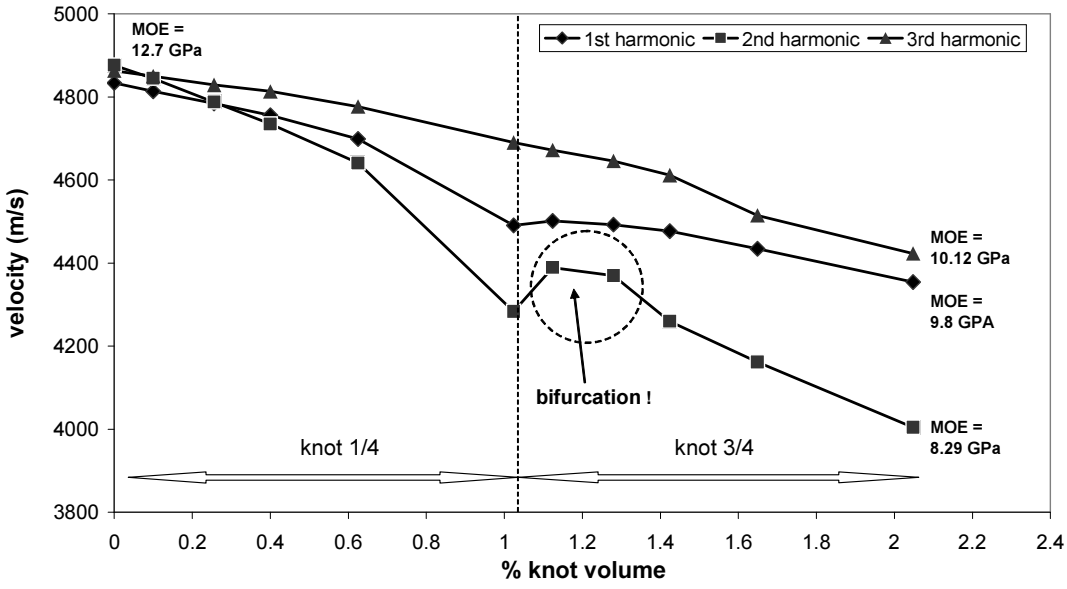

Figure 5-6: Velocity based on the first 3 harmonics versus percentage knot volume in a LVL-L beam with knots at 1/4 and 3/4.

The abrupt increase of velocity of the 2nd harmonic, when a second dowel was introduced at ¾ of the span, can be explained by bifurcation of the frequency spectrum in this range. The effects of bifurcation on the calculation of the elastic and damping properties are discussed in chapter 5.5.1.

When various 25 mm centreline holes were introduced at specific positions along the span of an LVL-L beam the velocities based on the first 3 harmonics were affected more similar (Figure 5-7). This test is analysed in detail on p 111 ff.

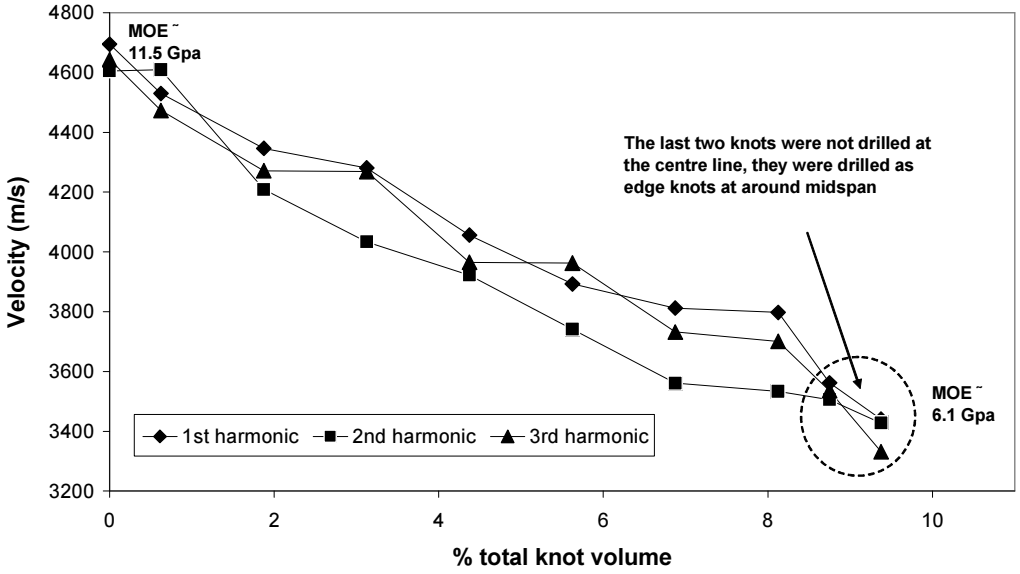

Figure 5-7: Velocity based on the first 3 harmonics versus percentage knot volume in an LVL-L beam with 25 mm knots at various positions along span.

The correlation coefficients (r^2) of these 3 tests for the velocity versus knot size (percentage knot volume) were between 0.54 and 0.99, which indicates that there is a reasonable relation between velocity of sound and knot size. However, if the velocities were to be used to calculate the MOE, different results would be obtained depending on the harmonic from which the velocity is taken. For the knot at midspan, (after the 32 mm dowel was drilled in) that would mean that the MOE based on the 1st harmonic was 9.93 GPa (Figure 5-5). The MOE based on the 2nd harmonic was 12.23 GPa and the MOE based on the 3rd harmonic was 10.25 GPa. Thus, a difference of 19% was evident between the MOE based on the 1st and the 2nd harmonic.

5.4.3 Influence of knot size and knot position on the damping ratio and the MOE

Knots at midspan

Figure 5-8 shows the effect on the damping ratio and the MOE (based on the 1st harmonic) of stepwise increases in the diameter of the knots at midspan which were drilled perpendicular to the individual layers (or growth rings) of the beams.

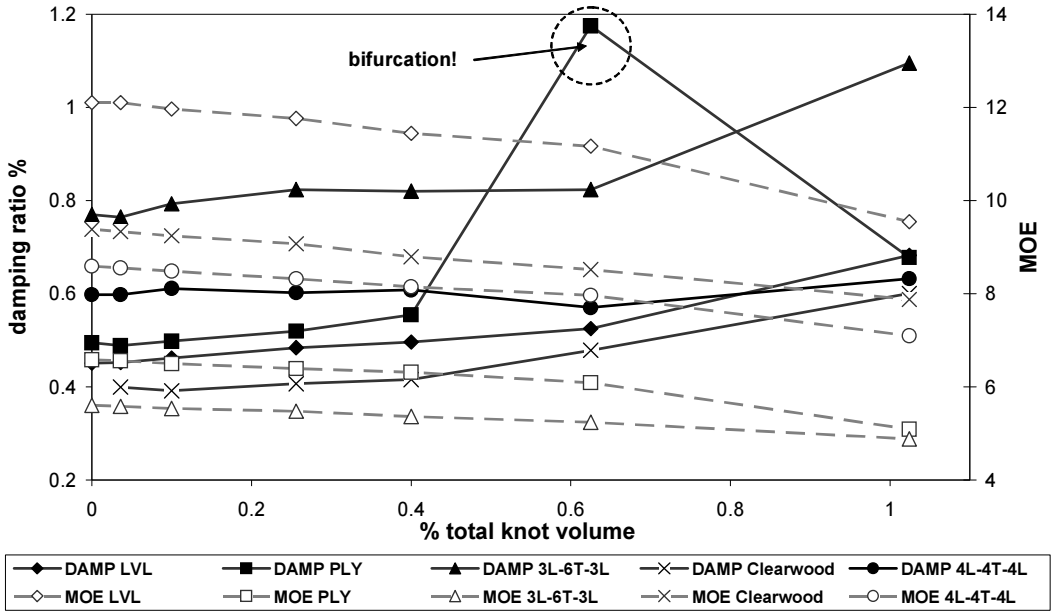

Figure 5-8: Influence of knots of increasing diameter at midspan on the damping ratio (solid black lines) and MOE (grey dashed lines) when drilled perpendicular to the individual layers.

The damping ratio increased by approximately 40% by the time the largest 32mm dowel had been introduced. In general, the damping ratio increased almost linearly up to the 20 or 25mm dowel. When the 32mm dowel was introduced, which occupies approximately 80% of the cross-section at midspan, or 1.024 % of the total beam volume, the damping ratio increased at a significantly higher rate.

It was obvious that the plywood beam showed an unusually high damping value when a 25 mm dowel was introduced to a beam. Surprisingly the damping ratio decreased again after the 32 mm dowel was drilled in. A second plywood beam was tested to confirm this unusual pattern; indeed, the second plywood beam test gave very similar results. These unexpected high values are probably a result of a split-peak or broadened peak of the fundamental which occurred at these stages of the experiment. This phenomenon is discussed in Chapter 5.5.1.

The damping ratio of the clearwood beam (without artificial knots) was 0.4%. A similar damping ratio (0.2% – 0.6%) was reported by Cai et al. (1997) for Douglas fir.

With increasing knot size the MOE (displayed as dashed grey lines) of all beams decreased almost linearly, falling by approximately 20% for the largest dowel (32 mm). However, bifurcation or broadening of the fundamental did not seem to have as much of an impact on the MOE as it had on the damping ratio.

When holes were drilled perpendicular to the individual layers, both the longitudinal layers and the transverse layers were cut. However, when the holes were drilled parallel to the layers, the situation was very variable depending on the position of the hole and the orientation of the unaffected veneer layers. Figure 5-9 illustrates the situation for a 4L-4T-4L beam having two edge knots 25 mm in diameter. Figure 5-9 shows that acoustic waves at midspan were forced to travel through wood of transverse orientation as the fastest path (the longitudinal layers) was completely cut and filled with a dowel which had its grain aligned perpendicular to the long axis of the beam.

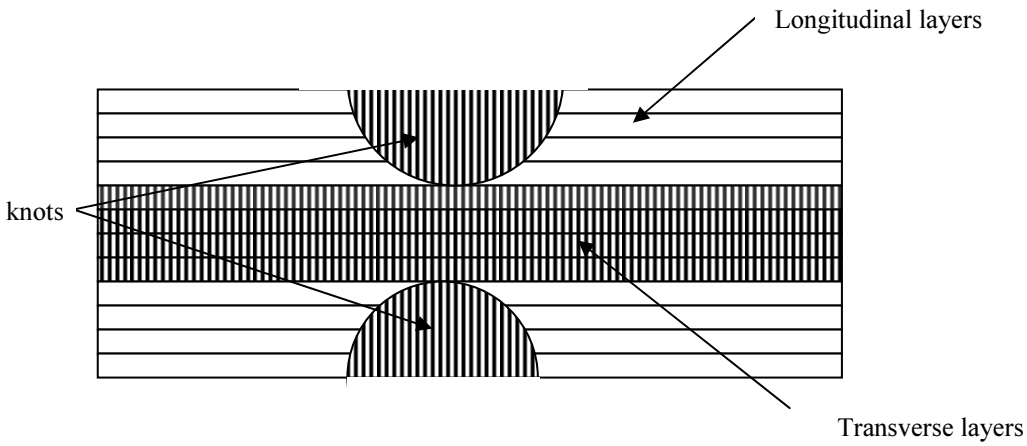

Figure 5-9: 25mm edge knots drilled parallel to the layers at midspan either side of a 4L-4T-4L beam.

A hole that is drilled through the centre and parallel to the layers would mainly (depending on its diameter) cut through the transverse layers of a 4L-4T-4L or a 3L-6T-3L beam. Hence the cut out material would be replaced by a dowel which has the same grain orientation as the surrounding transverse layers. Theoretically this should not have a significant impact on either the damping ratio or the MOE. On the other hand, a knot drilled parallel to the layers of plywood or a LVL-L beam would always also affect longitudinal layers, regardless of whether it is placed at the centre or on the edge.

When the holes were drilled parallel to the centre of the beams, the LVL-L beam showed the same increase of damping ratio and the same decrease of MOE as in the test where the holes were drilled perpendicular to the layers (Figure 5-10). As expected, the sandwiched beams showed different results. The 4L-4T-4L and the 3L-6T-3L beam were largely unaffected until the diameter of the dowel became bigger than the sandwiched transverse layers.

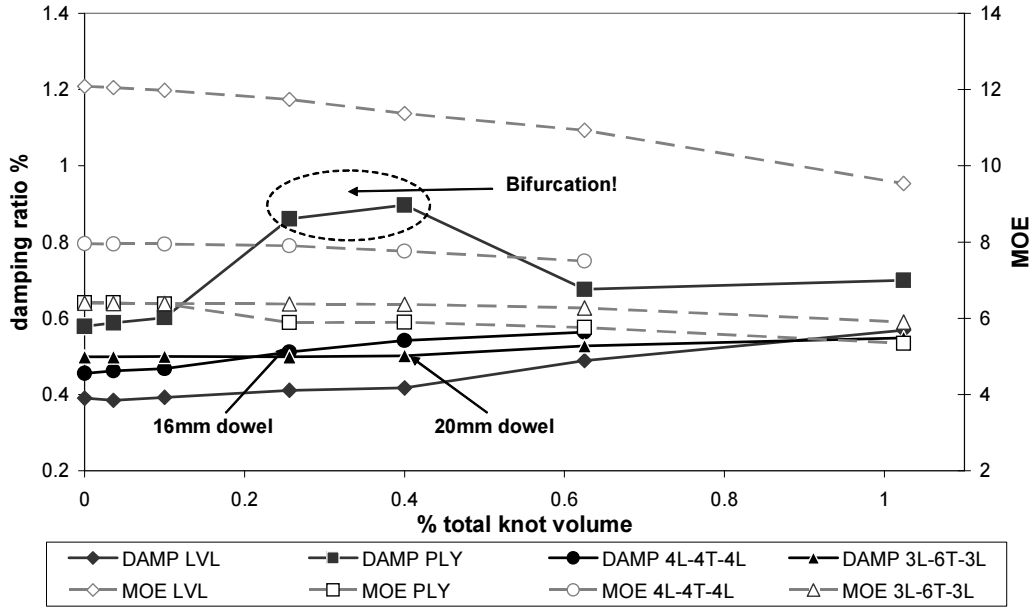

Figure 5-10: Influence of knots of increasing diameter at midspan on the damping ratio and MOE when drilled parallel to individual layers.

This is the case when a 16mm centreline dowel is fitted parallel to the layers of a 4L-4T-4L beam and a 20 mm dowel in a 3L-6T-3L beam respectively. Once those dowels were fitted, both the damping ratio and the MOE were affected. The damping ratio of sandwiched beams only increased by less than 10%, and likewise the MOE dropped less than 10%. The test for the 4L-4T-4L beam was stopped after the 25 mm dowel was fitted as it started to delaminate while the 32 mm hole was being drilled.

Where two hemispherical holes (edge knots) were drilled perpendicular to the layers of various beams at midspan (Figure 5-11) the graph shows similar results to the case where the holes were drilled perpendicular to the layers but through the centre at midspan (Figure 5-8). In both cases all of the layers were cut. The LVL-L beam showed a systematic increase in the damping ratio from 0.39 to 0.59, whereas the plywood beam again showed the highest damping ratio before the largest knot was introduced (Figure 5-11). As in the previous test, this peak occurred when approximately 0.6% of the beam's volume was filled with a dowel.

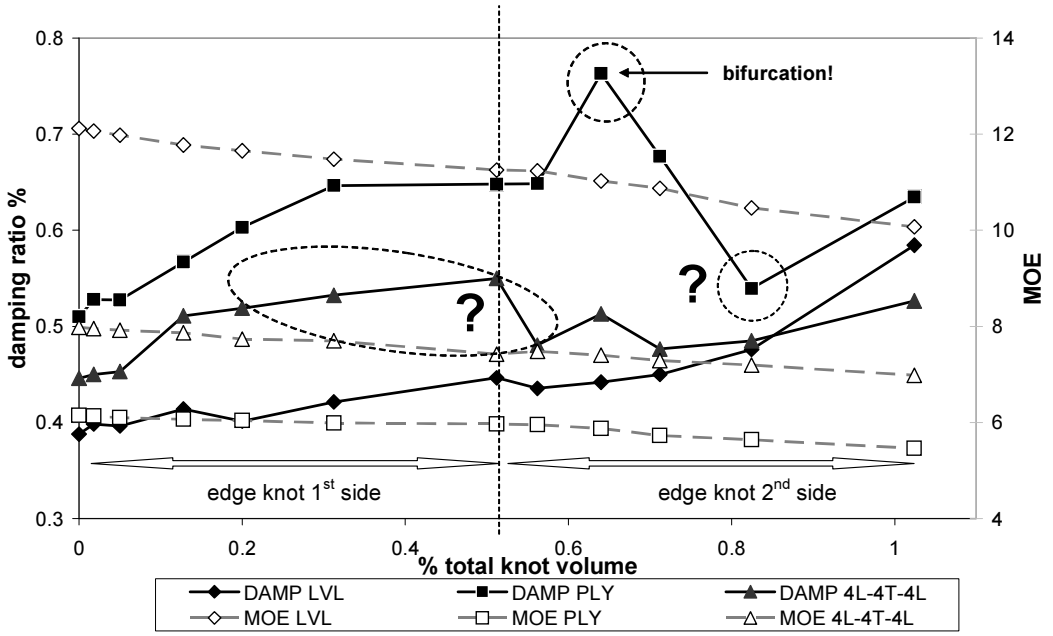

Figure 5-11: Impact of edge knots at either side at midspan drilled perpendicular the individual layers of the beams on the damping ratio and the MOE.

The damping ratio of the plywood beam and the 4L-4T-4-L beam showed no consistent response to an increasing knot volume of the beam. In contrast, the MOE of all three beams investigated in this test showed an almost linear decrease with increasing knot volume of the beam.

The situation was different where the holes were drilled parallel to the individual layers of the beams (Figure 5-12). The 3L-6T-3L and the 4L-4T-4L beam showed a significantly higher damping ratio (approximately 1.7 %) for this test series compared with the previous test Figure 5-11, where the knots were drilled perpendicular to the layers at midspan. The points at which the outer longitudinal layers were completely cut at midspan corresponded to the steepest slopes in Figure 5-12, that is, where the three longitudinal outer layers of one side of the 3L-6T-3L were cut after the 20 mm dowel was put in place. The 3L-6T-3L and the 4L-4T-4L curves for the damping ratio are slightly out of phase, which is probably caused by the additional longitudinal outer layer of the 4L-4T-4L beam requiring larger holes to be cut to penetrate this extra

longitudinal layer of veneer on either side. Unfortunately, it was not possible to finish the tests for the two sandwiched beams as they broke during the drilling process.

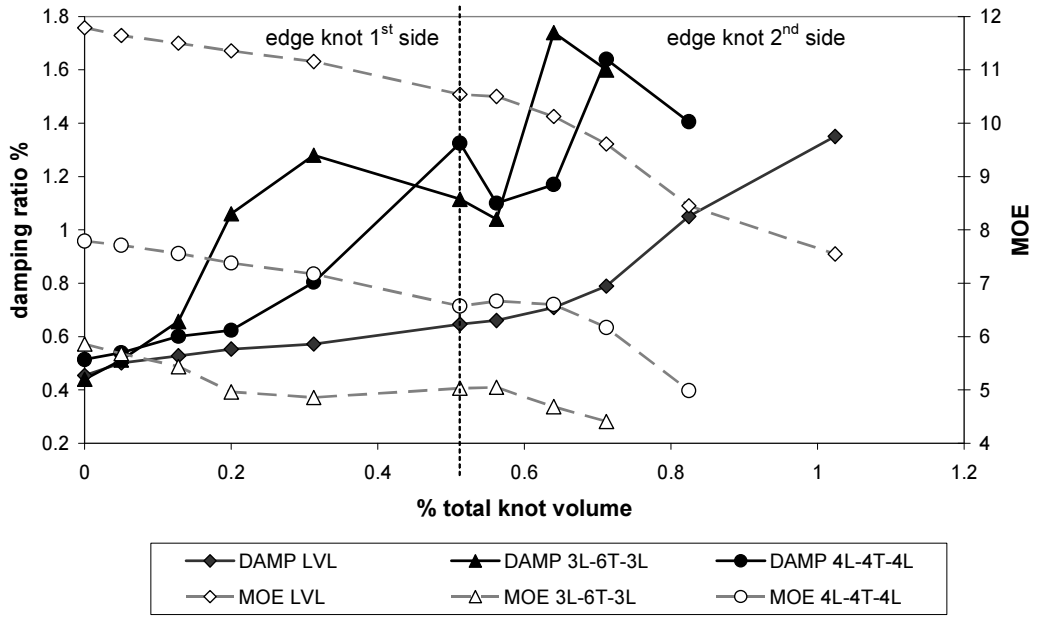

Figure 5-12: Impact of edge knots at either side at midspan drilled parallel the individual layers of the beams on the damping ratio.

The graphs for the MOE and the damping ratio of the LVL beam almost perfectly mirror one another, indicating that MOE and damping ratio are affected very similarly when the knot volume of edge knots was increased at midspan (it should be noted that the two Y-axes have different scales).

Knots at ¼ and ¾ of span

Figure 5-13 shows the impact of knots at ¼ and ¾ of the span on the damping ratio and the MOE. The MOE here was has been calculated from the 2nd harmonic, as the 2nd harmonic has its nodes for pressure at the quarter points when centrally drilled perpendicular to the layers. The dowels were first introduced at ¼ and then at ¾ of the span (distance from the end at which the beam was excited). The damping ratio and the MOE of the LVL-L beam were affected similarly to the beam in the test where the knots were introduced at midspan only. Especially when the knots were drilled at ¼

span, the damping ratio rises in a similar way as when the knot was drilled at midspan.

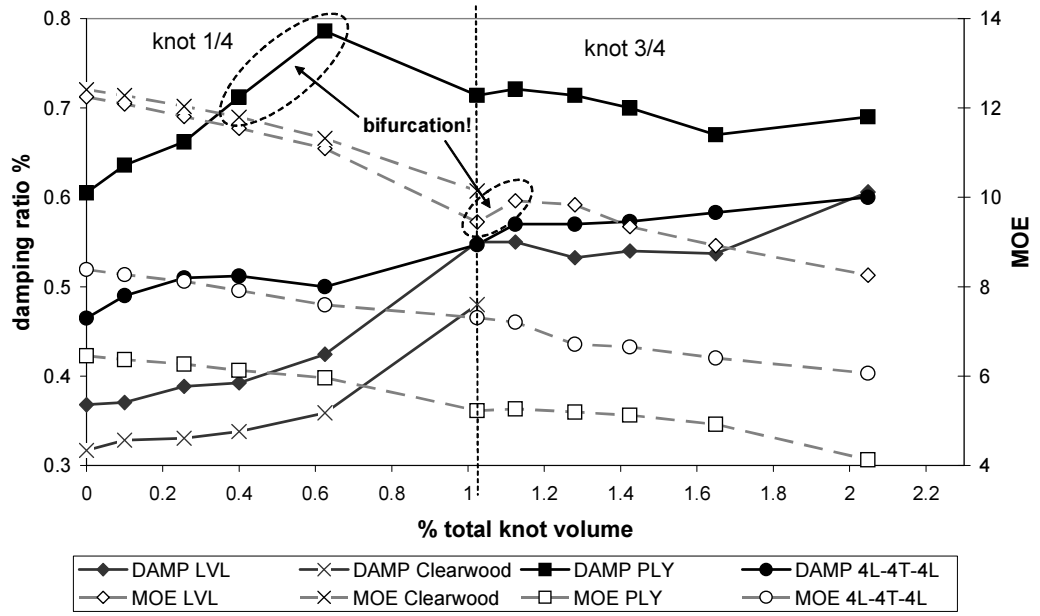

Figure 5-13: Impact of knots of increasing diameter drilled perpendicular to the individual layers at ¼ and ¾ span on the damping ratio.

However, when a second knot was added at the ¾ span, the damping ratio did not change significantly until the largest, 32 mm, knot was put in. The 32 mm knot at ¼ span increased the damping ratio by about 45%, whereas the second 32 mm knot at ¾ spanspan increased the damping ratio by only 15%. Again the graphed MOE of the LVL-L beam almost mirrors the graph for its damping ratio. When knots were first introduced at ¾ of the span, the damping ratio initially dropped and the MOE increased, but a closer look at the frequency spectrum revealed that the 2nd harmonic was undergoing bifurcation processes at that stage of the test. A second peak in the frequency spectrum started to develop when the 32 mm dowel was fitted at ¼ of the span such that when the 6 mm dowel was introduced at ¾ of the span, this second peak became bigger than the original peak which caused a shift to a higher resonance frequency for the second harmonic. Thus, the MOE calculations gave a higher value which can be explained by the shift of the resonance frequency for the second harmonic. Chapter 5.5.1 provides more detail discussion of this.

The damping ratio of the plywood beam again showed a peak at around 0.6% knot volume, while the MOE decreased systematically. The 4L-4T-4L beam showed a reasonably systematic pattern for both damping ratio and MOE.

Knots at various positions

A further test investigated whether the damping ratio and the MOE were affected at approximately the same rate if the total knot volume of the beam was increased stepwise to 10%. This was achieved by drilling various dowels (25 mm) perpendicular to the layers at specific positions along the span of a LVL-L beam (Figure 5-14). The first couple of knots were introduced at places where the 8th harmonic has its nodes for pressure. This was to protect the 8th harmonic and to show that other harmonics which have antinodes at these positions drop in frequency.

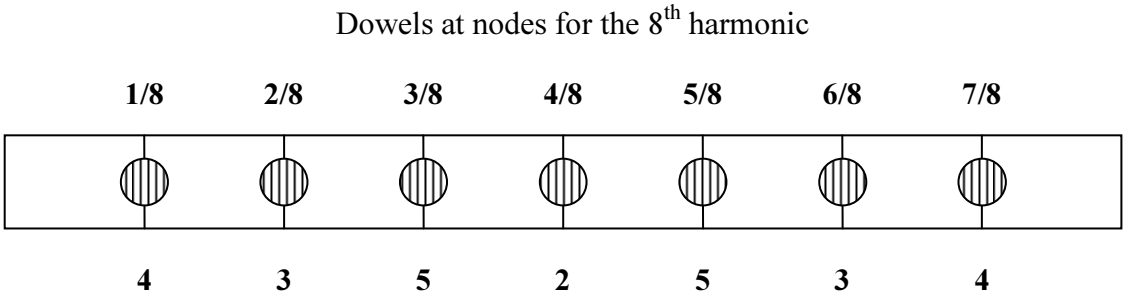

Figure 5-14: LVL beam with holes at various positions along the span. The numbers on the top mark the eighths of the span (nodes for pressure for the 8th harmonic) and the numbers on the bottom refer to the steps of the experience. Step 1 without holes. (Not drawn to scale).

The first knot was drilled at midspan (nodes for all even harmonics) followed by two knots at 2/8 and 6/8 of the span (nodes for the 4th and 8th harmonic); the next two knots were put at 1/8 and 7/8 (nodes for 8th harmonic); and then the last nodes for the 8th harmonic at 3/8 and 5/8 were filled with dowels.

After this knots were introduced at places where the 8th harmonic has antinodes for pressure.

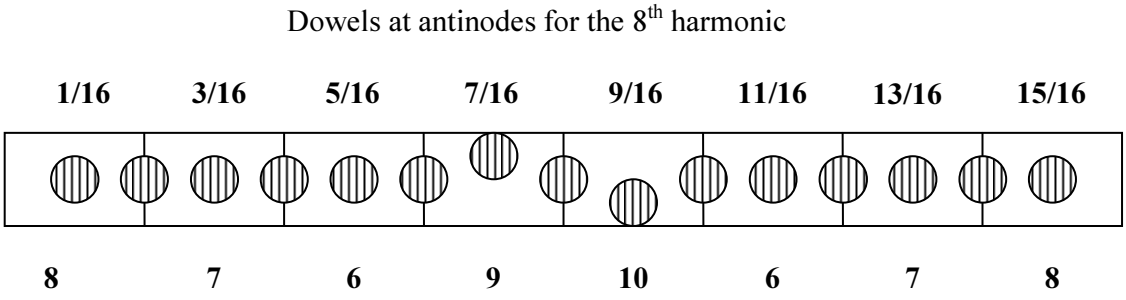

Figure 5-15: LVL beam with holes at various positions along the span. The numbers on the top mark the odd 16th of the span (anti-nodes for the 8th harmonic) and the numbers on the bottom refer to the steps of the experience. (Not drawn to scale).

First knots were put at 5/16 and 11/16 of the span; this corresponded to nodes for the 3rd harmonic. Thus, the 8th harmonic should have started to drop while the 3rd harmonic should not have been affected. Knots at 1/16 and 15/16 followed. So far all of the knots had been drilled in one straight line (centre line) perpendicular to the individual layers of the beam. Theoretically, there was still a continuous 7.5 mm × 40 mm clearwood strip remaining on either side of the dowels (40% of the cross section). The next step was to cut of one off these fast pathways by introducing a knot on one side of the beam at 7/16 of the span. Finally the last fast pathway was taken out by placing a knot on the opposite side at 9/16 of the span.

Figure 5-16 shows the response of the first 8 harmonics to the 10 steps of this test. Before the holes were drilled, the velocities as calculated from the first eight harmonics were reasonably close together. They were spread over 100 Hz. There was no discernable trend, for example, higher harmonics giving higher velocities.

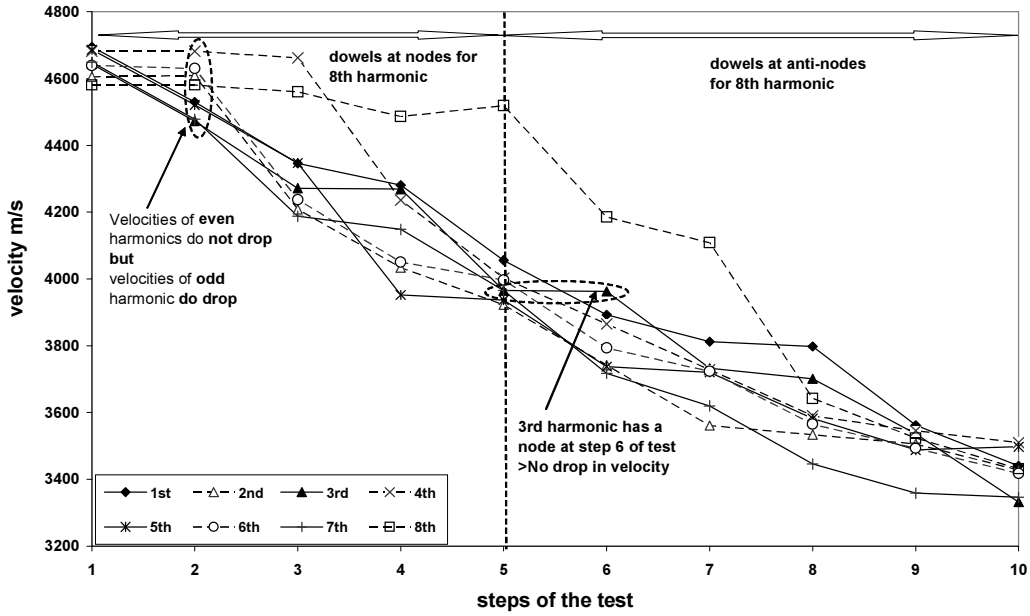

Figure 5-16: Change in velocity of the first eight harmonics when systematically increasing the knot volume of a LVL-L beam.

Figure 5-16 clearly shows that the dowels fitted at specific positions along the span of a LVL-L beam had a significant impact on the velocity of the first eight harmonics. When the first dowel was placed at midspan only, the odd harmonics which have an anti-node at midspan showed a drop in velocity. It was possible to protect the 8th harmonic by introducing knots at positions where the 8th harmonic has its nodes.

Figure 5-17 shows the damping ratio and the MOE of the LVL-L beam plotted against the increasing percentage of knot volume (same beam as in Figure 5-16). The MOE was either calculated from the average of the first eight harmonics; from the first harmonic; or from the harmonic which had the lowest velocity at each step of the test (For example, in the 2nd step, when the dowel at midspan was fitted, the 3rd harmonic showed the lowest velocity, at the 3rd step it was the 7th and so on).

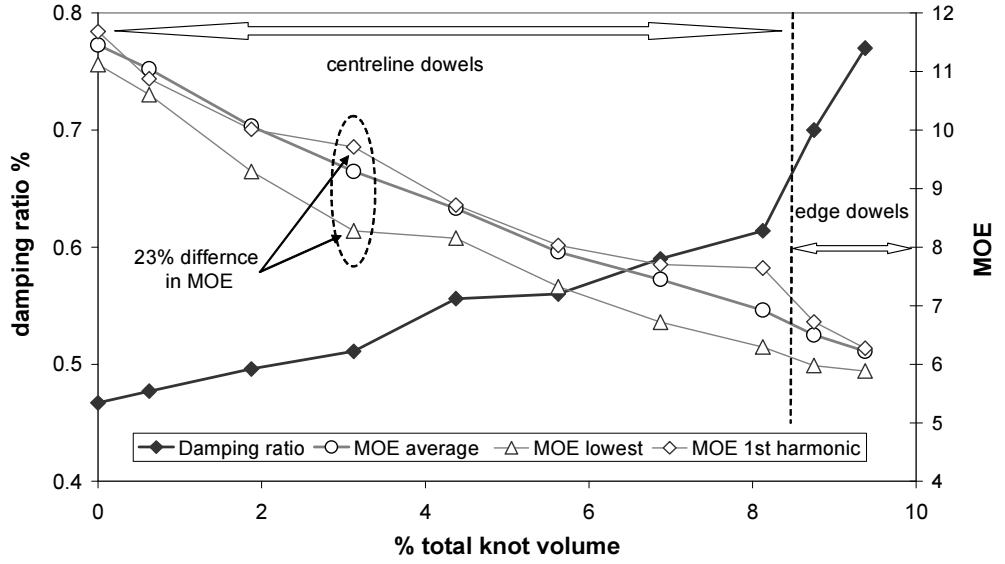

Figure 5-17: Impact of % knot volume on the damping ratio and MOE of a LVL-L beam.

The damping ratio increased almost linearly until the two edge knots were introduced. The correlation (r^2=0.98) between the damping ratio and knot volume can best be described by a linear regression line. Only with the last two steps did the damping ratio increase at a noticeably higher rate. Thus, cutting off the remaining fast pathways had a larger impact on the damping ratio than putting more dowels in line with the dowels already fitted.

The MOE as calculated from the average of the first eight harmonics dropped systematically with increasing knot volume (r^2= 0.99). However, the difference in MOE between the different calculations was as large as 23%. In all cases a negative exponential function brought the strongest correlation between MOE and knot volume. That indicates that the knottier the wood is, the weaker the impact becomes.

Predicting the MOE and the damping ratio of the knotty middle layer of a LVL-L beam by the law of mixtures

When 25 mm dowels are introduced along the centreline of a LVL-L beam, the laminate can be divided into three individual layers: the two outer layers are 12.5 mm thick and the middle layer, through which the dowels are drilled, is 25 mm thick. The calculations were based on the following equation:

$$E_{lam} = E_1 \frac{V_1}{V_0} + E_2 \frac{V_2}{V_0}$$

where;

E_{lam} = MOE of the laminate, E_1= MOE of longitudinal plies, E_2= MOE of the plies where the dowels are drilled in, V_0= total volume of the beam, V_1= volume of unaffected longitudinal plies and V_2= volume of the knotty plies.

The only unknown parameter in that equation is E_2.Which can then be easily calculated. The results are shown in Table 5-5.

Table 5-5: E_{lam} and E_2 of a LVL-L beam with increasing number of knots drilled on the centreline and perpendicular to individual layers as calculated from the 1st harmonic, from the harmonic with the lowest value and from the average of the first 8 harmonics.

E2 %knot volume	1st harmonic				harmonic with lowest value				average of first 8 harmonics			
	E_1	E_{lam}	E_2	E_2 %Change	E_1	E_{lam}	E_2	E_2 %Change	E_1	E_{lam}	E_2	E_2 %Change
0	11.68	11.68	11.68		11.12	11.12	11.12		11.45	11.45	11.45	
1	11.68	10.88	10.39	-11.04%	11.12	10.60	10.29	-7.43%	11.45	11.04	10.79	-5.74%
3	11.68	10.01	9.01	-7.63%	11.12	9.29	8.20	-8.77%	11.45	10.05	9.22	-6.49%
5	11.68	9.71	8.53	-5.39%	11.12	8.28	6.57	-8.18%	11.45	9.28	7.98	-6.05%
7	11.68	8.72	6.94	-5.80%	11.12	8.15	6.37	-6.10%	11.45	8.69	7.04	-5.50%
9	11.68	8.03	5.84	-5.56%	11.12	7.32	5.05	-6.07%	11.45	7.92	5.80	-5.48%
11	11.68	7.70	5.31	-4.95%	11.12	6.72	4.08	-5.76%	11.45	7.47	5.08	-5.06%
13	11.68	7.64	5.22	-4.25%	11.12	6.29	3.40	-5.34%	11.45	6.90	4.17	-4.89%

Percentage change is the change in E_2 caused per 1% knot volume. For example, the total knot volume in E_2 at step 8 of the test was 13% and the MOE (based on the 1st harmonic) dropped by 55% which gives a decrease of 4.25% per 1% knot volume. Table 5-5 clearly shows that, with increasing knot volume, the impact on the MOE decreases. However, there was considerable variation in the decrease of the MOE

when the knot volume increased depending on which harmonics were used for the calculation. Figure 5-18 shows the MOE of the knotty middle layer of the tested beam as calculated by the law of mixtures. The MOE calculated from the average of the first eight harmonics showed the strongest correlation (r^2=0.997) between the % knot volume and the MOE. The correlations for the lowest MOE (r^2=0.989) and the MOE of the first harmonic (r^2=0.974) were also equally strong. In all cases a negative exponential function brought the strongest correlation between MOE and % knot volume.

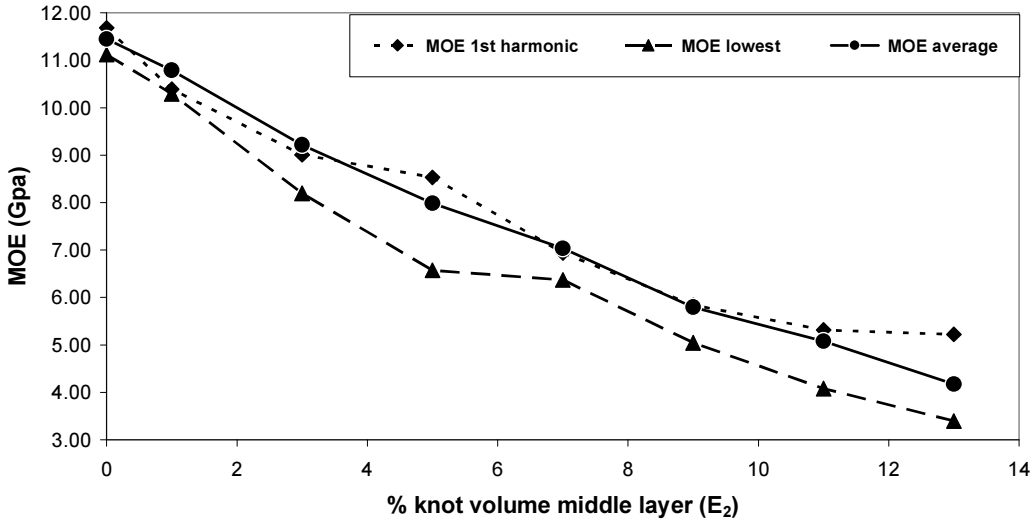

Figure 5-18: MOE of the middle layers of a LVL-L beam which are affected by increasing the number of knots drilled centred and perpendicular to the individual layers.

Table 5-6 shows the overall damping ratio of the beam and the damping ratio of the knotty middle plies as calculated by the law of mixture. In contrast to the MOE, the correlation (r^2=0.98) between the damping ratio and knot volume can best be described by a linear regression line. An increase of the knot volume of 1% caused on average a 3.4% increase of the damping ratio. The standard deviation was 0.44% and the coefficient of variation (COV) was 12%, indicating that the distribution can almost be considered a low variance (a COV below 10% is regarded as low variance).

Table 5-6: Damping ratio of a LVL-L beam with various holes drilled centred and perpendicular to the individual layers.

E2 % knot volume	damping ratio % unaffected plies	overall damping ratio %	damping ratio % knotty plies	% Change E2
0	0.467	0.467	0.467	
1	0.467	0.477	0.483	3.43%
3	0.467	0.496	0.513	3.31%
5	0.467	0.511	0.537	3.01%
7	0.467	0.556	0.609	4.36%
9	0.467	0.560	0.616	3.54%
11	0.467	0.590	0.664	3.83%
13	0.467	0.614	0.702	3.87%

5.4.4 Time of flight velocity versus resonance velocity

Table 5-7 compares the velocity of compression waves as calculated by the TOF method (PUNDIT) with the resonance method ("PULSE"). In this comparison the PUNDIT tester generated an electric pulse with a frequency of 54 kHz, while a hammer blow was used to calculate the resonance based velocity using "PULSE".

Table 5-7: TOF versus and resonance velocity in laminated beams.

Beam	configuration	Vel TOF	Resonance method		
			Vel 1st	Vel 2nd	Vel 3rd
LVL-L	no knot	4996	4717	4684	4757
	knot 32mm perpendicular midspan	4971	4372	4656	4353
PLY	no knot	3957	3487	3451	3507
	knot 32mm parallel midspan	3866	3184	3451	3183
PLY	no knot	4083	3564	3616	3620
	knots 32mm perpendicular 1/4+3/4	3944	3306	3164	3397
4L-4T-4L	no knot	4876	4026	3977	3994
	knot 32mm perpendicular midspan	4900	3659	3981	3615
3L-6T-3L	no knot	4075	3484	3410	3369
	knot 32mm parallel midspan	4042	3347	3412	3243
LVL-L	no knot	4975	4695	4605	4643
	various 25mm holes	4506	3440	3427	3332
4L-4T-4L	no knot	5026	4060	3989	3981
	knots 32mm perpendicular 1/4+3/4	4612	3742	3392	3740
LVL transverse	no knot	1090	925	957	947

Table 5-7 shows that the TOF velocities in laminated beams of various configuration were higher by approximately 10-20% compared with the resonance velocities before dowels were introduced. It is obvious that the largest discrepancy in wave velocity between the two methods was evident in the sandwiched beams. This indicates that the electric pulse of the PUNDIT finds its fastest path in the longitudinal layers of the sandwiched beams.

The velocity measurements based on the TOF method were far less affected by knots than the velocity measurements based on the resonance method. The resonance velocity decreased by approximately 10% (dependent on the harmonic from which it was calculated) when a single 32 mm centerline dowel was introduced at midspan, while the TOF velocity only dropped between 1-2%. When various 25 mm dowels were introduced to a LVL-L beam (Figure 5-15), the resonance velocity dropped by approximately 25% and the TOF velocity by 9% respectively.

5.4.5 Static MOE versus dynamic MOE

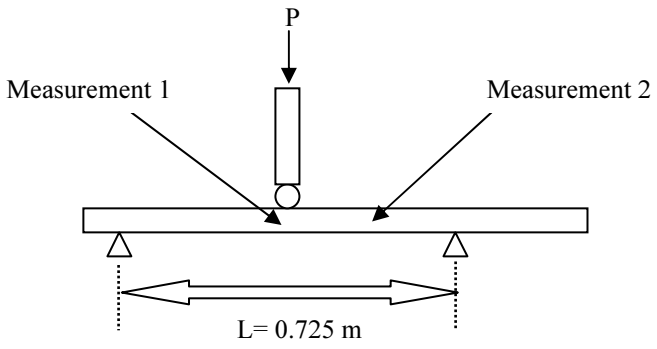

Figure 5-19: Schematic setup for the 3-point bending test.

The acoustic test results were compared with a 3-point bending test with centre point loading (crosshead speed 2mm/min). The same beams that had been used during acoustic testing were shortened to 0.95 m. During this process knots were eliminated. Thus a beam that had a knot at midspan was cut in two halves and had no knots. A

beam with knots at ¼ and ¾ of the span yielded only one clear beam for the bending test (being cut between ¼ span and ¾ span). The load was applied at two positions 15 cm apart from each other (Figure 5-19, measurement 1 and 2). At each position the deflection was measured when the beam was loaded both parallel and perpendicular to the layers of the beam. The two parallel and the two perpendicular readings were averaged and the static MOE was calculated using the following equation for a static bending test according to ASTM D-198 (2002):

$$E_f = \frac{PL^3}{48I\Delta}$$

where;
E_f= apparent MOE, P= applied load, L span and I= moment of inertia.

However, 3-point bending is not free of shear. Thus a correction factor has to be used to obtain “pure bending”.
The equation then changes to:

$$E = \frac{1}{E_j^{-1} - KG^{-1}(h/2)^2}$$

where;
E= MOE, G= Modulus of rigidity (shear modulus), K= shear coefficient and h= the depth of the specimen.

“K” is defined as the ratio of average shear strain on a section to shear strain at the centroid. Calculations on beams with rectangular cross-sections result in “K” values from 0.84 to 0.86. The shear modulus is calculated by the relation 1.2/K (ASTM D 198, 2002). However, it is questionable whether this correction factor can be applied to crossed laminates.

Table 5-8 compares the results of the acoustic dynamic MOE as calculated by the average of the first 3 harmonics with the MOE derived from static 3-point bending

tests. When the shear correction factor was applied to the static MOE for 3-point bending, the MOE increased by approximately 3.5%. For both methods the beams were free of dowels. The acoustic MOE was calculated as an average of the first three harmonics to obtain a better estimate of the overall stiffness of the beam than a test by the first harmonic which mainly tests the stiffness of the midspan area. However, the variation between the MOEs calculated from the first three harmonics was negligible. Each beam configuration was represented by three specimens.

Table 5-8: Comparison between the acoustic dynamic MOE and the static apparent MOE (measured when layers are oriented perpendicular (90°) as well as parallel (‖) to the applied load). E-modulus in GPa. Static MOE not corrected for shear.

Beam configu-ration	Acoustic MOE	Static MOE Layers 90°	Static MOE Layers ‖	Static MOE Average	Stat. MOE 90° / Acoustic MOE	Stat. MOE ‖ / Acoustic MOE	Stat. MOE average / Acoustic MOE
LVL-L	12.37	10.37	10.08	*10.23*	0.84	0.82	*0.83*
PLY	6.4	5.39	5.308	*5.35*	0.844	0.83	*0.84*
3L-6T-3L	5.49	2.96	4.638	*3.79*	0.54	0.84	*0.69*
4L-4T-4L	8.03	4.48	6.738	*5.60*	0.56	0.84	*0.7*
LVL-T	0.50	0.41	0.41	*0.41*	0.81	0.80	*0.81*
Clearwood	9.48	8.51	8.1	*8.30*	0.9	0.85	*0.88*

The dynamic MOE as calculated by the acoustic method was always significantly higher than the static MOE (average of the longitudinal and vertical alignment of the individual layers for 3-point bending). The highest dynamic MOE (12.4 GPa) was measured for the LVL-L beams, whereas the LVL-T beam had the lowest dynamic MOE (0.505 GPa). Moreover it is evident that the beams having 4 or 6 transverse layers sandwiched between the longitudinal layers are less stiff where the load was applied perpendicular to the layers. When these beams were loaded in the other plane the MOE was increased by 50% for the 4L-4T-4L beam and by 57% for the 3L-6T-3L beams. This observation does not match with the I-beam theory. When the sandwiched beams were loaded perpendicular to the individual layers, the situation was comparable to an I-beam. Therefore the sandwiched beams should have had a higher MOE when loaded perpendicular to the layers.

In the following, the theoretical value for the flexural stiffness, from which it is possible to derive the apparent MOE, is calculated. Figure 5-20 shows the parameters that are relevant to the calculation of the flexural MOE when the specimen was loaded perpendicular to its laminates. The measured values for the LVL-L and the LVL-T (Table 5-8) were taken as the values E_L and E_T to predict the MOE for the sandwiched beams and the plywood beams.

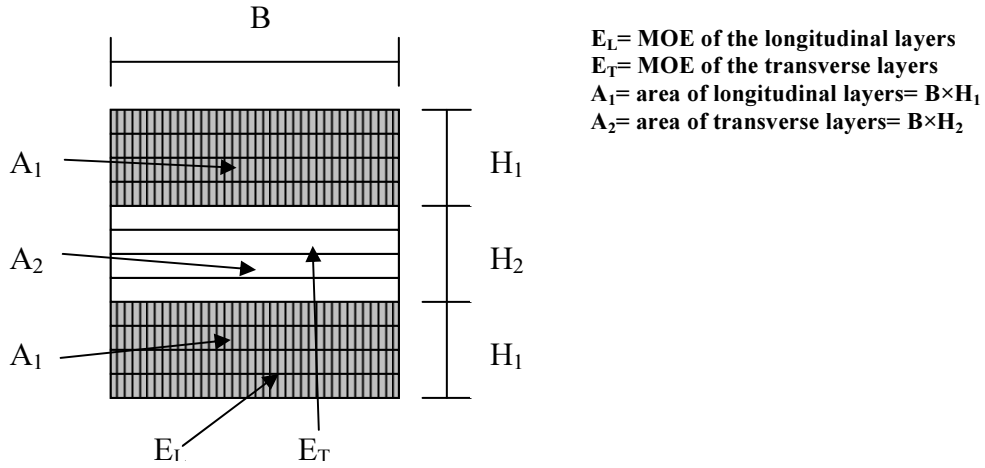

Figure 5-20: Parameters that are required for the calculation of the flexural stiffness of a laminate (sandwiched beam) loaded perpendicular to its laminates.

The following set of equations was used to calculate the theoretically apparent MOE of a laminate consisting of two longitudinal layers and one transverse layer that is loaded perpendicular to its laminates.

$$EI = E_L \times I_{A1} + E_T \times I_{A2} + E_L \times I_{A1}$$

$$EI = 2E_L \times I_{A1} + E_T \times I_{A2}$$

$$I_{A1} = \frac{B \times H_1^3}{12} + B \times H_1 \times \left(\frac{H_1 + H_2}{2} \right)^2$$

$$I_{A2} = \frac{B \times H_2^3}{12}$$

$$EI = 2E_L \times \left[\frac{B \times H_1^3}{12} + B \times H_1 \times \left(\frac{H_1 + H_2}{2} \right)^2 \right] + E_P \times \frac{B \times H_2^3}{12}$$

$$E_f = \frac{EI}{I}$$

$$I = \frac{B \times (H_1 + H_2 + H_1)^3}{12}$$

where; EI= flexural stiffness, E_f= apparent MOE and I= moment of inertia

When the same laminate is loaded parallel to its layers the following equations were used to calculate the theoretically apparent MOE:

$$EI = 2E_L \times I_{A1} + E_T \times I_{A2}$$

$$I_{A1} = \frac{H_1 \times B^3}{12}$$

$$I_{A2} = \frac{H_2 \times B^3}{12}$$

$$E_f = \frac{EI}{I}$$

$$I = \frac{(H_1 + H_2 + H_1) \times B^3}{12}$$

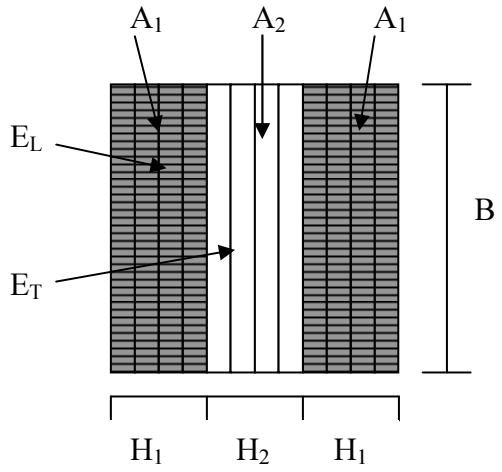

The prediction of the acoustic MOE was made using the law of mixtures. The following equation gives the MOE of a laminate consisting of n-layers of uniform thickness (Bodig and Jayne, 1982):

$$E_{lam} = E_L \frac{n_l}{n_0} + E_T \frac{n_t}{n_0}$$

where;

E_{lam}= elastic constant of the laminate, E_L= elastic constant in longitudinal direction of a ply, E_T= elastic constant in transverse direction of a ply, n_0= total number of plies, n_l= number of longitudinal plies and n_t= number of transverse plies.

Table 5-9 shows the MOE of various beams as measured acoustically; as calculated by the equations shown above; and as measured from 3-point-bending.

Table 5-9: Comparison of the theoretical MOE (predicted) with the MOEs measured from 3-point-bending and acoustic testing. Values in GPa.

Beam configuration	Acoustic MOE		Static MOE Layers 90°		Static MOE Layers ‖	
	measured	predicted	measured	predicted	measured	predicted
LVL-L	12.37		10.37		10.08	
PLY	6.40	6.44	5.47	6.63	5.38	5.25
3L-6T-3L	5.49	6.44	**2.98**	**9.13**	4.69	5.25
4L-4T-4T	8.03	8.41	**4.53**	**10**	6.85	6.86
LVL T	0.50		0.41		0.41	

The predicted values of the acoustic MOE and the static MOE when the beams were loaded parallel to their layers were reasonably close to the measured values. Moreover, the trend was that the acoustic measurements gave higher values (between 15-20%) for the MOE than the static bending tests. However, the measured values for the MOE of the sandwiched beams when loaded perpendicular to its layers did not match the predicted values. The 3L-6T-3L beams reached only 30% of the predicted value and the 4L-4T-4L beams showed a value that was 45% of the predicted value. An explanation for the discrepancy between the measured and the predicted values could be a result of delamination of the layers. A closer look at the transverse middle layers revealed that there was some local delamination between layers. Thus, the transverse middle layer was weakened and so was not behaving like the web of an I-beam. This would explain the greater differences between the measured and the predicted values of the sandwiched beams when they were loaded perpendicular to the layers, especially in the 3L-6T-3L and 4L-4T-4L configurations. As expected, acoustic measurements and their predicted values were far less affected.

5.5 Discussion

The acoustic testing of the laminated and the clearwood beams showed that artificial defects have a significant impact on both elastic and damping properties. This outcome is in accordance with a study by Ouis (2000). He drilled an increasing number of 10 mm holes through a wooden beam (70 ×7 × 7 cm) of Norway spruce,

which was set into longitudinal vibration, and determined the variation of the MOE and the loss factor (calculated from the reverberation time method) as the number of holes increased (Figure 5-21).

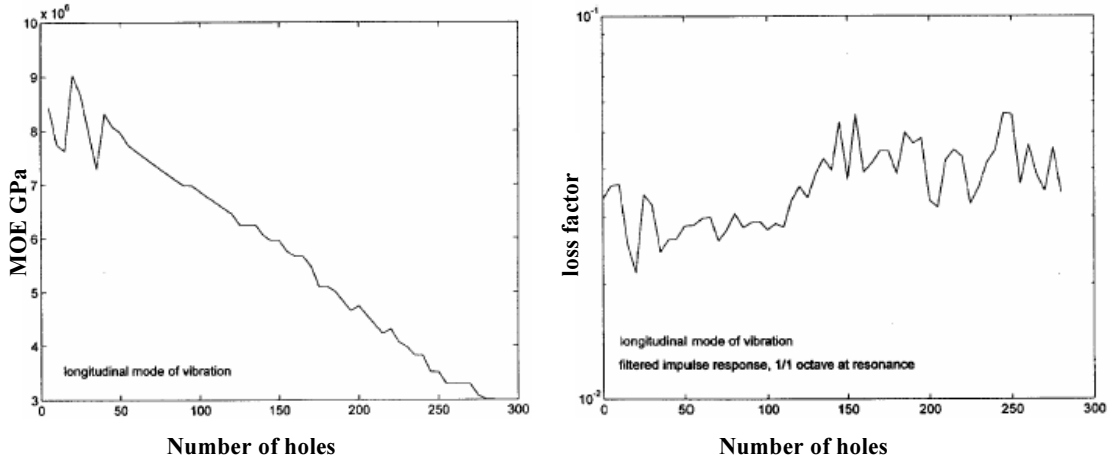

Figure 5-21: Variation of the MOE and the loss factor with the number of defects in the wooden bar. Adapted from Ouis 2000. The holes were drilled in various rows.

The curve of the MOE shows a clear monotonical decrease in MOE with increasing numbers of holes. Ouis (2000) explains that "the peculiar behaviour of the curve at the lowest number of defects may be due to the periodical pattern of the holes in the wood bar setting more resonances in its vibration". At the same time, the loss factor decreased before it started to increase with the increasing number of holes. However, the curve of the loss factor shows far more undulation than the curve of the MOE.

A comparable test in this study on a LVL-L beam showed very similar results for the MOE and the damping ratio (Figure 5-17). In this study the damping ratio, which is twice the loss factor, showed a more linear increase than in Ouis's (2000) study. However, the damping ratio in the plywood and the sandwiched beams often showed an erratic pattern when the knot volume in the beams increased.

Ouis (2000) states that it is important to distinguish between different types of damping when waves propagate in wooden beams. Material damping is the most important kind. Most of the energy loss in wood at the frequencies of some kHz is due

to fluid friction. However, energy is also dissipated at various boundaries of the beam, such as internal inhomogeneities or through sound radiation at the outer surfaces. Inhomogeneities within the laminated beam are for example: early and latewood zones, "real" knots, glue bonds, joints of the veneer within the same layer, resin pockets, cracks and the holes filled with dowels. Acoustic waves that travel through the beam are likely to be reflected and/or scattered at these inhomogeneities and thereby dissipated. The fact that the damping ratio of plywood and the sandwiched beams showed an inconsistent response to an increased knot volume might be explained by the higher degree of inhomogeneity within these beams than in LVL-L or clearwood beams.

Do different harmonics produce different results?

In this study it is clearly shown that different harmonics can give different results for the MOE. When the MOE was calculated for a beam that had the hole drilled at midspan (80% of the cross-section), the MOE as calculated from the 2nd harmonic was not affected at all while the 1st and 3rd harmonic showed a MOE that was lower by about 20-25% (Figure 5-5). Compared with the results of the eucalypt and pine logs (Chapter 4.4.2), it is obvious that knots and holes do influence the elastic behaviour of wood differently. This is discussed in Chapter 6.

In a test where various holes were introduced at specific positions along the stem, it was shown that it is possible to protect certain harmonics by drilling holes at positions that overlap with their antinodes for displacement or nodes for pressure (Figure 5-17). The MOE was calculated in three different ways: from the 1st harmonic, from the average of the first eight harmonics and from the harmonic that gave the lowest MOE. The difference between the MOEs as calculated in these three ways was as high as 23%.

This clearly shows that the MOE calculated from only one harmonic can give a value that is very different from the overall MOE value of the specimen. The first harmonic tests the specimen at around midspan. The closer inhomogeneities (defects) are

situated towards the ends of the specimen, the less they will influence the 1st harmonic. For the second harmonic, the situation is very different. While inhomogeneieties around midspan will not be detected, the 2nd harmonic is most sensitive to inhomogeneities at around ¼ and ¾of the span. The fact that the 1st and the 2nd harmonics investigate different parts of the specimen, could for example, be used to estimate the MOE at around midspan. If the MOE as calculated by the 1st harmonic is significantly lower than the MOE of the 2nd harmonic, this would then indicate that the specimen has defects (for example decay) at around midspan. However, it is not possible to detect defects that are very close to the ends of the specimen, as all harmonics have antinodes for displacement and nodes for pressure at the ends.

To obtain a reasonably close estimate of the overall MOE of the specimen, at least two harmonics should be considered to calculate the MOE. This should be one even and an one odd harmonic to balance out the parts of the log that are investigated because even harmonics are not affected by defects at midspan while odd harmonics are. If the first four harmonics are detectable, the average of the MOEs calculated from the 3rd and the 4th harmonics should give a reasonably close estimate of the overall stiffness of the specimen. Higher harmonics will be slightly more affected by defects that are close to the ends of the specimen, as their outer nodes for displacement shift closer towards the ends with increasing frequencies (Figure 5-22).

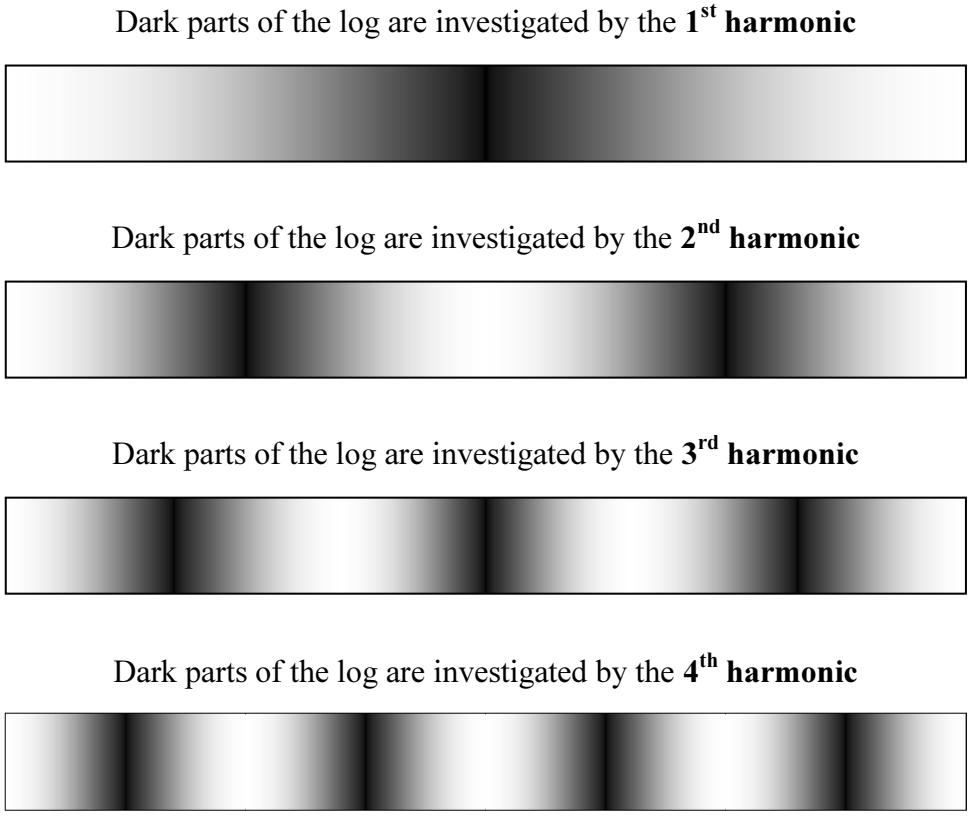

Figure 5-22: Anti nodes (dark areas) and nodes for pressure of the first four harmonics.

Differences between holes drilled perpendicular or parallel to the individual layers of the laminated beams

Edge knots drilled parallel to the layers of a LVL-L beam had a greater effect on the MOE and the damping ratio than edge knots drilled perpendicular to the individual layers. While the MOE of the LVL-L beam on average decreased by approximately 15% when holes were drilled perpendicular to the layers, the decrease when holes were drilled parallel to the layers was approximately 35%. The damping ratio increased by 50% when the holes were drilled perpendicular to the layers and it tripled when the holes were drilled parallel to the layers (Figure 5-11 and Figure 5-12). However, there was no difference in the MOE of a LVL-L beam between centreline knots drilled parallel or perpendicular to the layers.

Gerhards (1982) reported that the wavefront does not remain a planar front when it passes a knot but starts to become planar again after the knot is passed. In laminated beams, this could explain why the impact of holes is bigger when they are drilled parallel to the layers. In this case the wave front has to spread through the adjacent layers (and the glue lines) to build up a planar front again, whereas the perpendicular oriented dowels only cut out parts of any individual layer and, after a knot is passed, the wave front only has to spread out within each layer to reform a planar front. The latter scenario probably suffers less in terms of energy loss, which then would explain why dowels drilled parallel to he layers have a greater effect on the damping ratio.

5.5.1 The impact of bifurcation on the damping ratio and the MOE

In general the term bifurcation describes the phenomenon where the main body of one item splits into two parts. It is also possible for the main body to split into multiple parts. In this study trifurcation could be observed occasionally. However, bifurcation (trifurcation) is always a transition from a level of higher symmetry to one of lower symmetry and higher complexity. One possible explanation why bifurcation occurs is that parts of the wave front travel slower for a certain time during and after they have past the section of disturbance. Thus this part of the wave will have a slightly lower frequency which might become visible as a second peak in the same range of the frequency spectrum where the original peak can be found.

The calculation of the damping ratio is affected if the harmonic from which it is derived suffers from severe bifurcation. On some occasions the MOE can also be affected by bifurcation. This happens where one of the “new” peaks becomes larger in amplitude than the original peak, as shown in Figure 5-23.

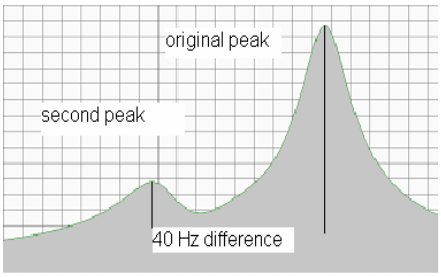

Test A: No hole test; a small second peak 40 Hz below the 1st harmonic

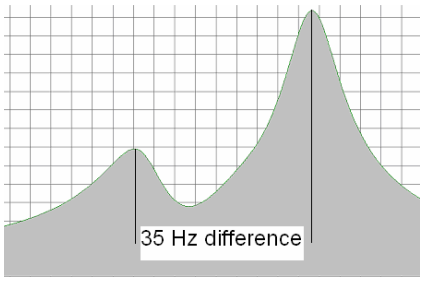

Test B: 10mm dowel test; second peak grows bigger and peaks come closer together

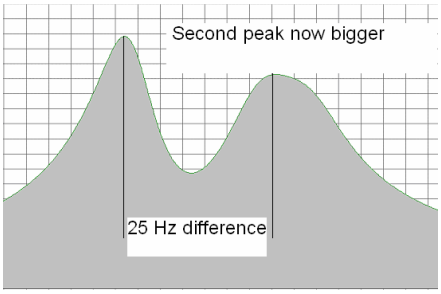

Test C: 20mm dowel test; second peak is now bigger, peaks only 25 Hz apart

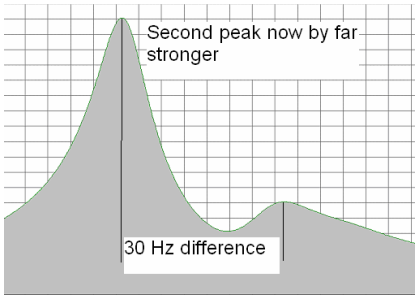

Test D: 25mm dowel test; second peak predominant and sharper than before

Figure 5-23: Bifurcation of the fundamental frequency of a plywood beam caused by a centreline dowel of increasing diameter drilled perpendicular to the individual layers at 3/8 of the span. Frequency (Hz) is displayed on the X-axis and the amplitude of acceleration (m/s^2) on the Y-axis.

The consequences of the bifurcation process in the example displayed in Figure 5-23 are summarised in the following table.

Table 5-10: Impact of bifurcation on the damping ratio and the MOE. Values in brackets are from the peak with lower amplitude.

Size of dowel	Fundamental frequency (Hz)		Damping ratio (%)	MOE (GPa)	
	Original peak	Second peak		Original peak	Second peak
Test A 0mm	**923**	(886)	**0.57**	**6.95**	(6.41)
Test B 10mm	**918**	(883)	**0.64**	**6.89**	(6.37)
Test C 20mm	(904)	**878**	**0.69**	(6.68)	**6.29**
Test D 25mm	(896)	**868**	**0.59**	(6.56)	**6.16**

In Test C (Figure 5-23) the amplitude of the second peak became larger than the amplitude of the original peak and consequently the frequency of the second peak was

then taken for the calculation of the MOE. The over proportional shift in frequency, effected by bifurcation, caused a larger decrease of the MOE than was expected.

The damping ratio is also influenced by the bifurcation of the fundamental frequency. Particularly, since the damping ratio in this study was calculated from the Q-factor method it is strongly affected by the bandwidth at the half power points of the fundamental frequency. If the peak broadens, the damping ratio increases. In test D (Figure 5-23) the second peak from which the damping ratio was calculated was much more pronounced than the original peak, and it was also narrower than in test C (Figure 5-23) which explains the decrease of the damping ratio.

The scenario discussed above is just one among many that can be induced by bifurcation. For example, it is also possible, that with increasing knot size, a second peak with a higher frequency progressively builds up and becomes larger than the original peak. At the point when the amplitude of the former smaller peak becomes larger than the original peak, the MOE will slightly increase even though a larger dowel is fitted (this was the case in Figure 5-13). Moreover it is possible that a second peak develops but does not become bigger in amplitude than the original peak. In such a case, which was mostly observed in this study, the calculation of the MOE is not affected. But, depending on the degree of bifurcation, the damping ratio can be strongly affected. It was also observed that the second peak was developing at a frequency that was only a few Hz away from the fundamental frequency. This peak could, for example, be called a shoulder peak. Shoulder peaks tend to widen the bandwidth at the half power points more obviously than peaks that are better separated in the frequency band.

5.5.2 Differences in static and dynamic MOE

When the MOE of the beams that had been used for acoustic testing (resonance method) was determined in static bending it was found that the MOE of the bending test was smaller by approximately 15% (Table 5-8). This discrepancy between static

and dynamic MOE has been observed by Jayne (1959) who found higher values (approximately 5%) for the dynamic method. Divos and Tanaka (2000) discussed the difference between a static bending test and a dynamic test. They did various 3-point bending tests with different velocities of the crosshead. According to Divos and Tanaka (2000), higher E-values were obtained for higher crosshead velocities. This means that, when loading the same beam with the same load but over a longer time (lower crosshead velocities), the MOE will slightly decrease. This is probably caused by creep processes within the wood. Andrews, Ilic and Walker (2003, unpublished) mention that relaxation during the bending test might be caused by rearrangements of the cell wall under stress, for example straightening of a segment of a hemicellulose chain. Divos and Tanaka (2000) established the following formula which takes account of the time factor during a bending test:

$$E_{t1} = E_{t2}(1 + 0.017\log(\frac{t_2}{t_1}))$$

where:

t_1: the characteristic time of Et_1 determination
t_2: the characteristic time of Et_2 determination

TOF versus resonance measurements

A comparison between the TOF and the resonance velocities on various laminated beams showed that the TOF method gave values that were higher by approximately 15% (Table 5-7). This discrepancy between TOF and resonance speed was described by Andrews (2002) and has been discussed in Chapter 2.4.3. It has to be mentioned that the TOF speed in this study was calculated by an electric pulse with a frequency of 54 kHz, while a hammer blow was used to calculate the resonance-based velocity.

Table 5-7 shows that the TOF velocities in laminated beams of various configurations were higher by approximately 10% to 20% compared with the resonance velocities

before dowels were introduced. It is obvious that the biggest discrepancy in wave velocity between the two methods was evident in the sandwiched beams. This indicates that the electric pulse of the PUNDIT finds its fastest path in the longitudinal layers of the sandwiched beams. However, the velocity based on the resonance method is an average velocity of the whole system. This was demonstrated in a test conducted by Carter, Chuahan and Walker (2006) in which they tested logs, cants and boards from 24-year-old radiata pine trees using the resonance based tool Director HM200. They found that the acoustic velocity of the diametral cant was very close to the volume-weighted average velocity for all the boards cut from the diametral cant.

The velocity measurements on various laminated beams based on the TOF method were far less affected by holes filled with dowels than the velocity measurements based on the resonance method. The resonance velocity decreased by approximately 10% (dependent on the harmonic from which it was calculated, and the configuration of the laminated beam) when a single 32mm centerline dowel was introduced at midspan, while the TOF velocity only dropped between 1-2% (Table 5-7). When various 25mm dowels were introduced to a LVL-L beam, the resonance velocity dropped by approximately 25% and the TOF velocity by 9%. This clearly shows that local defects have a significantly lower impact on the TOF wave speed in wood compared with the resonance wave speed. The reason for this is that the TOF velocity is based on the fastest path that is evident between the active probes. The 9% decrease in TOF velocity for the various hole test (Figure 5-15) of a LVL-L beam seems to be very high compared with a 25% decrease for the resonance-based velocity. This can be explained by the fact that, at the end of the test, there was no straight-through pathway left, since the last two holes were drilled at the edge of either side of the centerline.

5.6 Conclusion

It has been shown that velocity of sound in the longitudinal direction of a veneer sheet is five times higher than in the transverse direction. This indicates that the wood of

radiata pine is about 25 times stiffer parallel to the grain than across the grain. The damping ratio in the transverse direction was four times higher than the damping ratio in the longitudinal direction. The damping ratio for the clearwood beams and the LVL-L beams was between 0.35% and 0.47% and between and 0.45% and 0.6% for cross laminated beams. The increase of the damping ratio (maximum of 1.7%) was strongly affected by the knot volume and the orientation of the knot. It was found that edge knots placed parallel to the layers of the laminated beams had a greater impact on the damping ratio than a knot that was oriented perpendicular to the layers. Another important outcome of this study that the damping ratio can be used to detect defects (knots) in timber. However, it seems that the damping ratio cannot be applied to test engineered wood products that have a high degree of inhomogeneity such as plywood, as the frequency spectrum shows more discontinuities which are enhanced by introducing artificial defects.

It was found that the MOE is more suitable for describing the impact of artificial knots on clearwood and on laminated beams (especially if the orientation of the layers changes). In this context it should be noticed that it is not appropriate to base the calculation of the MOE on only one harmonic. This is because harmonics only detect defects in areas that are close to an anti-node for pressure. It was shown that the accuracy of the MOE prediction can be increased when it is based on the average of an even number of harmonics (half of them odd, half of them even).

When various knots were introduced to a LVL-L beam it was found that the MOE dropped negative exponential while the increase of the damping ratio could be best described as a linear regression line.

Static bending tests on the beams led to MOE values that were lower by 15-20 %, depending on the configuration of the beam, compared with the MOEs derived from acoustic testing.

Chapter 6: General discussion and conclusion

6.1 General discussion

When comparing the results from the eucalypt and pine logs (Chapter 4.4) with the results from laminated beam tests (Chapter 5.4) it is obvious that the MOE as calculated from various harmonics responded differently when knots or holes were at specific locations. For example, the logs that had knots at midspan had the highest MOE when the 1st and 3rd harmonics were used for the calculation while a hole drilled at midspan gave significantly lower values for the 1st and the 3rd harmonics The 2nd harmonic showed the highest MOE.

How differences between knots and holes affect the acoustic properties of logs and beams

Branch nodes or nodal whorls in logs are very different from holes drilled in beams. A hole drilled through a wooden beam simply reduces the cross-section of the beam at the very position where it is drilled. Filling the hole with a dowel of corresponding size keeps the mass of the beam nearly constant, but the dowel does not contribute to the mechanical properties of the beam. The situation may be compared to a loose knot in a beam. Although the fibres surrounding a loose knot will be deflected, the fibres surrounding a drilled hole are obviously more or less straight grained.

Moreover, beams are even shaped while logs are usually tapered and sometimes may be crooked or have an oval shaped cross-section. Branch nodes and nodal whorls usually cause what is known as nodal swelling; an increase of the diameter at the location of branch nodes and nodal whorls. An increase in diameter enlarges the cross-section of the log at the positions of branch nodes and nodal whorls. Moreover, branch nodes and nodal whorls are parts of a stem that have a higher mass compared with “knot-free” parts of the stem. The reason for this is twofold: firstly, nodal swelling increases the diameter which then increases the volume and consequently the

mass; secondly, branches usually increase the density of wood because reaction wood, which amongst others can be found in branches, is usually of higher density than "normal" wood tissue.

Therefore, logs that have branch nodes or nodal whorls at midspan have an area of increased mass and a bigger cross-section at midspan, whereas a beam through which a hole is drilled at midspan has a reduced cross-section of wood material. As discussed in chapter 2.4.2, a vibrating (compression waves) log or beam can be described as a mass spring system. Figure 6-1 illustrates the situation as sensed by the 1st harmonic.

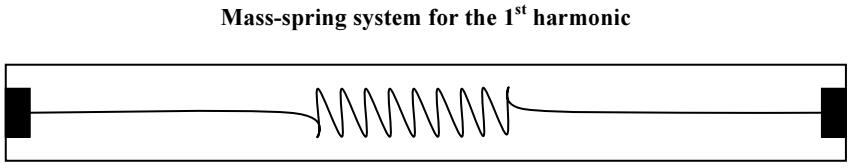

Figure 6-1: Mass-spring system of a log for the 1st harmonic as sensed by acoustics.

The equations below show that a bigger cross-section (A), caused by nodal swelling, increases the spring constant (k). A higher spring constant causes less deflection which then results in a higher MOE value.

$$k = \frac{EA}{l}$$

and

$$MOE = \frac{F}{A} \times \frac{l}{\Delta l}$$

Holes drilled through beams at midspan decrease the cross-section and thereby decrease the spring constant. Hence, a smaller MOE will be sensed by the 1st harmonic.

The mass-spring as sensed by the 2nd and 3rd harmonic is shown in Figure 6-2. For the 2nd harmonic it consists of three masses and two springs which are attached in series.

The motion of systems with multiple springs and masses is clearly much more complex than that of a single spring. In this study the full complexity of multiple spring and mass systems is not analysed. The equivalent spring constant of multiple springs attached in series can be found in the following equation:

$$\frac{1}{k_{eq}} = \frac{1}{k_1} + \frac{1}{k_2} + ...\frac{1}{k_n}$$

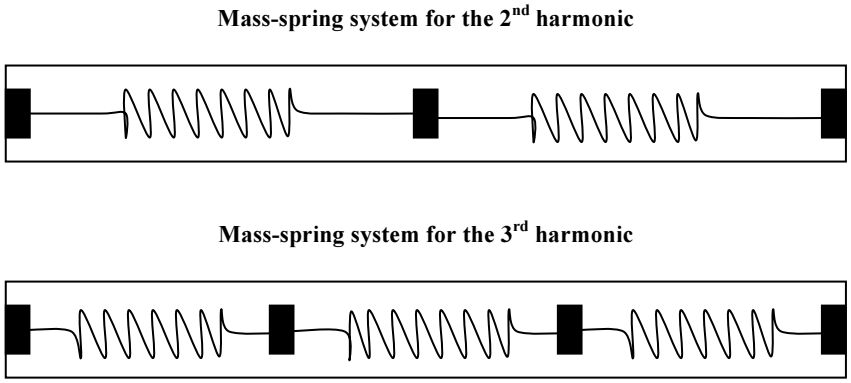

Figure 6-2: Mass-spring system of a log for the 2nd and 3rd harmonic as sensed by acoustics.

The 2nd harmonic will detect the higher mass at midspan of logs that have nodal swelling at midspan (increased mass) which then will cause higher deflection and consequently a lower MOE. A hole at midspan, filled with a dowel, will not change the mass. Thus it has no impact on the elastic behaviour of the beam.

The situation for the 3rd harmonic is similar to the situation for the 1st harmonic. Theoretically, the impact of knots or holes on the 3rd harmonic should be smaller than the impact of knots or holes on the 1st harmonic, because only one out of the three springs is affected. The actual testing gave a MOE for the 3rd harmonic which was smaller by 3% than the MOE based on the 1st harmonic (Figure 5-5).

The theoretical reasoning above has been founded on a simplified model that describes the acoustic properties of a log or a beam in longitudinal vibration by a set

of masses and springs. However, the impact of knots on the mechanical properties of trees, logs and beams is certainly much more complex.

Nardin et al., (2000) state that the mechanical properties of clear wood are well known, but that relatively little is known about the impact of knots on the mechanical behaviour of wood. They found that the fracture energy, tensile strength, stiffness and density decreases with the distance from the knot. Tension and shear tests were conducted on small test specimens of Norway spruce (40 ×40 × 6 mm), which were cut from boards with a single knot, or boards that had a minimum distance of 100 mm between the knots. The specimens were taken at different distances from the knot. The specimens were only tested in the radial-longitudinal orientation and the tangential-longitudinal orientation. These findings are in accordance with the outcome of the acoustic tests of eucalypt and pine logs in chapter 4 of this study. It was observed that harmonics which tested the "knotty" parts of the stem showed significantly higher MOE values than harmonics which tested the "clear wood" parts of the log.

6.2 General conclusion

TOF measurements

In Chapter 3 it has been shown that TOF measurements in standing trees can be used to detect differences in outerwood stiffness that have been caused by different pruning and thinning treatments. Pruning significantly increased the outerwood stiffness of 14-year-old *Pinus radiata* trees by up to 25%. The theory that the distance to the green crown has an impact on the type of wood (juvenile or mature) that is produced at a certain position of the trunk, could not be tested in this study, because the trees were all pruned to the same height. Thinning operations also had an impact on the MOE, although this was not as noticeable as pruning. Reducing the initial stand density of 1000 stems/ha to 500 stems/ha had no significant impact on the MOE. When the stand density was decreased to 250 stems/ha, the MOE of the outerwood was significantly lower (8.5%) than in the high stand density plots.

Resonance measurements

Defects had a significant impact on damping and elastic properties of wood. It was found that different harmonics respond differently to defects that are situated at specific locations. Holes filled with dowels, drilled through dry laminated beams at specific locations, reduced the MOE of the beam. But only harmonics that have antinodes for pressure (nodes for displacement) at the locations where the holes were drilled, responded with a decrease in MOE. Harmonics which have nodes for pressure (antinodes for displacement) were not affected. However, branch nodes and nodal whorls in green logs gave higher MOE values when harmonics which investigated the "knotty" parts of the stem were used for the calculations.

The damping properties of laminated beams were also highly affected when holes were drilled through specific locations at midspan. The damping ratio of LVL-L beams and clearwood beams increased systematically when the knot volume of the beam increased. Beams of higher inhomogeneity (plywood and sandwiched beams) usually suffered severe bifurcation processes which can cause heavy distortion of the frequency response spectrum. Thus, the damping ratio of these beam configurations often showed an unsystematic pattern when the knot volume of the beam increased.

6.3 Practical conclusions

Acoustics provide a fast method to estimate the stiffness of trees (outerwood stiffness only), logs and timber. The general opinion is that relatively small defects like knots are not detectable when testing with acoustic waves of a few kHz, because the wave length of the first 4 harmonics is somewhere between 1 and 10 metres when testing normal sized logs. However, in this study it was found that defects, even if they are much smaller than the wavelength, have a measurable impact on the acoustic properties of wood.

Another crucial outcome of this study is that different harmonics can give significantly different values for stiffness. Different harmonics investigate different parts of the stem owing to the fact that their distribution pattern for nodes and antinodes for pressure as well as for displacement systematically changes with increasing frequency. Therefore it is strongly recommended that the MOE calculations of logs and timber should be based on the first two, or better still on the first four harmonics. This would give a MOE value that is a better estimate of the overall stiffness of the specimen than a MOE value calculated from only one harmonic.

6.4 Areas for further research

The evidence suggests that there are still many "unknowns" in the acoustics of wood. In this study a total of 288 trees, 30 logs and approximately 40 laminated beams have been tested using various acoustic techniques. To verify the results of the resonance measurements on small logs, a larger study would be required. The studies on the damping ratio of laminated beams had a scoping character. Further research is required to establish relationships between the damping properties and the mechanical properties of wood.

Moreover, further research areas of interest are:

- Comparison of the transmitted energy of the signal for various harmonics: this study only made use of the maximum amplitude of the transmitted signal.

- Bifurcation: it has only been possible to observe bifurcation processes in the frequency response spectrum, but it is not fully understood what causes bifurcation.

- Impacts of knots in beams: it was observed that branch nodes and nodal whorls increase the “acoustic” stiffness in logs. This may be due to nodal swelling.

- Bending waves in standing trees: so far it is only possible to estimate the outerwood stiffness by using the TOF method (based on compression waves). However, it might be possible to use bending waves, which would investigate the whole cross-section of the stem, to obtain a better estimate of the overall stiffness of a standing tree.

References

American Society for Testing and Materials. (2002). *Annual book of ASTM standards.* Astm. Philadelphia.

Andrews, M. K. (2002). Which acoustic speed? *Proceedings of the 13th International Symposium on Non-destructive Testing of Wood, university of California, Berkeley Campus California, USA.*

Bamber, R. K., & Burley, J. (1983). *The wood properties of Radiata Pine.* Slough: Commonwealth Agriculture Bureaux.

Barnett, R., & Jeronimdis, G. (2003). *Wood quality and its biological basis*. Cornwall, UK.: Blackwell Publishing.

Bascuñán, A., Moore, J., & Walker, J. C. F. (2004). Influences of wind on wood quality: known unknowns and unknown unknowns. *Proceedings of the Workshop on wood quality. Albury, Australia,* August 2004.

Bodig, J., & Jayne, B. A. (1982). *Mechanics of wood and wood composites*. New York: Van Nostrand Reinhold Co., Inc.

Bootle, K. R. (2005). *Wood in Australia*. McGraw-Hill Australia Pty Ltd

Brooker, M. I. H. (2002). Eucalypts of south-eastern Australia. Collingwood: CSIRO Publishing.

Brüel & Kjær. (1994). Technical note "Digital Filter Techniques vs. FFT Techniques for Damping Measurements (Part 1+2).

Brüel & Kjær. (1999). Technical document no. 3560: APPLICATION NOTE: How to Determine the Modal Parameters of Simple Structures. by Gade. S., Herlufsen. H., & Konstantin-Hansen, H.

Buccur, V. (1995). *Acoustics of wood.* Boca Raton: CRC Press.

Buccur, V. (1996). Acoustics of Wood as a Tool for Nondestructive Testing. Presented at: NDT 1996 proceedings: *10th internationall Symposium on Nondestructive Testing of Wood. Lausanne, Switzerland.*

Burdon, R. D., Kibblewhite, R. P., Walker, J. C. F., Megraw, R. A.; Evans, R; Cown, D. J. (2004) Juvenile Versus Mature Wood: A New Concept, Orthogonal to Corewood Versus Outerwood, with Special Reference to *Pinus radiata* and *P. taeda*. *Forest Science 50*, 399-415.

Burmester, A. (1965). Relationship between velocity of sound [ultrasonic waves] and morphological, physical, and mechanical properties of wood. *Holz als Roh und Werkstoff 23*, 227-236.

Butterfield, B. G. (2003). Wood anatomy in relation to wood quality. In: Barnett & Jeronimidis (Eds), *Wood quality and its biological basis.* (pp 30-52). Cornwall, UK.: Blackwell publishing.

Cai, Z.; Hunt, M. O.; Fridley, K. J.; & Rosowsky, D. V. (1997). New technique for evaluating damping of longitudinal free vibration in wood-based materials. *Journal of testing and evaluation 25,* 456-460.

Carter, P., Chauhan, S. S. & Walker, J. C. F. (2006). Sorting logs and lumber for stiffness. using Director HM200. *Wood and Fibre Science 38*, 49-54.

Cave, I. D. (1968). The anisotropic elasticity of the plant cell wall. *Wood Science and technology 2,* 268-278.

Chauan, S., Entwistle. K. M., & Walker. J. C. F. (2005). Differences in acoustic velocity by resonance and transit-time methods in an anisotroic laminated wood medium. *Holzforschung 59,* 428-434.

Cown, D. J. (1973). Effect of severe thinning and pruning treatments on the intrinsic wood properties of young radiate pine. *New Zealand Journal of Forestry Science 3*, 379-389.

Cown, D. J., McConchie, D. L., & Young, G. D. (1991). Radiata pine: wood properties survey. NZ Forest Research Institute Bulletin No. 50.

Cown, D. J. (1992). Corewood (juvenile wood) in pinus radiata – should we be concerned? *New Zealand Journal of Forestry Science 22*, 87-95.

Cremer, L. & Heckl, M. (1988) Structure Borne Sound, 2nd edition. Berlin: Springer Verlag.

De Olivera, F. G. R., De Campos, J. A. O., Pletz, E., & Sales, A. (2002). Assessment of mechanical properties of wood using an ultrasonic technique. *Proceedings of the 13th International Symposium on Non-destructive Testing of Wood, university of California, Berkeley Campus California, USA*.

Divós, F., Dániel, I., & Bejó, L. (2001). Defect Detection in Timber by Stress Wave Time and Amplitude. NDT.net - March 2001, Vol. 6 No. 03.

Divos, F. & Tanaka, T. (2000). Effects of Creep on Modulus of Elasticity Determination of Wood. Journal of vibrations and acoustics 122, 89-92.

Fabris, S. (2000). Influence of cambial ageing, initial spacing, stem taper and growth rate on wood quality of three coastal conifers. Ph.D. thesis, Faculty of Graduate Studies, Department of Forestry, University of British Columbia, Vancouver, B.C.

Fang, S., Yang, W., &Tian, Y. (2006). Clonal and within-tree variation in microfibril angle in poplar clones. *New Forests 31*, 373-383.

Feeny, F., Chivers, R., Eversten, J., & Keating, J. (1996). The influence of inhomogeneity on the propagation of ultrasound in wood. *10th internationall Symposium on Nondestructive Testing of Wood. Lausanne, Switzerland.*

Ferry, J. D., (1980) Viscoelastic Properties of Polymers. 3rd edition New York: Wiley.

Forde, M. B. (1966). Pinus radiata in California. *New Zealand Journal of Forestry 11,* 20-42.

Funada, R., Kubo, T., Tabuchi, M., Sugiyama, T., & Fushitani, M. (2001). Seasonal variations in endogenous indole-3-acetic acid and abscisic acid in the cambial region of *Pinus densiflora* Sieb. et Zucc. stems in relation to earlywood–latewood transition and cessation of tracheid production. *Holzforschung 55*, 128–134.

Gartner, B. L., North, E. M., Johnson, G. R. & Singleton, R. (2002). Effects of live crown vertical patterns of wood density and growth in Douglas-fir. *Canadian Journal of Forest Research 32,*439-447.

Gerhards, C. C. (1982). Longitudinal stress waves for lumber stress grading: factors affecting applications: state of the art. *Forest Products Journal 32*, 20-25.

Grabianowski, M. (2003). Measuring acoustic properties in lumber and trees. Masters thesis University of Canterbury, New Zealand.

Halliday, D., Resnick, R., & Walker, J. (1997). *Fundamentals of Physics Extended, 5th Ed*, John Wiley & Sons Inc.

Harris, J. M. (1981).Wood quality of radiata pine. *Appita 35*, 211-215.

Harris, P., & Andrews, M. (1999). Emerging technologies for Evaluating wood quality for processing. *Presented at 3rd Wood Quality Symposium in Rotorua, N.Z.*

Jayne. B. A. (1959). Vibrational properties of wood as indices of quality. Forest Products Journal 9, 413-416.

Kane, J. W., & Sternheim, M. M. (1988). *Physics 3rd edition*. John Wiley & Sons Inc.

Kovac M. Murphy B. W, Lawrie J. W. (1990). Soil Landscapes of the Bathurst 1:250 000 Sheet, Soil Conservation Service of NSW, Sydney.

Larson, P. R. (1963). Stem form development of forest trees. *For. Sci. Monogr. 5*, 1–42.

Lasserre, J. P., Mason, E. & Watt, M. (2004). The influence of initial stocking on corewood stiffness in a clonal experiment on 11-year-old *Pinus radiata* D. Don. *N.Z. J. For. 44*, 18-23.

Lavery, P. M., Mead D. J. (1998). *Pinus radiata*: a narrow epidemic from North America takes on the world. . In: Richardson D.M. *Ecology and Biogeography of Pinus*. Cambridge University Press.

Libby, W. J, Bannister, M. H & Linhart, Y. B. (1968). The pines of Cedros and Guadalupe Islands. *J. For. 66*, 846–853.

Lindström, H., Harris, P., Nakada, R. (2002). Methods of measuring stiffnes in young trees. *Holz als Roh- und Werkstoff 60,* 165–174.

Macdonald, R. G., Franklin, J. N. (1969) *Pulp and Paper manufacture 2nd Ed.* New York: McGraw-Hill.

Megraw, R. A., Leaf, G., Bremer, D. (1998). Longitudinal shrinkage and microfibril angle in Loblooly pine. *Proceedings of the IAWA/IUFRO International Workshop on the significance of Microfibril Angle to Wood Quality*, Westport, New Zealand, November 1997.

Meyers, A. M. (1994). *Dynamic behaviour of Materials.* New York: John Wiley and sons. Inc.

Millar, C. I. (2000). Evolution and biogeography of Pinus radiata with a proposed revision of its Quaternary history. *New Zealand Journal of Forest Science 29*, 335-365.

Nardin, A. Boström, L., Zaupa, F. (2000). The effect of knots on the fracture of wood. *World Conference on Timber Engineering Whistler Resort, British Columbia, Canada.*

Ouis, D. (2000). Effect of Artificial Structural Defects on the MOE and Damping Properties of a Wood Element. *Proceedings of the 6th World Conference on Timber Engineering, Whistler, BC, Canada.*

Ouis, D. (2002).On the frequency dependence of the modulus of elasticity of wood *Wood Science and Technology 36*, 335–346.

Pape, R. (1999). Effects of thinning regime on the wood properties and stem quality of Picea abies. *Scand. J. For. Res. 14*: 38–50.

Price R. A., Liston, A., Strauss, S. H. (1998). Phylogeny and systematics of *Pinus*. In: Richardson D.M. *Ecology and Biogeography of Pinus*. Cambridge University Press.

Ross, R. J., & Pellerin, R. F. (1994). Nondestructive testing for assessing wood members in structures: A review. Gen. Tech. Rep. FPL-GTR-70 (Rev.). Madison, WI: U.S. Department of Agriculture, Forest Service, Forest Products Laboratory.

Sandoz, J. L., Benoit Y., & Demay, L. (2000). Wood testing using Acousto-ultrasonic. *World Conference on Timber Engineering Whistler Resort, British Columbia, Canada.*

Savidge, R. A. (2001). Intrinsic regulation of cambial growth. *J. Plant Growth Regul. 20*, 52–77.

Schniewind, A. P. (1989). *Concise encyclopedia of wood and wood-based materials.* Oxford: PergamonPress.

Smith, B. J., Peters, R. J., & Owen, S. (1996). *Acoustics and noise control*. Addison Wesley Longman Limited.

Smith, J. H. G. (1980). Influences of spacing on radial growth and percentage latewood of Douglas-fir, western hemlock, and western redcedar. *Canadian Journal of Forest Research 10,* 169-175.

Snedecor, G. W., & Cochran, W. G. (1967). *Statistical Methods*. Iowa State University Press. Ames, Iowa, USA.

Sundberg, B., Ericsson, A., Little, C. H. A., Näsholm, T., & Gref, R. (1993). The relationship between crown size and ring width in*Pinus sylvestris* L. stems: dependence on indole-3-acetic acid, carbohydrates and nitrogen in the cambial region. *Tree Physiol. 12*, 347–362.

Tsehaye, A. (1995). Within and- and between-tree variation in the wood quality of radiate pine. Thesis, Doctor of Philosophy in Forestry, School of Forestry. University of Canterbury. Christchurch.

Toulmin, M. J., & Raymond, C. A. (2007). Developing a sampling strategy for measuring acoustic velocity in standing *Pinus radiata* using the TRETAP time of flight tool. *New Zealand Journal of Forestry Science 37.*

XU, P. (2000). The mechanical properties and stability of radiate pine structural timber. Thesis, Doctor of Philosophy in Forestry, School of Forestry. University of Canterbury. Christchurch.

Xu, P., & Walker, J. C. F. (2004). Stiffness gradients in radiate pine trees. *Wood Science Technology 38*, 1-9.

Walker, J. C. F., & Nakada, R. (1999). Understanding corewood in some softwoods: a selective review on stiffness and acoustics. *International Forestry Review 1*, 251 -259.

Walker, J. C. F. (2006). *Primary wood processing 2nd edition.* Dordrecht: Springer Verlag.

Wang, S.Y., Lin, F. C., Jane, M. C., Lin, C.J., & Hung, C.P.. (2000). Effects of thinning and pruning on DBH and ultrasonic wave velocity in *Taiwania Cryptomerioide.* World Conference on Timber Engineering Whistler Resort, British Columbia, Canada.

Wang, S.Y., Lin, C. J., Chiu, C. M., Chen, J. H., & Yung, T. H. (2005). Dynamic modulus of elasticity and bending properties of young Taiwania trees grown with different thinning and pruning treatments. *Journal of wood science 5,* 1-6.

Zobel, B. J., & van Buijtenen, J.P.(1989). *Wood variation, its causes and control*. Berlin: Springer-Verlag.

Zobel B. J., Sprague, J. R. (1998). *Juvenile wood in forest trees*. Berlin: Springer Verlag.